



University of Kentucky  
UKnowledge

---

Theses and Dissertations--Mechanical  
Engineering

Mechanical Engineering

---


2018

## ASSISTED DEVELOPMENT OF MESOPHASE PITCH WITH DISPERSED GRAPHENE AND ITS RESULTING CARBON FIBERS

Aaron Owen

University of Kentucky, amow224@g.uky.edu

Author ORCID Identifier:

 <https://orcid.org/0000-0003-0858-3151>

Digital Object Identifier: <https://doi.org/10.13023/etd.2018.454>

[Right click to open a feedback form in a new tab to let us know how this document benefits you.](#)

---

### Recommended Citation

Owen, Aaron, "ASSISTED DEVELOPMENT OF MESOPHASE PITCH WITH DISPERSED GRAPHENE AND ITS RESULTING CARBON FIBERS" (2018). *Theses and Dissertations--Mechanical Engineering*. 126.

[https://uknowledge.uky.edu/me\\_etds/126](https://uknowledge.uky.edu/me_etds/126)

This Master's Thesis is brought to you for free and open access by the Mechanical Engineering at UKnowledge. It has been accepted for inclusion in Theses and Dissertations--Mechanical Engineering by an authorized administrator of UKnowledge. For more information, please contact [UKnowledge@lsv.uky.edu](mailto:UKnowledge@lsv.uky.edu).

## **STUDENT AGREEMENT:**

I represent that my thesis or dissertation and abstract are my original work. Proper attribution has been given to all outside sources. I understand that I am solely responsible for obtaining any needed copyright permissions. I have obtained needed written permission statement(s) from the owner(s) of each third-party copyrighted matter to be included in my work, allowing electronic distribution (if such use is not permitted by the fair use doctrine) which will be submitted to UKnowledge as Additional File.

I hereby grant to The University of Kentucky and its agents the irrevocable, non-exclusive, and royalty-free license to archive and make accessible my work in whole or in part in all forms of media, now or hereafter known. I agree that the document mentioned above may be made available immediately for worldwide access unless an embargo applies.

I retain all other ownership rights to the copyright of my work. I also retain the right to use in future works (such as articles or books) all or part of my work. I understand that I am free to register the copyright to my work.

## **REVIEW, APPROVAL AND ACCEPTANCE**

The document mentioned above has been reviewed and accepted by the student's advisor, on behalf of the advisory committee, and by the Director of Graduate Studies (DGS), on behalf of the program; we verify that this is the final, approved version of the student's thesis including all changes required by the advisory committee. The undersigned agree to abide by the statements above.

Aaron Owen, Student

Dr. Rodney Andrews, Major Professor

Dr. Alexandre Martin, Director of Graduate Studies

ASSISTED DEVELOPMENT OF MESOPHASE PITCH WITH DISPERSED  
GRAPHENE AND ITS RESULTING CARBON FIBERS

---

THESIS

---

A thesis submitted in partial fulfillment of the requirements  
for the degree of Master of Science in Mechanical  
Engineering in the College of Engineering at the University  
of Kentucky

By

Aaron Owen

Lexington, Ky

Director: Dr. Rodney Andrews, Professor of Mechanical Engineering

Copyright © Aaron Owen 2018

<https://orcid.org/0000-0003-0858-3151>

## ABSTRACT OF THESIS

### ASSISTED DEVELOPMENT OF MESOPHASE PITCH WITH DISPERSED GRAPHENE AND ITS RESULTING CARBON FIBERS

The efficacy of dispersed reduced graphene oxide (rGO) as a nucleation site for the growth of mesophase in an isotropic pitch was investigated and quantified in this study. Concentrations of rGO were systematically tested in an isotropic petroleum and coal-tar pitch during thermal treatments and compared to pitch without rGO. The mesophase content of each thermally treated pitch was quantified by polarized light point counting. Further characterization of softening temperature and insolubles were quantified. Additionally, the pitches with and without rGO were melt spun, graphitized, and tensile tested to determine the effects of rGO on graphitized fiber mechanical properties and fiber morphology.

KEYWORDS: Mesophase, Reduced graphene oxide, Melt spinning, Carbon fiber

Aaron Owen

---

December 5, 2018

---

Date

ASSISTED DEVELOPMENT OF MESOPHASE PITCH WITH DISPERSED  
GRAPHENE AND ITS RESULTING CARBON FIBERS

By

Aaron Owen

Dr. Rodney Andrews

---

Director of Thesis

Dr. Alexandre Martin

---

Director of Graduate Studies

December 5, 2018

---

Date

## ACKNOWLEDGMENTS

Thank you to my patient wife who has graciously dealt with my long days and late nights throughout this process.

Also, thank you to everyone in the Carbon Group at CAER that helped guide me along to be a better engineer and scientist and dealt with my constant barrage of questions.

Lastly, thank you to my advisor, Rodney Andrews and co-advisor Matt Weisenberger for taking the time to guide me in my research and thesis work.

## TABLE OF CONTENTS

ACKNOWLEDGMENTS .....	iii
TABLE OF CONTENTS.....	iv
LIST OF TABLES .....	vii
LIST OF FIGURES .....	ix
Chapter 1. BACKGROUND .....	1
1.1 Introduction.....	1
1.2 History of Pitch.....	4
1.3 Petroleum Pitch Origin .....	6
1.4 Coal-tar Pitch Origin.....	7
1.5 Isotropic and Mesophase .....	10
1.6 Previous Pitch Improvement Methods.....	16
1.7 Fiber Processing.....	18
1.7.1 Melt Spinning.....	18
1.7.2 Oxidation.....	24
1.7.3 Carbonization and Graphitization .....	24
1.8 Conclusion .....	27
Chapter 2. GRAPHENE AS A SEED CRYSTAL FOR MESOPHASE DEVELOPMENT .....	29
2.1 Introduction.....	29
2.2 Experimental Materials and Methods .....	30
2.2.1 Materials .....	30
2.2.2 Experimental Methods.....	30
2.2.3 Temperature Control.....	33

2.2.3 Heat Treatment.....	34
2.2.4 Insoluble Testing.....	35
2.2.5 Dynamic Mechanical Analysis (DMA) .....	36
2.2.6 Polarized Light Microscopy.....	37
2.3 Results.....	39
2.3.1 Petroleum Pitch.....	39
2.3.2 Coal-tar Pitch .....	49
2.3.3 Observations During Heat Treatments.....	57
2.2.5 Milled Mitsubishi and THF Insolubles .....	58
2.4 Conclusion .....	59
Chapter 3. MELT SPINNING .....	61
3.1 Introduction.....	61
3.1.1 Wayne Extruder (WEXT) Spinning.....	63
3.1.2 Pressure Spinning Capsule.....	67
3.1.3 Melt Pool Spinning .....	71
3.1.4 Lessons Learned.....	72
3.2 Method .....	73
3.3 Results.....	74
3.4 Conclusion .....	76
Chapter 4. THERMAL CONVERSION AND CARBON FIBER PROPERTIES .....	77
4.1 Introduction.....	77
4.2 Mechanical Properties.....	78
4.2.1 Thermal Conversion.....	78
4.2.2 Microscopy .....	79
4.2.3 Tensile Testing.....	83



4.3 Results.....	84
4.4 Conclusion .....	87
Chapter 5. CONCLUSION.....	89
5.1 Future Work.....	91
APPENDIX.....	92
REFERENCES .....	94
VITA.....	98

## LIST OF TABLES

Table 1.1 CHN Analysis of various pitches. Carbon (C), hydrogen (H), nitrogen (N), sulfur (S), oxygen (O) and carbon: hydrogen ratio (C/H). Percentages are by weight.....	6
Table 1.2 Representative properties of carbon fibers from various precursors. ....	13
Table 1.3 Mechanical properties of graphitized fibers with various textures. Diameter ( $\emptyset$ ), tensile strength (TS), Young's modulus (E), compressive strength (CS).....	24
Table 2.1 Average temperatures at each treatment time with deviation.....	40
Table 2.2 Comparing rGO wt.% with closer average temperatures. Target temperature was 370 °C.....	42
Table 2.3 Comparison of mesophase percentages for the 0.5-hour treatment samples that had the smallest deviation of average pitch temperature. ....	43
Table 2.4 Average temperature during the heat treatment for all coal-tar samples and the deviation of temperatures.....	50
Table 2.5 Comparing rGO wt.% with closer average temperatures. Target temperature was 370 °C.....	52
Table 2.6 Mesophase percentage for coal-tar pitch samples with same average temperature heat treated for 0.5-hours. ....	53
Table 3.1 Initial spinning parameters for experimental pitches. Filter pore size, nitrogen pressure (P), spinneret diameter ( $\emptyset$ ), spinneret temperature (Spin Temp), take-up spool setting (RPM), and meters per minute (m/min) of fiber collected.....	73
Table 3.2 Optimization of spinning conditions for each heat-treated pitch; petroleum (Pet.) and coal-tar (Coal) with listed mesophase percentage (M), softening temperature ( $T_{sp}$ ), controlled spin temperature (Spin T), monitored pitch temperature (Pitch T), nitrogen pressure (P), and spool take-up speed (RPM) .....	75
Table 4.1 Change in lengths and masses for the petroleum (P) and coal-tar (C) pitches with 0 wt% and 0.01 wt % rGO. Initial green fiber carbon yield (CY) after graphitization. ....	79
Table 4.2 Diameter ( $\emptyset$ ) of the four graphitized fibers samples as measured by SEM. Petroleum (P) and coal-tar (C) pitch. ....	82

Table 4.3 Break Tenacity (T)(cN/dtex) and Initial Modulus (E)(cN/dtex), and Coefficient of Variance (COV) of the graphitized pitch fibers. Shown are petroleum (P) and coal-tar (C) with 0 wt.% and 0.01 wt.% rGO..... 84

## LIST OF FIGURES

Figure 1.1 Tensile properties of carbon fibers from various precursors. ....	2
Figure 1.2 PAN and Pitch, raw material to carbon fibers. ....	3
Figure 1.3 Representative of the type of molecular structure expected to find within (a) coal-tar pitch and (b) petroleum pitch.....	6
Figure 1.4 Coal coke oven where coal-tar pitch production is a by-product. ....	8
Figure 1.5 Solvent refining process where pitch or coke can be produced. ....	8
Figure 1.6 Fischer-Tropsch process to produce diesel and gasoline. Pitch is a by-product towards the beginning of the process.....	9
Figure 1.7 Polarized light image of a mesophase pitch. Here, the sample is 100% mesophase. ....	11
Figure 1.8 Graphitic radial texture in graphitized fibers derived from 100% mesophase (polymerized naphthalene AR pitch). ....	12
Figure 1.9 Mesophase spheres (magenta and cyan) within an isotropic matrix. ....	14
Figure 1.10 Viscosity comparison of isotropic and mesophase pitches ....	19
Figure 1.11 The alignment of discotic mesophase during melt spinning. ....	20
Figure 1.12 Pitch green fiber that has a "bulge" in the fiber most likely caused by insolubles in the pitch. This nodule is a defect in the fiber and yields significantly lower mechanical properties. ....	21
Figure 1.13 Melt-spinning extruder process. ....	22
Figure 1.14 Internal morphology for graphitic mesophase fibers, classified as radial, onion-skin, random, flat-layer, radial-folded, and line-origin. ....	23
Figure 1.15 Graphite AB structure. Basal plane view showing the AB stacking offset... ..	25
Figure 1.16 Top view of graphite AB stacking. The A plane is a solid line and the B plane is a dotted line. ....	26
Figure 2.1 Test matrix followed for testing rGO in coal-tar and petroleum isotropic pitch. Each treatment time and rGO wt.% were replicated at least once leading to 60 separate thermal treatments.....	31
Figure 2.2 Thermal treatment arrangement. ....	33

Figure 2.3 A comparison of the pitch temperature during heat treatments with the temperature being controlled by the pitch thermocouple or the mantle thermocouple. ...	34
Figure 2.4 Example of a DMA analysis to determine the softening temperature of a pitch. The derivative of displacement with respect to temperature is plotted and the peak of this curve is representative of the softening temperature. ....	36
Figure 2.5 Example of a polished “puck” of pitch inside an epoxy. This “puck” was used for polarized light microscopy to determine the mesophase percentage of the heat-treated pitch. Puck was 1 inch in diameter. ....	38
Figure 2.6 The average temperature of the pitch during the heat treatment for every petroleum pitch sample tested.....	40
Figure 2.7 Petroleum mesophase percentage as determined by polarized light microscopy. Three samples were tested at three rGO weight percentages: 0 (baseline), 0.01, and 0.10. ....	41
Figure 2.8 The mesophase percentage compared with less deviation in the average temperatures.....	42
Figure 2.9 Isotropic petroleum-based pitch under polarized light. No mesophase content is present. The two white dots are epoxy.....	44
Figure 2.10 Mesophase growth comparison by polarized for 0.5-hours of thermal treatment for the 0 wt.% (i) 0.01 wt.% (ii) and 0.10 wt.% (iii) samples. Scale bar is 50 $\mu\text{m}$ . ....	45
Figure 2.11. Mesophase content for the petroleum sample at treatment times of 1 hour (i), 2-hour (ii), 3-hour (iii), and 4-hour (iv). ....	47
Figure 2.12 Softening temperatures of the pitches by DMA compression test for all petroleum pitches tested. The softening temperature was determined by a controlled force test. Then the derivative of displacement with respect to temperature was plotted. ....	48
Figure 2.13 Quinoline insolubles (QIs) for all the petroleum pitches tested. As expected, the QIs increased with increased mesophase percentage.....	49
Figure 2.14 The average temperature of the pitch during the heat treatment for every coal-tar sample tested.....	50

Figure 2.15 Coal-tar pitch mesophase percentage as determined by polarized light microscopy. Three samples were tested at three rGO weight percentages: 0 (baseline), 0.01, and 0.10.....	51
Figure 2.16 The mesophase percentage compared with less deviation in the average temperatures.....	52
Figure 2.17 Isotropic coal-based pitch under polarized light. No mesophase content is present. The white dot is epoxy. ....	54
Figure 2.18. Mesophase content for the petroleum sample at treatment times of 0.5-hours (i), 1-hour (ii), 2-hour (iii), 3-hour (iv), and 4-hour (v). ....	55
Figure 2.19 Softening temperatures of the pitches by DMA compression test for all coal-tar pitches tested. The softening temperature was determined by the derivative of displacement with respect to temperature. ....	56
Figure 2.20 Quinoline insolubles (QIs) for all the coal-tar pitches tested. As expected, the QIs increased with increased mesophase percentage.....	57
Figure 3.1 Representative shear rate sweep for a 100% mesophase pitch.....	62
Figure 3.2 Extruder screw for the WEXT.....	63
Figure 3.3 Side view of the WEXT with the listed monitored (M) and controlled (C) parameters. ....	64
Figure 3.4 Controlled temperatures zones for the WEXT where the pitch transitions from right to left. Melt temperature and pressure transducer location are shown. ....	65
Figure 3.5 Extruder melt spun mesophase carbon fibers.....	67
Figure 3.6 UKY CAER pressure spinning capsule with monitored pitch temperature, controlled spinneret temperature, and controlled nitrogen flow. ....	68
Figure 3.7 Melt spinning apparatus used for spinning green fibers. A 20 $\mu\text{m}$ fritted metal filter was used during spinning to filter out particulates. The parameters controlled for pressure spinning are shown: nitrogen pressure, spinneret temperature, and take-up spool RPM. ....	69
Figure 3.8 Green fibers after being pressure spun for a mesophase pitch (i). Graphitized mesophase fiber with desired graphitic sheets and undesired voids in the fiber (ii). ....	71

Figure 3.9 Melt pool spinning where only the exit of the spinneret is shown at 330 $\mu\text{m}$ (A), the pitch exits and begins to swell to a pool size of 3.774 mm (E) and decreases to 2.867 mm once pulled into a fiber (F). .....	72
Figure 3.10 Green fiber melt spun pitch sample. The collection of fiber forms a band around the spool. Individual filaments are highlights in the callout image. ....	76
Figure 4.1 SEM images of melt-spun graphitized (i) petroleum pitch 0 wt.% rGO (ii) petroleum pitch 0.01 wt.% rGO (iii) coal-tar pitch 0 wt.% rGO (iv) coal-tar pitch 0.01 wt.% rGO. ....	81
Figure 4.2 Example of a fiber that had non-uniform shrinkage during thermal conversion. Here the fiber was approximately 120 mm in length and approximately 30 $\mu\text{m}$ in diameter.....	82
Figure 4.3 Break stress of the graphitized petroleum (P) and coal-tar (C) pitch fibers in textile units (cN/dtex) with mesophase percentage. ....	86
Figure 4.4 Modulus of the graphitized petroleum (P) and coal-tar (C) pitch fibers in textile units (cN/dtex) with mesophase percentage. ....	87
Figure 5.1 Distribution of the tensile stress against probability of failure using a Weibull analysis of graphitic fibers .....	93

## Chapter 1. BACKGROUND

### 1.1 Introduction

Materials science has made great advancements over the last twenty years. There has been a significant focus on making materials both stronger and lighter. Composites are an excellent choice because they are composed of a reinforcing material within a matrix material, which combine to provide advantageous mechanical, thermal, or electrical properties. Composite materials are of high value in industries where weight reduction and high strength are imperative, as in aerospace and, increasingly, automotive applications. A commonly used material in these industries is carbon fiber reinforced composite (CFRC), which is comprised of high modulus and strength reinforcing carbon fibers within, typically, a polymeric matrix, often epoxy. The matrix protects the fibers and imparts shape and toughness to composite parts.

Polyacrylonitrile (PAN) based carbon fibers dominate the field of carbon fiber composites. The main reason the PAN-based carbon fibers are the primary product on the market is the high strength and high strain to failure, or high fiber toughness. A potential alternative is pitch-based carbon fibers. Pitch-based carbon fibers have two primary sources: coal-tar pitch, and petroleum pitch. In Figure 1.1 the respective properties of PAN-based and pitch-based carbon fibers are shown. The mesophase pitch fibers have a lower tensile strength but show an exceedingly high tensile modulus with high thermal conductivity, while the PAN-based fibers are high in tensile strength, but do not have as high tensile modulus.



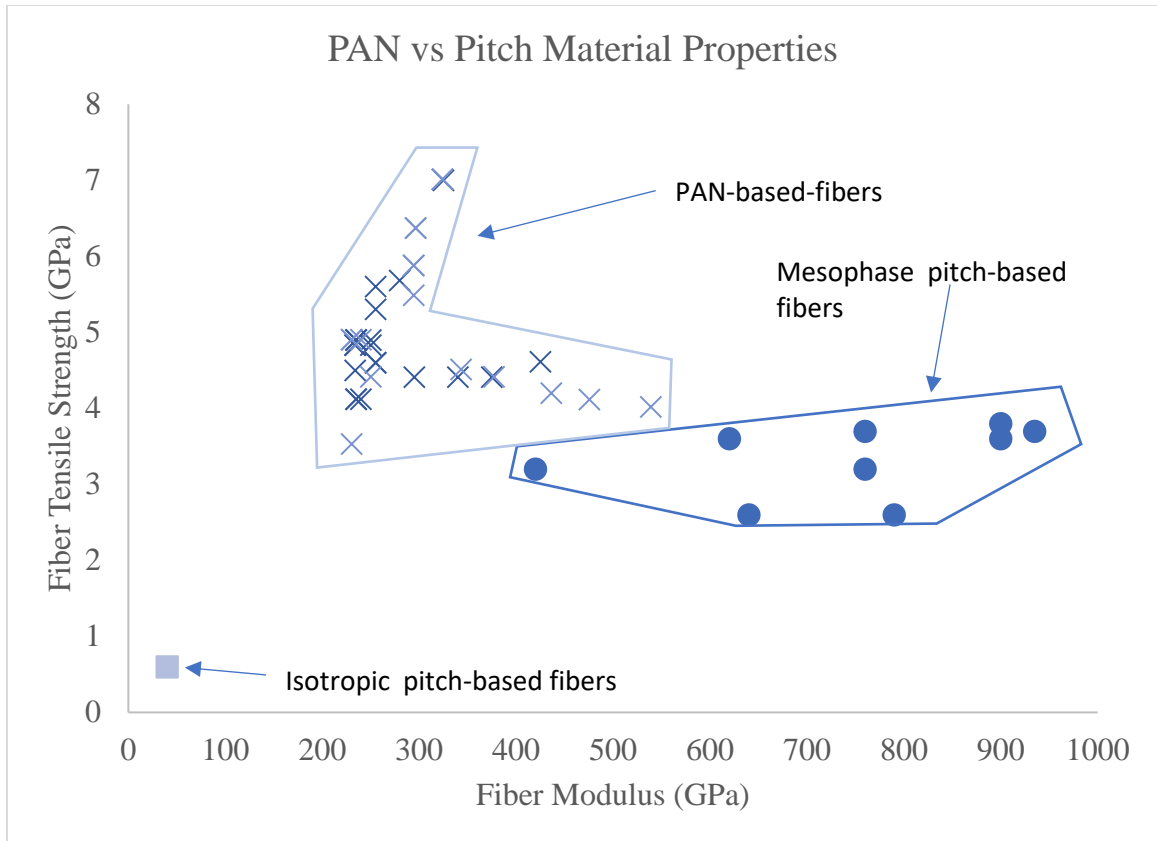


Figure 1.1 Tensile properties of carbon fibers from various precursors[1], [2].

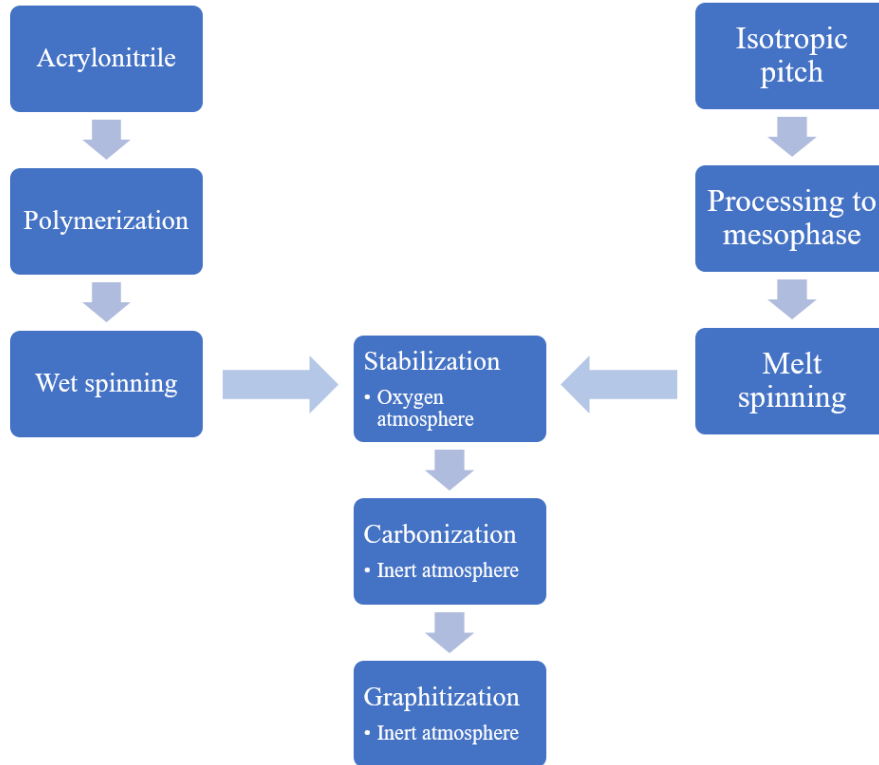


Figure 1.2 PAN and Pitch, raw material to carbon fibers.

Figure 1.2 outlines the steps to convert raw pitch and PAN to carbon fiber. The pitch spinning process varies significantly from the PAN, solution spinning process. First, pitch requires processing to promote the stacking of polyaromatic hydrocarbons (PAH) in an isotropic matrix to generate a liquid crystalline state called mesophase. Melt spinning then gives the fiber the proper molecular orientation and therefore, stretching is not needed during thermal conversion. The molecular orientation occurs when the disc-like mesophase is forced through the capillary of the spinneret and the mesophase aligns in the capillary of the spinneret before vitrifying shortly after exiting the spinneret. The thermal conversion process: oxidation and carbonization follow a similar path to the PAN fiber.

There are many reasons why pitch-based precursor fiber should be a candidate to produce low-cost carbon fiber. For example, the isotropic pitch is cheaper than acrylonitrile[3] and pitch can be melt spun thus avoiding costs associated with solution

spinning PAN. Moreover, the carbon fiber carbon yield (from precursor fiber) for mesophase pitch is approximately 80% by weight, while for PAN it is 50% to 55% [4].

One advantage of melt spinning is that solvent recovery is not necessary as is required during PAN precursor fiber production. For the PAN precursor fiber production, it is estimated for every 1 kg of precursor fiber generated, 40 kg of solvent wash water is generated. The elimination of this portion of the spinning process could potentially help offset some of the additional processing costs of the production of green (as-spun, non-oxidized) pitch fiber, which primarily consists of the cost to process isotropic pitch to mesophase pitch. Also, the physical footprint of the melt spinning process is considerably smaller than that of the PAN precursor fiber production. However, the green fiber is considerably more fragile than PAN precursor fiber. Therefore, extreme care must be taken when collecting and handling the green fiber before oxidation which is not the case with PAN precursor fiber. While the cost of mesophase pitch has been coming down in recent decades, the cost of PAN-based carbon fibers is still lower at \$10-30 per pound versus mesophase pitch at \$50+ per pound [5].

## 1.2 History of Pitch

Pitch is derived from three common products: petroleum, coal, and plants. Plant-derived pitch has been utilized for thousands of years to seal sailing vessels. This pitch was a product of the distillation of wood, aptly named “wood tar.” In production, wood was heated until pitch (tar) was dripping from the wood and left behind charcoal. While pitch and tar are used interchangeably, at room temperature pitch is usually solid, while tar exists in a liquid state.

The history of pitch-based carbon fibers dates back to 1970 where the Kureha Corporation industrialized an isotropic carbon fiber using a method invented by Otani [6]. Higher performance pitch-based carbon fibers were achieved by the Union Carbide Corporation (currently Cytec Solvay Group) using another method invented by Otani [7]. These high-performance fibers exhibited anisotropic (mesophase) characteristics. Other companies have been involved with the production of high-performance mesophase

fibers since the 1980s including Exxon and Du Pont but have since ceased production. In modern production methods, the refining of crude oil and coking of metallurgical coal generate pitches as by-products. The current economic climate is favorable to produce pitch-based carbon fibers because there is considerable interest in using coal-tar pitch as a raw material. Currently, there is one United States-based pitch carbon fiber manufacturer (Solvay-Cytec Industries) and four Japan-based manufacturers (Nippon Graphite Fiber Co., Ltd.; Mitsubishi Plastics, Inc.; Kureha Corp.; and Osaka Gas Chemicals Co., Ltd.)[8].

Petroleum and coal-tar pitches can vary significantly. For petroleum and coal-tar pitch of comparable densities, petroleum pitch has little to no native quinoline-insolubles (QI) while coal-tar pitch has significant QI due to the coking process, which introduces small amounts of soot into the pitch. Native QI is a measure of the cumulative mineral matter, coke, and quite high molecular weight hydrocarbons in the pitch. Therefore, native QI is a significant characterization factor in the production and categorization of coal-tar pitch as a raw material, while it is less significant for petroleum pitch as a raw material. Another important characterization for pitches is softening temperature which is the temperature when the pitch begins to soften (without a phase transition) and resembles a viscous liquid. This softening is a transition for the pitch from a glassy solid to a glassy liquid. The isotropic raw material pitch used for processing to carbon fibers generally has an initial softening temperature of approximately 100 °C.

The chemical structure of coal-tar and petroleum-derived mesophase pitch varies for several reasons. While both consist of a polyaromatic hydrocarbon (PAH) molecular structure, petroleum pitch has been shown to have aliphatic carbon while coal-tar pitch has not been observed to have significant aliphatic carbon. Figure 1.3 shows a representative molecular structure for coal-tar and petroleum pitches. The coal-tar pitch is primarily planar, which allows for strong intermolecular forces, while the petroleum pitch molecular structure is more mobile because of the aliphatic carbon areas[9]. This mobility in petroleum-derived pitches allows for the rearrangement of molecules more readily and mesophase generally grows more quickly than in coal-derived pitches and the aromaticity of coal-tar-derived pitch is higher than petroleum-derived pitch.

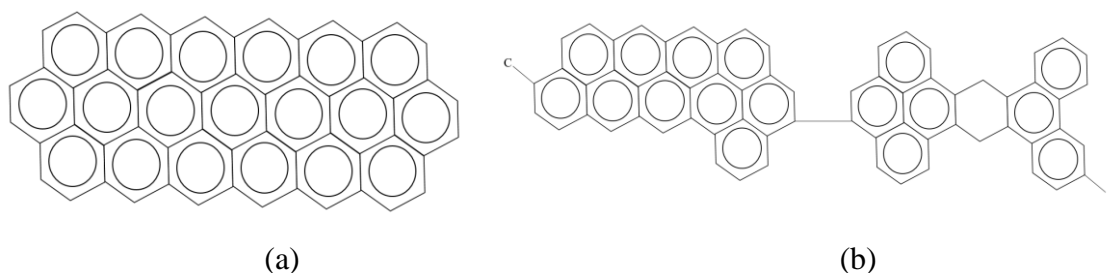


Figure 1.3 Representative of the type of molecular structure expected to find within (a) coal-tar pitch and (b) petroleum pitch[9].

The aromaticity of a pitch can be estimated by a CHN (carbon, hydrogen, nitrogen, oxygen by subtraction) analysis. The larger the carbon/hydrogen ratio (C/H), the more aromatic a pitch is. Using these ratios, the aromaticity of the coal-tar pitch can be seen to be higher than the petroleum pitch. Synthetic pitches which were produced with an HF-BF<sub>3</sub> catalyst (section 1.6), range in aromaticity, namely Mitsubishi AR and Mitsubishi LSP (Table 1.1).

Table 1.1 CHN Analysis of various pitches. Carbon (C), hydrogen (H), nitrogen (N), sulfur (S), oxygen (O) and carbon: hydrogen ratio (C/H). Percentages are by weight.

<u>Sample</u>	<u>Type</u>	<u>%C</u>	<u>%H</u>	<u>%N</u>	<u>%S</u>	<u>%O</u>	<u>C/H</u>
Mitsubishi AR	Synthetic	93.64	5.14	<0.01	0.00	1.22	18.22
Mitsubishi LSP	Synthetic	93.49	5.89	<0.01	0.00	0.62	15.87
Petroleum	Petroleum	93.09	5.50	0.04	0.60	0.74	16.93
Coal-tar	Coal-tar	93.11	5.00	0.82	0.52	0.55	18.62

### 1.3 Petroleum Pitch Origin

The production of petroleum pitch stems from the distillation of crude oil during the process of producing fuels and chemicals. The types of petroleum pitch produced are

highly dependent on the processing conditions of the crude oil and the severity of the process.

Fluid catalytic cracking (FCC) is a traditional method for processing crude oil and generating heavy bottoms which then can be processed to make pitch. This process has become more popular than traditional thermal cracking methods because FCC produces gases that are more aromatic. During the FCC process the feedstock, or crude oil, is heated to a high temperature and moderate pressure with the addition of a catalyst. This catalyst breaks the long chain hydrocarbons into shorter chains creating a vapor. These vapors flow through the reactor and are distilled into end products including naphtha, fuel oil and off gas. The petroleum naphtha is further processed to produce fuels, and from this processing, and further processing of the heavy bottoms of the cracking towers, a low softening point (<50°C) pitch-like material is formed. Through further filtration and distillation, the softening point rises to approximately 100 °C, and is formed into isotropic pitch.

#### 1.4 Coal-tar Pitch Origin

Three main production processes yield coal-tar pitch: coking, solvent extraction, and gasification. The coking process is the most widely used that produces pitch as a by-product. This process is outlined in Figure 1.4[10]. The coal is heated in the coking ovens, called batteries, to produce a nearly pure carbon solid fuel called coke. The volatiles captured during the process are collected as a sludge. This sludge is again heated to a gaseous form, then steam distilled. The by-product of this steam distillation is coal-tar pitch. The coal-tar pitch produced can vary drastically based on the parent coal.

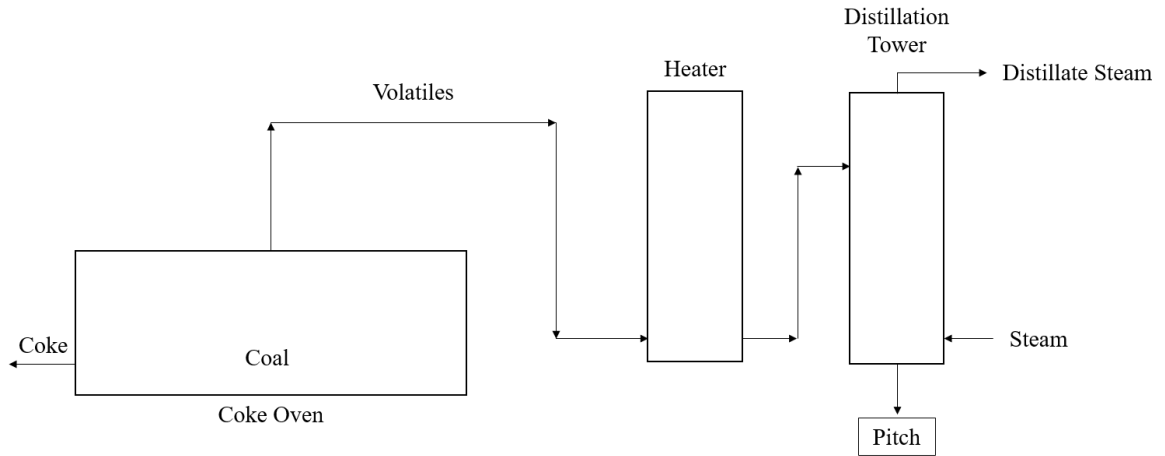


Figure 1.4 Coal coke oven where coal-tar pitch production is a by-product.

Solvent extraction of coal is another method by which products are made, one of which is pitch. One solvent extraction process is outlined in Figure 1.5[11]. Here, the coal is mixed with a solvent feed (e.g., anthracene oil) inside the reactor tank. The mixed feed is then processed to remove virtually all the mineral matter present in the coal. Once this coal solution has been gathered, it may be processed into coke or pitch.

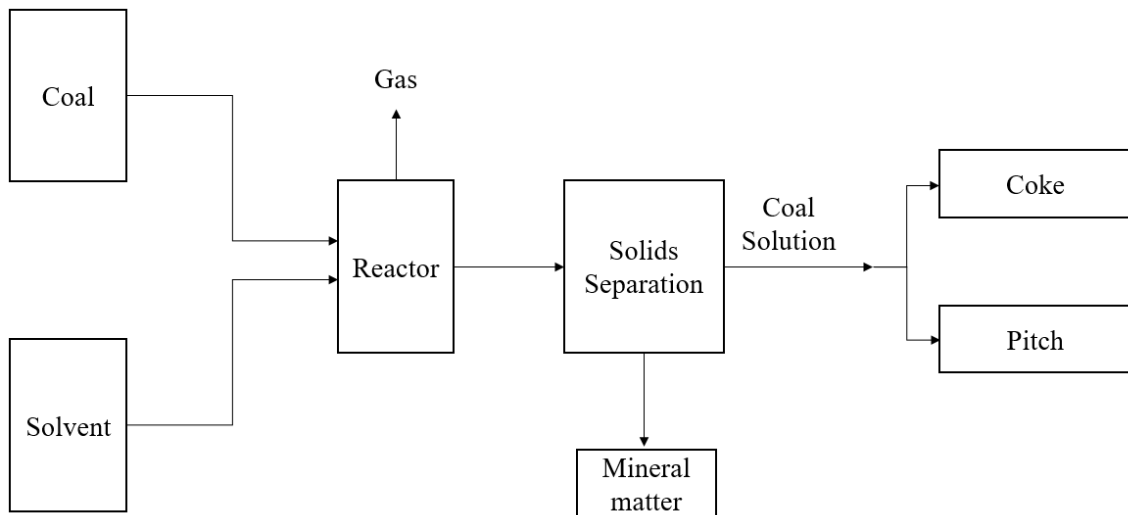


Figure 1.5 Solvent refining process where pitch or coke can be produced[11].

Lastly, gasification is another process for refining coal that produces pitch as a by-product, which relies heavily on the Fischer-Tropsch process<sup>9</sup>. Synthesis gas is produced from coal using steam and oxygen in Lurgi gasifiers, which are vertical distillation units used to capture gas off-take with the introduction of hot steam to gasify the coal. Many of the by-products gathered during the gasification process are the tar distillates which are further refined to gasoline and diesel fuel. The heavy oils and waxes produced during the process are fractionated and refined. Figure 1.6 shows the coal refining process for producing fuels, where pitch is a by-product during the purification stage.

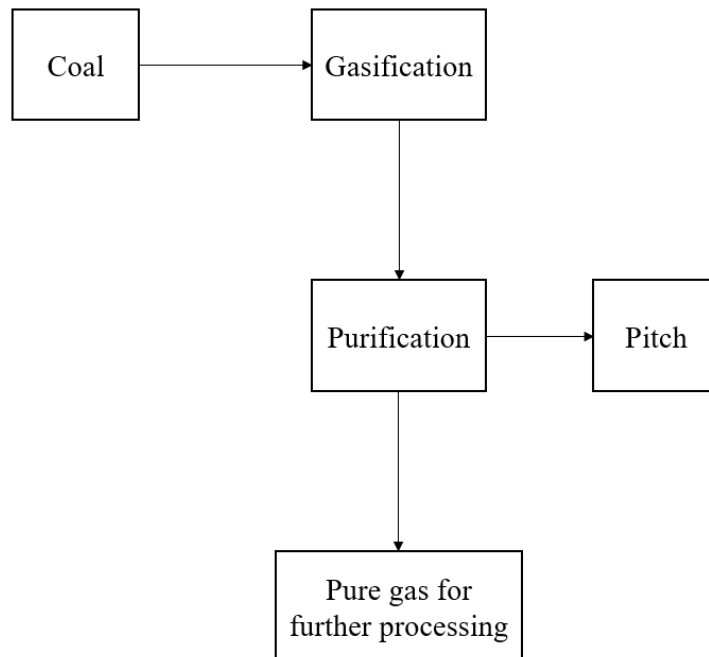


Figure 1.6 Fischer-Tropsch process to produce diesel and gasoline. Pitch is a by-product towards the beginning of the process.



## 1.5 Isotropic and Mesophase

The types of pitch used for pitch-based carbon fibers can be divided into two categories: isotropic and mesophase. Isotropic pitches consist of smaller aromatic molecules that are arranged in random order while mesophase pitches consist of larger, stacked aromatic molecules that can arrange into liquid crystal domains. Isotropic pitch-derived fibers, which are considerably easier to process than mesophase-derived fibers, do not achieve a graphitic structure even with high-temperature treatment and therefore are considered general use carbon fibers. In this sense, isotropic pitch is a non-graphitizable carbon[12]. Mesophase fibers do achieve a graphitic structure with heat treatment above 2000 °C and are considered high-performance fibers, exhibiting moderate tensile strength, very high modulus, and impressive thermal conductivity. The graphitic structure forms due to the liquid crystalline nature of the mesophase – resulting in domains of pre-stacked mesogen (or polyaromatic hydrocarbon) units, which readily condense to AB stacked graphite upon high heat treatment under inert conditions. Figure 1.7 shows polarized light images of the liquid crystalline state of mesophase (at room temperature). With the anisotropic material, the crystalline structure causes the polarized various wavelengths across the sample (a material property called birefringence), yielding the variation of colors. An isotropic pitch analyzed under polarized light shows no variation in color regardless of orientation. Figure 1.8 shows the graphitic sheets formed in the graphitization of mesophase fibers.

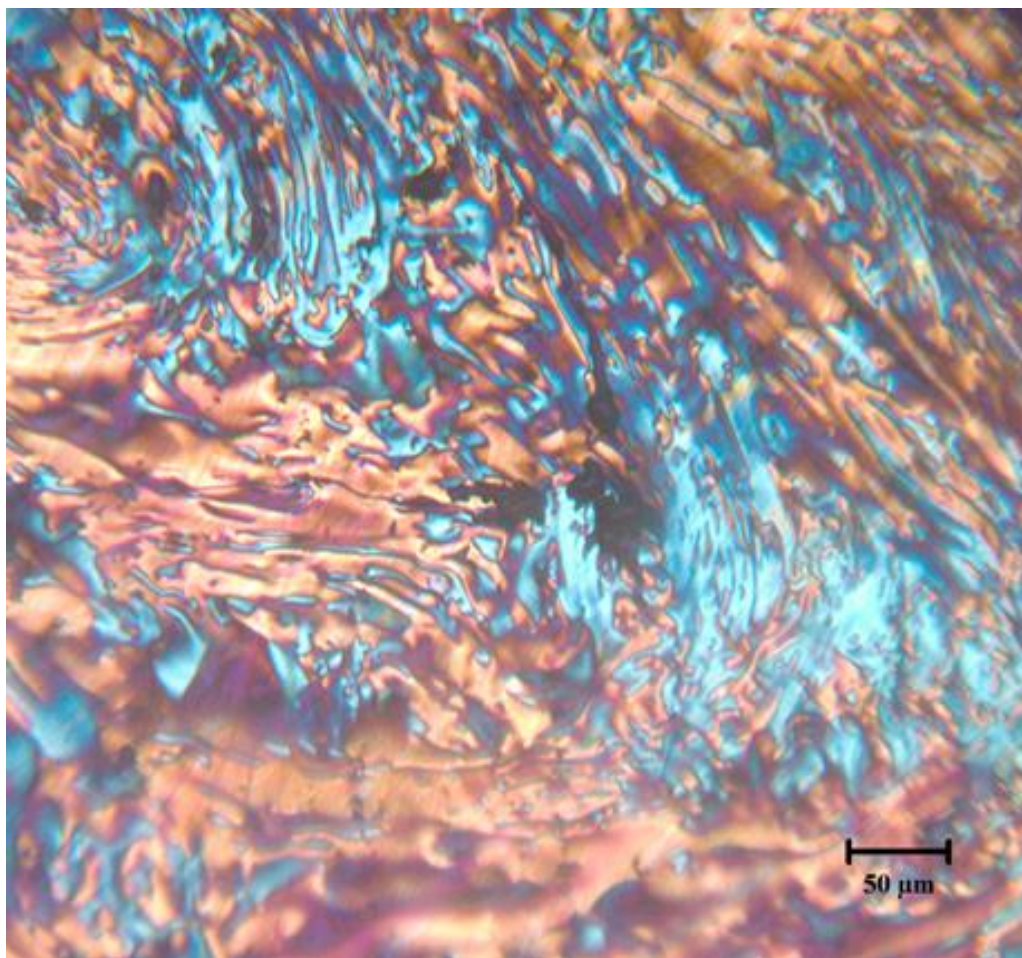


Figure 1.7 Polarized light image of a mesophase pitch. Here, the sample is 100% mesophase.

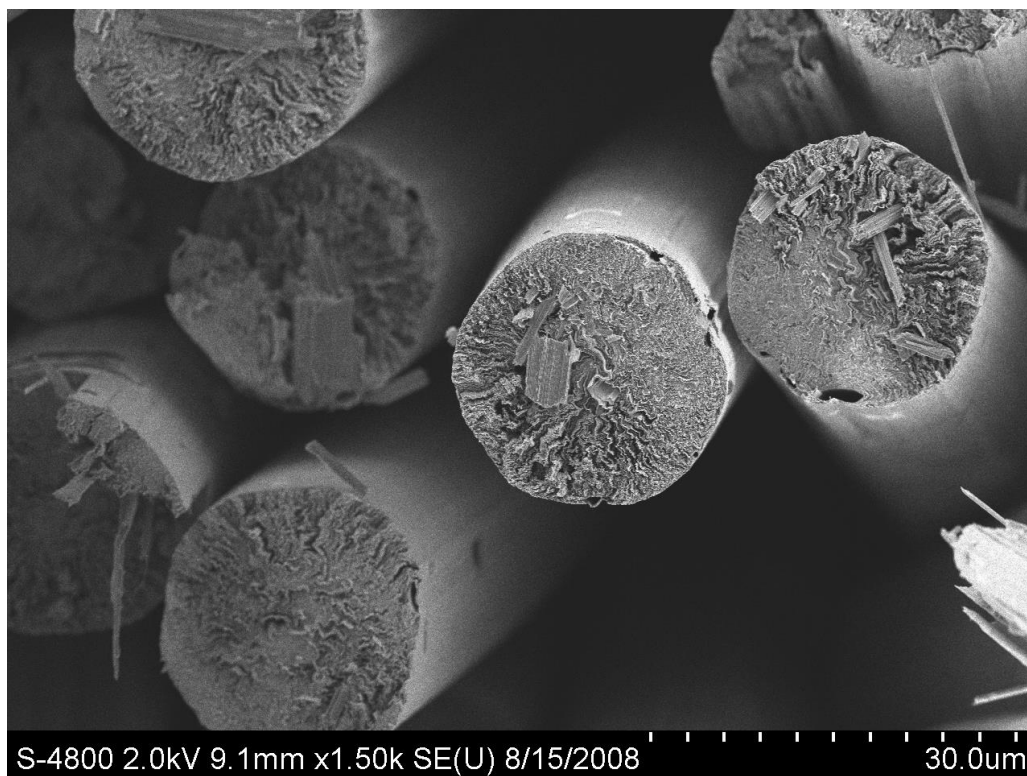


Figure 1.8 Graphitic radial texture in graphitized fibers derived from 100% mesophase (polymerized naphthalene AR pitch).

Clean (low-QI), isotropic petroleum or coal-tar pitch is a relatively easy substance to melt spin into green fiber. This isotropic matrix is forgiving to temperature fluctuations and multiple ranges of spinning speeds[4]. However, the isotropic pitch generally has a lower softening point ( $< 150\text{ }^{\circ}\text{C}$ , mesophase  $> 220\text{ }^{\circ}\text{C}$ ) since the molecular structure of the isotropic pitch consists of lower molecular weight species. This softening point is an important distinction because if it is too low, the fibers are susceptible to fusion during thermal conversion. The softening point can be increased through an oxygen-rich air blowing heat treatment[13], causing the aromatic molecules to cross-link via oxygen linkages. This reaction can be inhibitive to the growth of mesophase. The final isotropic fiber product will not have the required mechanical or thermal properties that are needed to make pitch-based carbon fiber an attractive product for the structural materials market. Mesophase derived carbon fiber, with its high modulus, moderate strength and thermal conductivity, has value for structural composites. Isotropic pitch derived carbon fiber does not, and has been used as activated, chopped carbon fiber and thermal insulation.

Table 1.2 shows a comparison of general mechanical properties for isotropic-based carbon fiber, mesophase-based carbon fiber, and traditional PAN-based carbon fiber<sup>12</sup>.

Table 1.2 Representative properties of carbon fibers from various precursors[2].

<u>Material</u>	<u>Fiber Modulus (GPa)</u>	<u>Fiber Tensile Strength (GPa)</u>
PAN	234	4.8
Mesophase	790	2.6
Isotropic	40	0.6

Brooks and Taylor first observed mesophase (anisotropy) in 1965[12], which was deemed a liquid crystal. Experiments with hot-stage microscopy using polarized light gave them the ability to observe the sequential steps of the liquid crystalline mesophase spheres nucleation, growth, and coalescence. However, if the temperature became too high during these observations, the pitch would form infusible coke. The images first captured by Brooks and Taylor detail the structures of the mesophase within an isotropic pitch matrix[12]. These aromatic self-organizing spherical domains, after the coalescence phase, have two poles which correspond to the ends of the axis of the sphere. These poles are related to the layered structure and the arrangement of the aromatic rings and signify the intersection of the axis of symmetry with the planar sections.

The reason the aromatic sheets would form into spherical domains was presumed to be the mesophase minimizing its interface with the isotropic phase. Brooks and Taylor observed these spheres growing with a high molecular order in the isotropic matrix of the pitch and initially suggested that the underlying molecular structure was tens of aromatic rings in length. They observed during the heat treatment process the spheres coalescing and with appropriate shear formed into a flow field of mesophase, as in Figure 1.7. They also observed that as the mesophase sphere grew, it would be deformed by any insoluble present, such as dispersed coke particles. No insoluble particle was observed in the sphere, only at the interface of the mesophase and the isotropic matrix. This suggested insolubles present in the pitch would prevent further growth of mesophase. Specifically, they observed the growth of mesophase with mica and graphite present. The mesophase remained non-wetting on the mica surface while it thoroughly wetted the surface of the

graphite. This observation is essential to the work of this thesis which will be discussed in section 1.8.

The two most important factors in the growth of the mesophase were temperature and time. The lower temperature at which the spheres were formed was observed to be approximately 400 °C. With increased temperature, the mesophase formed quicker, but the risk of coking the pitch was higher. Upon graphitization, they observed the carbonaceous mesophase spheres would form graphitic structures.

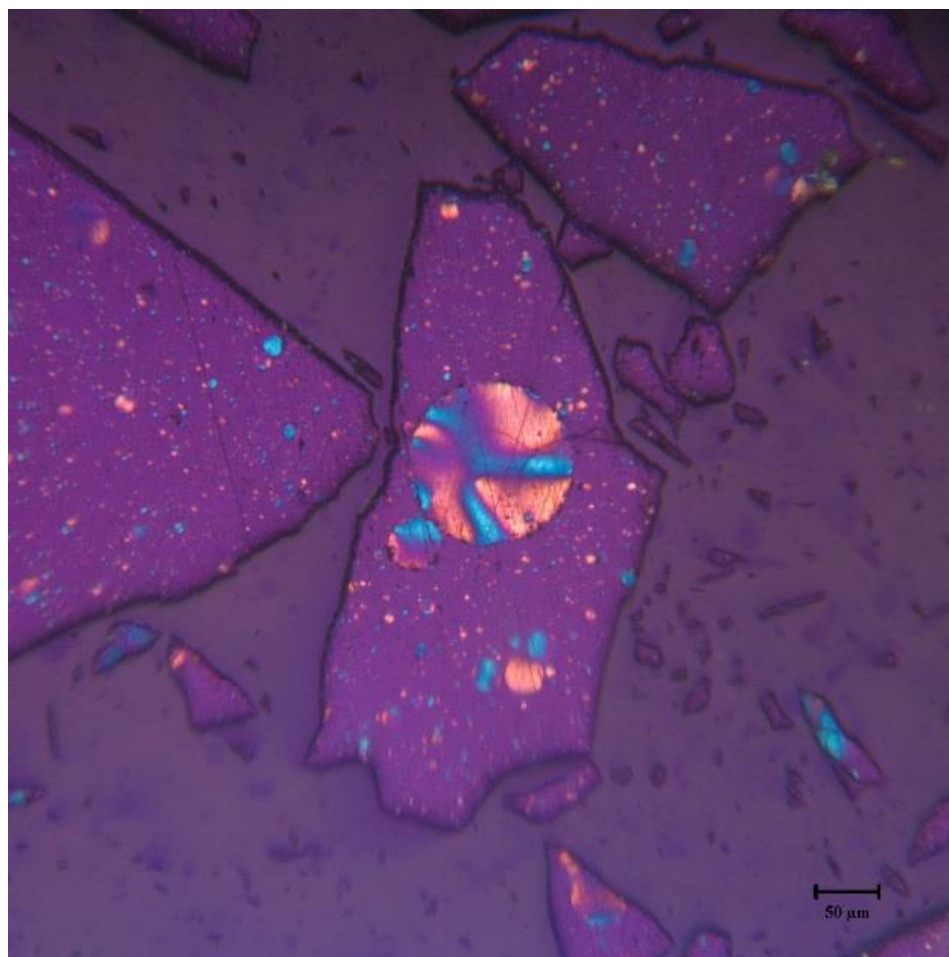


Figure 1.9 Mesophase spheres (magenta and cyan) within an isotropic matrix.

Mesophase pitch exhibits thermotropic and lyotropic properties, meaning the liquid crystalline state can form through heat or addition of a solvent, respectively[14]. Liquid crystals are fluids that have relatively long-range order with the rod-like or disc-

like constituent molecules. A common orientation of liquid crystalline mesophase can be seen in Figure 1.9 where a mesophase sphere is quiescent within an isotropic matrix of pitch.

Although mesophase is considered a liquid crystal, it possesses several differences from traditional liquid crystalline phases. Two-dimensional, planar, PAH formations are the building blocks of the graphitic structure. Generally, the carbonaceous mesophase forms primarily upon heating, although some studies[15] have shown that it may form under specific cooling conditions. Also, the growth of mesophase depends on the liquid crystalline mobility (which is enhanced by shear). The elevated temperatures during the heating process are responsible for molecular arrangement which promotes the growth of the mesogens in two directions, stacking and coalescing, as well as volatilizing the lighter weight species. Therefore, there is a higher concentration of large molecules once heat treatment is complete.

The structure of mesophase pitch has been thoroughly studied by Mochida et al. who proposed mesophase is formed by aromatic rings that stack to allow  $\pi$ - $\pi$  bonding interactions. These aromatic rings are thought to be 0.6 to 1.5 nm in diameter and linked together through methylene bridges giving the molecular structure a weight range of 400 to 4000 amu. It is believed that the alkyl groups contribute to the solubility and fusibility[16] (Figure 1.3).

Through various heat treatments in a nitrogen atmosphere, the volatilization of lower weight species and the polymerization of the aromatic molecules encourages the growth of mesogens into mesophase. The lower molecular weight species allow for the fusibility of the mesophase pitch and act as a solvent by increasing mobility of mesogens; making their interactions more frequent. Therefore, it is important not to be too aggressive during the removal of lightweight species because they are essential in forming a viable mesophase pitch product. It should be noted that petroleum and coal-tar pitch are constituted by thousands of individual molecules and it is tremendously difficult to get an exact molecular model for a given pitch material.

## 1.6 Previous Pitch Improvement Methods

A high carbon content makes the pitch a viable candidate in the production of precursor carbon fiber. However, since the mechanical and thermal advantages are realized with mesophase pitch that requires processing from isotropic pitch, it can be an expensive process. Various methods have been utilized to produce mesophase pitch cheaper and are discussed in this section.

As mentioned by Mochida, the evolution of treatment began with heat-treatment by Otani[17]. Then, Signer et al.[18] and Union Carbide Co. (UCC) effectively produced a mesophase pitch with a softening point below 350 °C by using a vigorous nitrogen flow, with the goal being to remove the low molecular weight, non-mesophase, species which were attributed to the isotropic phase of the material. Using nitrogen and heat was effective for generating mesophase but it was discovered that long, vigorous nitrogen treatments led to the condensation reactions of the low reactive species. These condensation reactions may produce infusible solids in the pitch as well as remove the solvent in which the mesophase forms.

Solvent extraction is another method used to create a viable mesophase pitch. This was proposed by Diefendorf, with support from Exxon, to create a pitch that was more than 75% mesophase[19]. The pitch used was an Ashland A240 isotropic petroleum pitch that was dissolved in 70% toluene-30% heptane mixture, then the separated insoluble pitch was heated to 350 °C at 10 °C/min. This fraction had a softening point of 375 °C. With a further heat treatment at 400 °C for 10 minutes, the pitch was converted to greater than 75% mesophase material and was stated as having less than 25% QIs.

The next evolution in mesophase generation and separation was heat treatment through high-temperature centrifugation. Strehlow was the first to write that the mesophase matrix of the pitch could be separated from the isotropic matrix of the pitch through high-temperature centrifugation. The mesophase fraction is higher density than the isotropic phase fraction causing the mesophase to settle at the bottom of the vessel during centrifugation. This was accomplished with a coal-tar pitch at temperatures up to 525 °C[20].

Further refinement of the pitch improvement process included work by Mochida in using hydrogenation with a catalyst during heat treatment. Mochida discovered that the short alkyl chain groups are essential in maintaining a lower softening point for stable spinning[15]. Mochida was able to achieve a synthetic mesophase pitch by using naphthalene, methylnaphthalene, and ethylene tar as a base product and using HF-BF<sub>3</sub> as the catalyst. This new pitch, called AR mesophase, was said to have very similar properties to heavy oil residues or coal-tar pitch using heat soak methods. Moreover, since the preparation of the mesophase pitch was carried out at lower temperatures (200-300 °C) through polymerization, it prevented the creation of infusible solids. The HF-BF<sub>3</sub> allowed the formation of large polyaromatic ring structures, which made the rapid growth of mesophase possible. The softening point of this synthetic mesophase was approximately 286 °C by a controlled force, Dynamic Mechanical Analysis (DMA) test. This softening temperature allowed the pitch to be melt processed and permitted for a more rapid and stable oxidation process. Therefore, AR mesophase pitch became highly studied, and subsequent research was completed studying its melt-viscosity[21] and spinability[22].

With any pitch improvement method, it is important to assess the percent yield of mesophase and the processability of the improved pitch. The distribution of molecular weight is essential for both isotropic and mesophase pitch to be a melt processible pitch. A method of understanding the molecular weight distribution of the pitch is by dissolving the pitch in a solvent and measuring the insolubles. The insolubles of the pitch dissolved in various solvents (quinoline, toluene, tetrahydrofuran) can be used to get a general understanding of the molecular weight distribution of a pitch. The most common solvent used in understanding the molecular weight and dispersed solids in the pitch is quinoline. There is a sharp distinction between native quinoline insolubles (QIs) and QIs generated through heat treatment. Generally, a pitch with native QIs above 1 wt.% will not be a viable product for fiber spinning because the insolubles make it challenging to form mesophase by inhibiting their growth.

Quinoline is a strong solvent, capable of dissolving high molecular species, while toluene and tetrahydrofuran dissolve smaller molecular weight species. Certain resins



including alpha-resins (quinoline insolubles) – highest molecular weight, beta-resins (quinoline solubles less the toluene insolubles) – moderate molecular weight, and gamma resins (toluene solubles) – lower molecular weights, have been characterized. Beta-resins have been shown to produce mesophase in some studies and are discussed at length by Oberlin[23]. Solvent fractionation methods are used to narrow the molecular weight distribution of pitch and to provide a more homogeneous matrix with similar softening temperatures and flow characteristics. The utilization of solvents to accomplish this makes it an economically unfavorable process, as it would be more cost effective to produce the homogenous material during heat treatment, i.e., without solvents. Additionally, QIs may also be used to estimate the mesophase percentage of pitch after thermal treatments since mesophase is not soluble in pitch.

## 1.7 Fiber Processing

### 1.7.1 Melt Spinning

The treated coal or petroleum pitch can be melt spun into green fibers. Green fibers are simply as-spun pitch fibers which have yet been given any thermal conversion treatment. There are various extrusion methods by which to accomplish this which include using a screw, gas overpressure, or a plunger to force the pitch through a small capillary. For most processes, the operating temperature at the spinnerette is generally 30-40 °C above the softening point of the pitch. For mesophase pitches, molecular alignment of the mesophase with the flow direction occurs in the spinneret capillary during the melt spinning process. This means the choice of a spinnerette capillary diameter and aspect ratio is crucial. D. Edie et al. have conducted extensive studies on mesophase liquid crystalline behavior during spinning[4]. Also, studies have analyzed the viscosity of the mesophase and isotropic pitch[4], [21], [24]–[26]. Isotropic pitch has been shown to follow Newtonian behavior but becomes non-Newtonian (exhibiting shear thinning) once mesophase is formed. The viscosity of mesophase pitch is also highly temperature dependent[4]. Together, a small window of processing temperature results, and is one of the main factors influencing the difficulty of mesophase pitch spinning. Even a small change in temperature of 3.5 °C could cause a 15% variation in diameter of fibers[27], [28]. This temperature dependence can be seen in Figure 1.10 where the two mesophase

itches have a sharp change in viscosity over small temperature changes, which is not the case for the isotropic pitch shown.

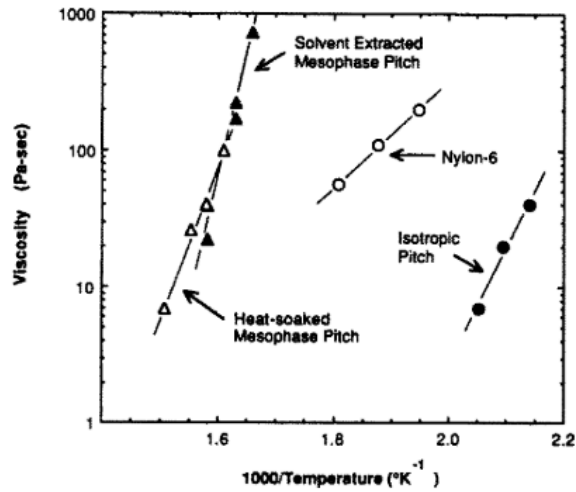


Figure 1.10 Viscosity comparison of isotropic and mesophase pitches. *Reprinted from Carbon, 27(5), Edie DD, Dunham MG, Melt spinning pitch based carbon fibers,647-655, 1989, with permission from Elsevier.*

As mentioned, mesophase is a liquid crystal and the molecular orientation of the pitch green fiber is determined during melt spinning[29] (Figure 1.11). Pitch molecular arrangement is advantageous because, upon heating, PAN chains tend to randomize, while mesophase will retain its alignment – even through the oxidation heat treatment which stabilizes the fibers to render them infusible with its neighboring filament. The spinning capsule, which is a heated chamber where pitch is placed for gas pressure spinning (simple rendering Figure 1.11), can vary the flow characteristics by its shape and therefore the orientation of the pitch during spinning. The orientation of the pitch during spinning can also vary greatly depending on the L/D (length over diameter) ratio and shape of the spinneret capillary. The manipulation of either one of these conditions may result in a drastically different fiber even with the same raw material. The spinneret diameter sizes ranging from 0.15 mm - 0.660 mm and a L/D of approximately 5[30] can produce good mesophase carbon fibers.

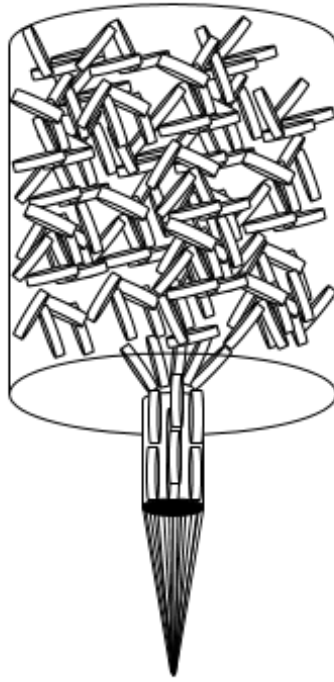


Figure 1.11 The alignment of discotic mesophase during melt spinning.

Achieving a pitch softening temperature below 300 °C (but above 200 °C to prevent fusion during oxidation) is desirable because the spinning temperature must be below approximately 350 °C. The higher the spin temperature, the more reactive pitch will be inside the equipment and with air once it exits the spinneret, which can cause excessive polymerization and pyrolysis that can significantly vary the green fiber. Some of these disadvantages may be addressed by the addition of heated air or nitrogen quench surrounding the fiber as it exits the spinneret. The elevated quench temperature decreases the delta temperature between the ambient air and the spinning temperature[4], thus, decreasing the reactivity of the molten pitch to air.

If insoluble particles are present in the pitch during spinning, they will not melt or deform. These insolubles cause the isotropic or mesophase matrix to behave unpredictably, clog the capillaries, and become embedded in the green fiber. Insoluble particles embedded in fibers, as shown in Figure 1.12, are considered a gross defect that cause the fiber to be generally useless for mechanical applications.

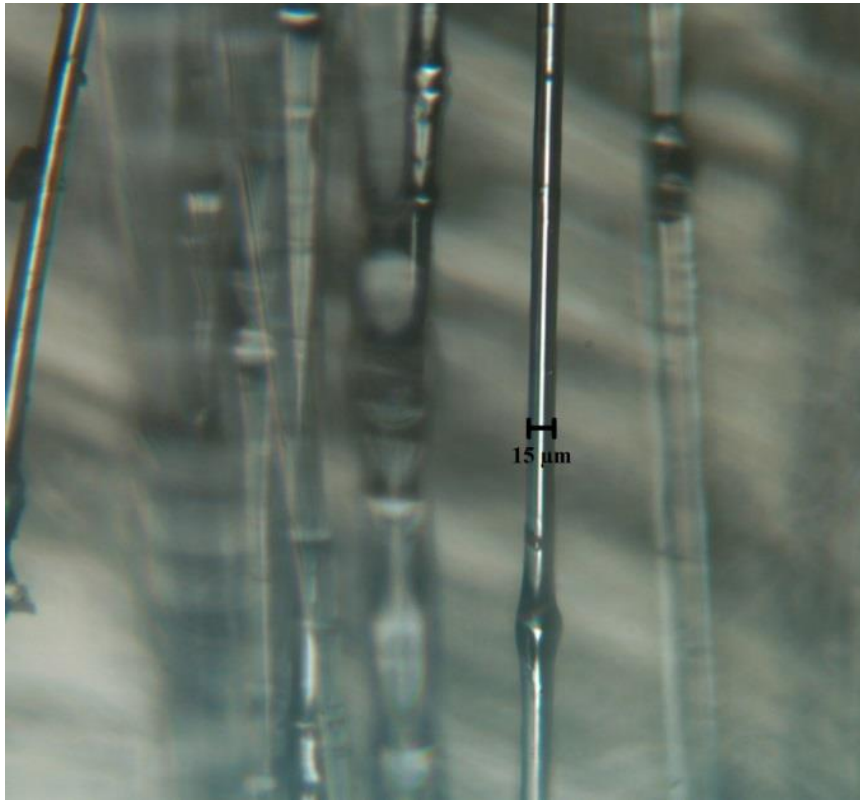


Figure 1.12 Pitch green fiber that has a "bulge" in the fiber most likely caused by insolubles in the pitch. This nodule is a defect in the fiber and yields significantly lower mechanical properties.

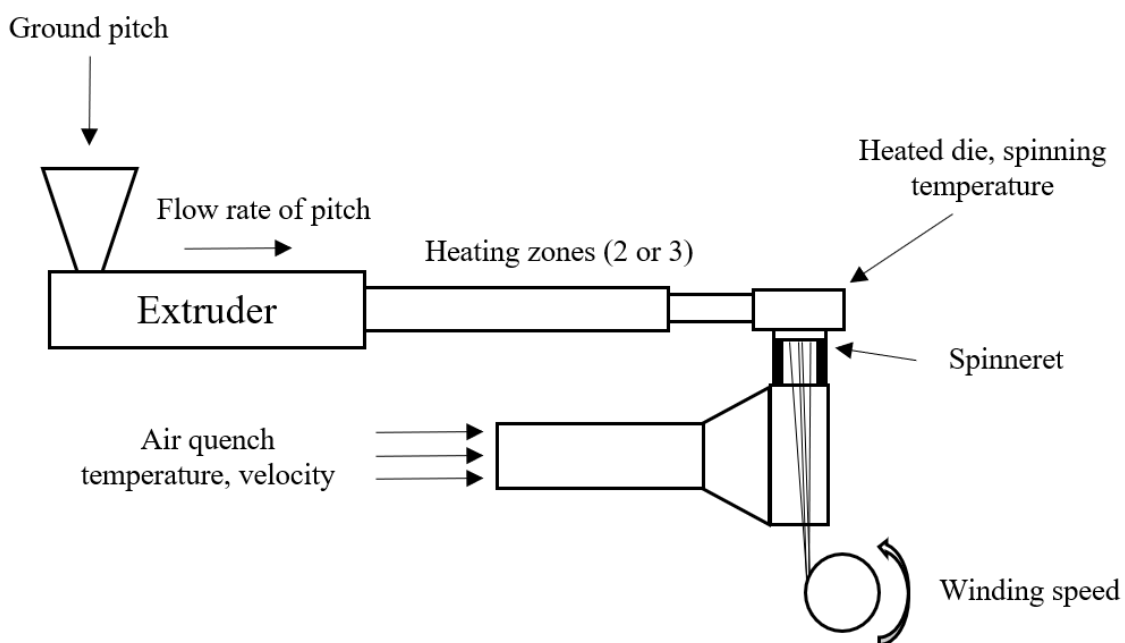


Figure 1.13 Melt-spinning extruder process.

For an industrial operation, continuous fiber spinning by a melt extrusion process is used. A representative melt extrusion process is shown in Figure 1.13. Ground pitch (<1.00 mm pellet) is fed into a hopper where an extruder melts and meters the liquid pitch through a spinneret. The primary variables to control during melt spinning are temperature, extrusion rate (or pressure), spinneret capillary diameter, quench air flow rate, quench air temperature, and winding speed. There are generally four primary temperature zones which need controlling. Three are in the “Heating Zones” portion of the process where the pitch is gradually melted as it travels along the extruder screw. The fourth primary temperature to control is the “Heated die”, which sets the spinning temperature for the pitch and is the last heating zone before the pitch exits the spinneret.

For melt spun fibers, the internal morphology for graphitic mesophase fibers is classified as radial, onion, or random texture, as shown in Figure 1.14. The graphitic sheet stacking is easily seen in all molecular orientations, along with the presence microdomains (subsets of the crystalline region) in the structure. In a study by Mochida et.al[31], the radial and onion-skin textures showed a homogeneous structure. The

benefits of having a homogeneous distribution of orientation with the random fibers are realized during oxidation, carbonization, and graphitization where the fiber should have uniform shrinkage in all directions. The non-homogeneous orientation of the molecular structure of the radial and onion-skin orientations led to non-uniform shrinkage during high-temperature heat treatments. The non-uniform shrinkage can lead to defects and have a significant effect on the mechanical properties of the fibers. The mechanical properties for the different molecular textures can be seen in Table 1.3 with the random texture having the highest tensile strength at 3.6 GPa and radial having the highest modulus at 800 GPa. The main variables affecting the internal carbon fiber texture are the chemistry of the precursor, controlling the flow of the pitch as the precursor fiber is formed, and the tensile forces the pitch is exposed to while spinning. Controlling the flow includes the capillary shape of the spinneret and the temperature of the spinneret. As the temperature increases, these textures have been shown to form in order of lower temperature to a higher temperature: onion-skin, random, radial-folded, radial, radial with open-wedge[27] (sometimes referred to as ‘pac man’ shaped fibers).

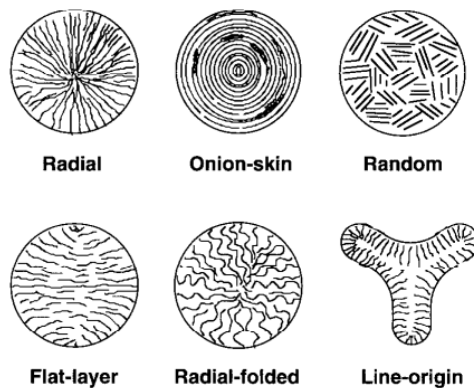


Figure 1.14 Internal morphology for graphitic mesophase fibers, classified as radial, onion-skin, random, flat-layer, radial-folded, and line-origin. *Reprinted from Carbon, 36(4), Edie DD, The effect of processing on the structure and properties of carbon fibers,345-362, 1998, with permission from Elsevier.*

Table 1.3 Mechanical properties of graphitized fibers with various textures. Diameter ( $\emptyset$ ), tensile strength (TS), Young's modulus (E), compressive strength (CS). *Reprinted from Carbon, 36(4), Edie DD, The effect of processing on the structure and properties of carbon fibers, 345-362, 1998, with permission from Elsevier.*

<u>Texture</u>	<u><math>\emptyset</math></u> ( $\mu\text{m}$ )	<u>TS</u> (GPa)	<u>E</u> (GPa)	<u>CS</u> (GPa)
Radial with open wedge	11.0	2.8	740	-
Skin Radial-core random	8.1	3.4	800	0.4
Random	9.2	3.6	780	0.7
Quasi-onion	10.4	2.6	720	-

### 1.7.2 Oxidation

Oxidation is a process that introduces oxygen to diffuse through the fibers and react to crosslink PAHs, dramatically increasing the softening temperature such that the filaments are infusible upon further heating and carbonization [8]. This process can be a difficult task for pitch fibers that require 1-24 hours to complete because the fibers are susceptible to fusion. Generally, this process begins with no tension on the fibers with a temperature of 100-150 °C, then the temperature gradually increases to a range of 300-400 °C. The higher the softening point of the treated pitch, the faster the rate of temperature increase may be during oxidation without inter-filament fusing. For lower softening point fibers (< 200 °C) the oxidation process could span days to ensure the fibers do not re-soften and fuse. Therefore, it is essential the softening temperature of the pitch be closer to 300 °C for pitch fibers to be economically practical for an industrial process where the oxidation process needs to be less than a couple hours.

### 1.7.3 Carbonization and Graphitization

After the pitch fibers have been stabilized to prevent fusing, the carbonization process is analogous to the PAN fiber carbonization process with the exception, again, that pitch fibers do not require tension. The goal of this process is to introduce the stabilized fibers to an inert environment at temperatures 900-1200 °C for many minutes. The carbon yield of pitch fibers is generally 70-80 wt% of the precursor green fibers. With mesophase fibers, the mechanical and thermal property advantages are realized

once the fibers are graphitized. During thermal conversion at temperatures of 2300-2700 °C for many minutes, the graphite crystalline structure is formed[8].

The graphite structure that is formed during graphitization gives the mesophase derived fibers excellent strength and rigidity as well as attractive thermal properties. The graphite layers formed by carbon-carbon double bonds expand in-plane to give the graphite layer a direction. These layers are stacked together through weak Van Der Waals bonds and give the layers an AB stacking sequence. This stacking sequence can be seen in Figure 1.15 and Figure 1.16 where the advantageous properties are ‘in-plane’, not ‘through-plane’.

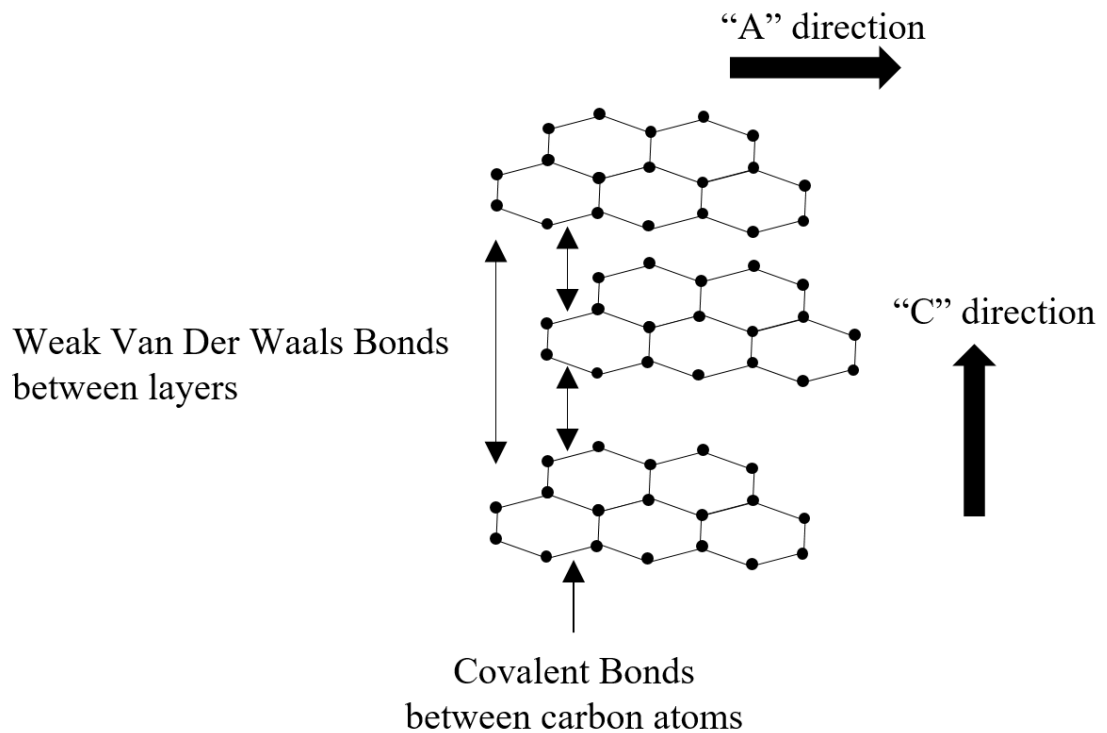


Figure 1.15 Graphite AB structure. Basal plane view showing the AB stacking offset.



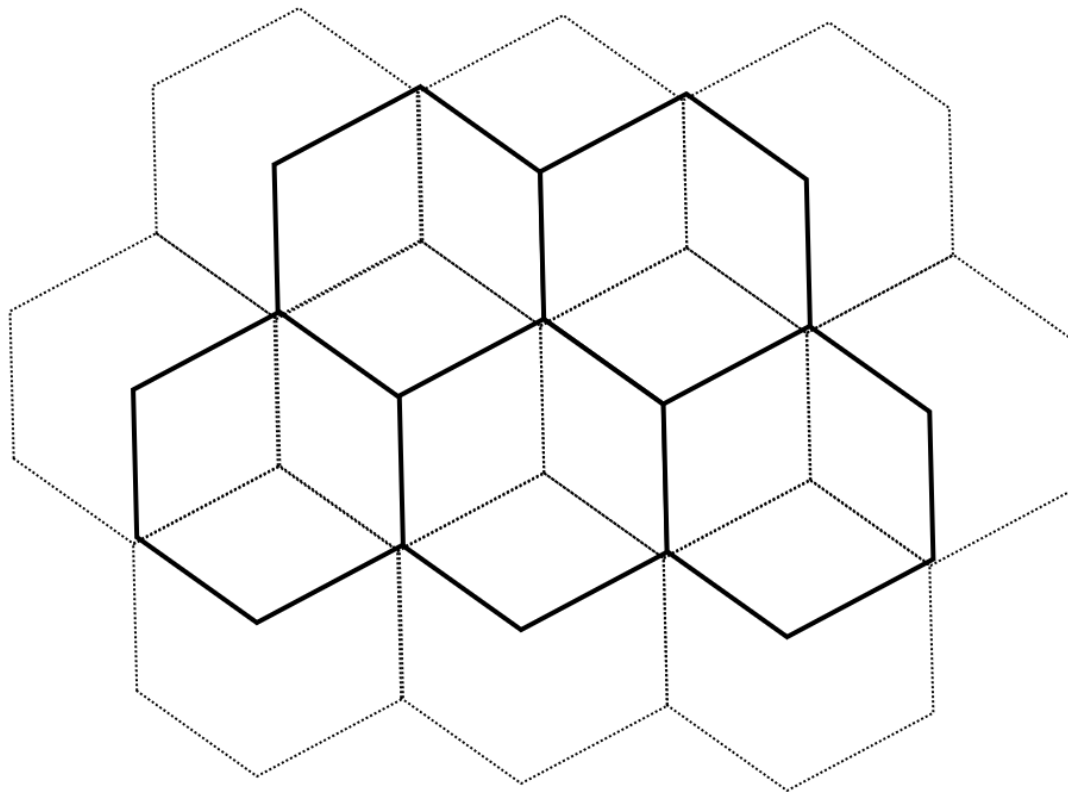


Figure 1.16 Top view of graphite AB stacking. The A plane is a solid line and the B plane is a dotted line.

This graphite crystal is not realized in isotropic pitch derived fibers because they do not possess discotic mesogen molecules (capable of forming into graphitic layers upon high heat treatment). Therefore, isotropic fibers have low strength, low modulus, and low thermal conductivity and are only useful for general fiber applications where mechanical properties are not essential.

Graphene, which is the base structure of graphite with no basal edges (1 layer) is similar to the desired mesophase and subsequent graphitic structure in graphitized fibers. However, pure graphene is difficult and expensive to produce. Therefore, an effective way to produce nearly pure graphene is to use graphite, which is readily available, that is oxidized to produce graphite oxide. Then, exfoliation in a solvent by sonication is used to break the 3-dimensional structure of graphite oxide to single layered graphene oxide

(GO). The GO can then be reduced to produce nearly pure graphene, which is called reduced graphene oxide (rGO).

## 1.8 Conclusion

Recent economic factors have rekindled interest in pitch as a favorable candidate to produce carbon fibers. The goal of producing low cost pitch-based carbon fiber requires the large-scale production of mesophase pitch from which high modulus and high thermal conductivity carbon fibers are derived. Mesophase pitch production is an energy intensive process and needs significant optimization before pitch fibers can reach more of the carbon fiber market. A process that can simplify and reduce the processing time for the growth of the mesophase will commensurately increase carbon fiber production efficiency.

As mentioned before, the energy barrier of mesophase formation can be high and take up to one day[32] for the sufficient formation of mesophase. Therefore, the addition of a catalyst to decrease the activation energy required for the formation of mesophase could drastically improve the time required for the formation of mesophase. If a catalyst is added to the isotropic pitch to facilitate mesophase growth, its effect as a quinoline insoluble in pitch and therefore its influence on the melt spinning process is of chief concern. Consequently, the catalyst used to promote the growth of mesophase would need to be indistinguishable in the mesophase spheres. As seen with the Brooks and Taylor experiments with hot-stage microscopy, as the mesophase coalesced, it was deformed by insoluble particles (e.g. mica) present in the isotropic matrix. However, when graphite was present within the isotropic matrix, the mesophase spheres readily wetted the surface of the graphite. This observation suggests mesophase growth and coalescence may be accelerated with a graphite-like structure present that resembles the mesophase structure.

With this conclusion milled graphite would be a candidate to disperse in pitch to promote the growth of mesophase. However, the large surface area of the milled graphite relative to the aromatic ring structure of mesophase would limit the sites upon which

mesophase could nucleate. Additionally, the milled graphite which has basal edges is a large insoluble in pitch and could become embedded in the fiber during melt spinning. This insoluble embedded in melt spun fibers cause mechanical properties to drastically decrease and can even prevent the formation of fibers. Therefore, the nucleation site must be small enough not to interfere with melt spinning but still resemble the molecular structure of graphite. Graphene is an attractive candidate as a seed crystal (catalyst) to provide a nucleation site where mesophase growth would readily occur and is small enough to be soluble in the pitch. This is because the structure of graphene is similar to the desired mesophase and subsequent graphitic structure in graphitized fibers.

In this study, the efficacy of dispersed graphene (as rGO), in the isotropic parent pitch, to serve as a nucleation site for the accelerated growth of mesophase will be investigated.

The results will be discussed and quantified by systematic thermal treatment experiments with a petroleum and coal-tar derived isotropic pitch. This hypothesis stems from the work by Brooks and Taylor[12] which showed that mesophase tended to wet graphite.

The specific questions studied in this thesis are;

1. Determining if graphene influences the growth of mesophase in an isotropic petroleum and coal-tar pitch
2. If the addition of graphene influences the processability of the created mesophase pitch into carbon fibers (melt spinning, thermal conversion)

Furthermore, the thermally treated pitch (with and without the use of graphene) will be melt spun into precursor green fiber. The green fiber will be graphitized to determine mechanical properties and the structure analyzed by scanning electron microscopy (SEM) and the effects of graphene on the final graphitized fibers will be evaluated.

## Chapter 2. GRAPHENE AS A SEED CRYSTAL FOR MESOPHASE DEVELOPMENT

### 2.1 Introduction

The ease of processing needs to be considered when attempting the difficult task of promoting the growth of mesophase within isotropic pitch. Therefore, heat treating, which was the most straightforward method to transition an isotropic pitch to a mesophase pitch, was used in the following experiments. For the purposes of this study, heat treatment refers to heating pitch to a specific temperature in an inert atmosphere while introducing shear, by nitrogen sparging, to the molten pitch. Nitrogen sparging created an inert atmosphere to help prevent the polymerization of pitch at higher temperatures while the flow of nitrogen directed into the molten pitch introduced shear by bubbling and mixing the molten pitch. The goal of the heat treatments was to create a thermodynamically favorable environment that encouraged the arrangement of the PAHs present in the isotropic pitch into stacked layers of PAHs, which is the base structure of mesophase. Stacking of the aromatic structures occurred because this was a lower energy state for the molecules and happened readily because the high-temperature environment allowed the PAHs to become more mobile. The shear increased the chances of the aromatic structures becoming aligned into stacked layers.

The two main challenges of using graphene as a seed crystal were: reducing graphene from graphene oxide (GO) and using efficient method to disperse graphene homogeneously throughout the pitch. For this study, microwave reduction of graphene oxide was used which excites the functional groups of the GO to break bonds with the aromatic rings then quickly form new bonds. The newly bonded compounds were then off-gassed from the microwave[33]. The dispersion of the rGO was conducted by sonication in a pitch: tetrahydrofuran (THF) mixture which allowed the rGO to be dispersed homogeneously throughout the pitch.

To test the efficacy of the rGO as a seed crystal, milled Mitsubishi AR was also tested as a nucleation site. To test the effect of THF insolubles present in the pitch, a heat

treatment experiment was conducted with insolubles removed from the pitch: THF: rGO mixture by centrifugation.

## 2.2 Experimental Materials and Methods

### 2.2.1 Materials

An isotropic petroleum pitch and an isotropic coal-tar pitch were used for the heat treatments. The graphene oxide (GO) was supplied from Apply Nano Solutions out of Alicante, Spain. Initial softening points of the pitches were approximately 100 °C for the coal-tar pitch and 110 °C for the petroleum pitch as determined by Dynamic Mechanical Analysis (DMA). The coal-tar and petroleum pitch had QIs of 0.36 wt.% and 1.00 wt.%, respectively and showed excellent spinnability as a baseline, isotropic pitch.

### 2.2.2 Experimental Methods

For each of the base pitches, two concentrations of rGO were examined, 0 wt.% (baseline), 0.01 wt.% and 0.10 wt.%. These weight percentages were chosen to determine if the added rGO nucleated the mesophase at a very small concentration (0.01 wt.%) and a relatively higher concentration (0.10 wt.%). Additionally, a mesophase pitch was tested as a seed crystal to determine the novelty of using rGO (section 2.2.5). Five treatment times were chosen to study the effect of mesophase formation with rGO as compared to the mesophase formation of the base pitches. The test matrix is shown in Figure 2.1.

Pitch	Treatment Time (hr)	rGO wt.%		
		0	0.01	0.10
Coal-tar	0.5			
	1			
	2			
	3			
	4			
Petroleum	0.5			
	1			
	2			
	3			
	4			

Figure 2.1 Test matrix followed for testing rGO in coal-tar and petroleum isotropic pitch. Each treatment time and rGO wt.% were replicated at least once leading to 60 separate thermal treatments.

The example test matrix shows the plan for a 30-test experiment with at least one replication for each wt.% and treatment time, leading to a total of 60 individual experiments. All processing parameters for the heat treatments such as treatment set temperature, treatment time, nitrogen flow rate, and pitch: solvent ratio remained constant except for the addition of rGO.

Graphene oxide was reduced using microwave energy before dispersion in the parent pitch and subsequent thermal treatments[34]. For the 0.01 wt.% and 0.10 wt.% concentrations, the GO was reduced by placing 0.25-0.50 g of GO in a 250 ml beaker with fiberglass covering the opening of the beaker, inside a 1200 W microwave for one minute. This reduction was done immediately before the pitch-THF mixture was placed on the hotplate. The masses of the GO and reduced GO (rGO) were recorded to quickly ensure reduction, with an average mass loss of 15 wt.%.

The pitch preparation and treatment method were as follows. For all samples, a 500 ml beaker was tared on a scale and 20 g of coarsely ground pitch was added. The solvent: pitch ratio of 1 g: 10 ml was used, therefore 200 ml of THF was added in the

beaker and the beaker was placed on a hotplate. A one-inch long magnetic stirrer was placed in the beaker and set to 50 RPM and the temperature was set to 50 °C to ensure the pitch dissolved in the THF. The rGO was added to the pitch-THF mixture once it was placed on the hotplate. A watch glass covered the top of the beaker to prevent evaporation of THF. A k-type thermocouple placed on the heating surface on the hotplate was monitored by a portable digital thermometer to verify the temperature of the hotplate. The pitch was left to dissolve for 2-hours.

After 2-hours of magnetic stirring on the hotplate, the mixture was then sonicated continuously at room temperature. A Fisherbrand™ Model 505 Sonic Dismembrator was used for two hours at 15% power to give a homogeneous dispersion of the rGO, also with magnetic stirring (one-inch magnetic bar). The beaker of pitch-THF-rGO was placed in ice during sonication to help prevent the evaporation of THF. The mixture was transferred to a 500 ml three-neck flask where a THF flush of the beaker was used to ensure all pitch-rGO was removed from the beaker. The 500 ml flask was then placed in a Brisk HM0500MC1™ mantle heater with a k-type thermocouple placed between the bottom center of the flask and the mantle heater. A second k-type thermocouple 0.125-inch probe was placed through the center neck of the flask and positioned near the bottom of the pitch-THF-rGO mixture to monitor the temperature of the mixture during processing. The temperature was controlled using a PID controller by monitoring the mantle temperature which was set to 425 °C for all samples in an attempt to achieve a pitch temperature of 370 °C. Temperatures were logged using a Graphtec GL240 data logger at a sampling rate of 1-point/sec.

The nitrogen was supplied through a rubber bung into a stainless-steel tube that was placed near the bottom of the pitch-THF-rGO mixture to ensure sparging throughout the entire heat treatment process. The arrangement can be seen in Figure 2.2. The stainless-steel tube for nitrogen and the pitch thermocouple were placed a few inches apart to help prevent error in the temperature readings. Prior to beginning the heat treatment, the THF was evaporated from the pitch by setting the mantle temperature to 100 °C and condensing the THF in a connected flask placed on ice. Once the majority of

the THF appeared to have evaporated from the pitch, the controller was set the 425 °C for the thermal treatment.

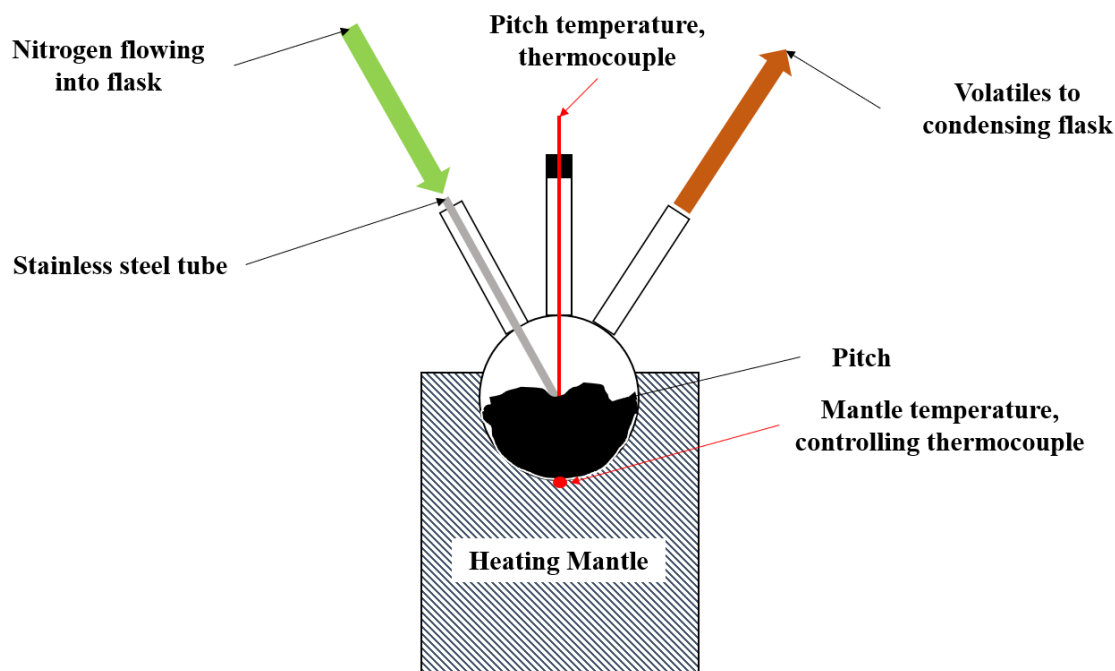


Figure 2.2 Thermal treatment arrangement.

### 2.2.3 Temperature Control

With mesophase being a thermotropic liquid crystalline material, the temperature control during heat treatment was an important factor. The goal of the heat treatment experiments was to set the pitch to a consistent and repeatable temperature of approximately 370 °C for all heat treatments. Two options were explored to determine the best method to control the temperature of the pitch. Using a mantle heater, the temperature was controlled by a k-type thermocouple placed under the treatment flask to set the temperature of the mantle. Additionally, a 12-inch, 0.125-inch diameter k-type thermocouple probe was placed in the pitch to control the treatment temperature, as in Figure 2.2. Logging the temperature showed that controlling the temperature by the mantle thermocouple produced a less variable treatment temperature and was closer to the desired temperature of 370 °C throughout the run. The variation in the pitch-controlled thermocouple run was from the lag of the controller relay turning on, then



turning on the heating mantle, and finally the time to get the pitch to the set point. With a mantle temperature of 425 °C, the pitch reached the desired temperature of approximately 370 °C more consistently than a pitch-controlled temperature set to 370 °C. These results can be seen in Figure 2.3, where the variation in temperature for the pitch-controlled sample was significantly larger than the variation in the mantle-controlled temperature.

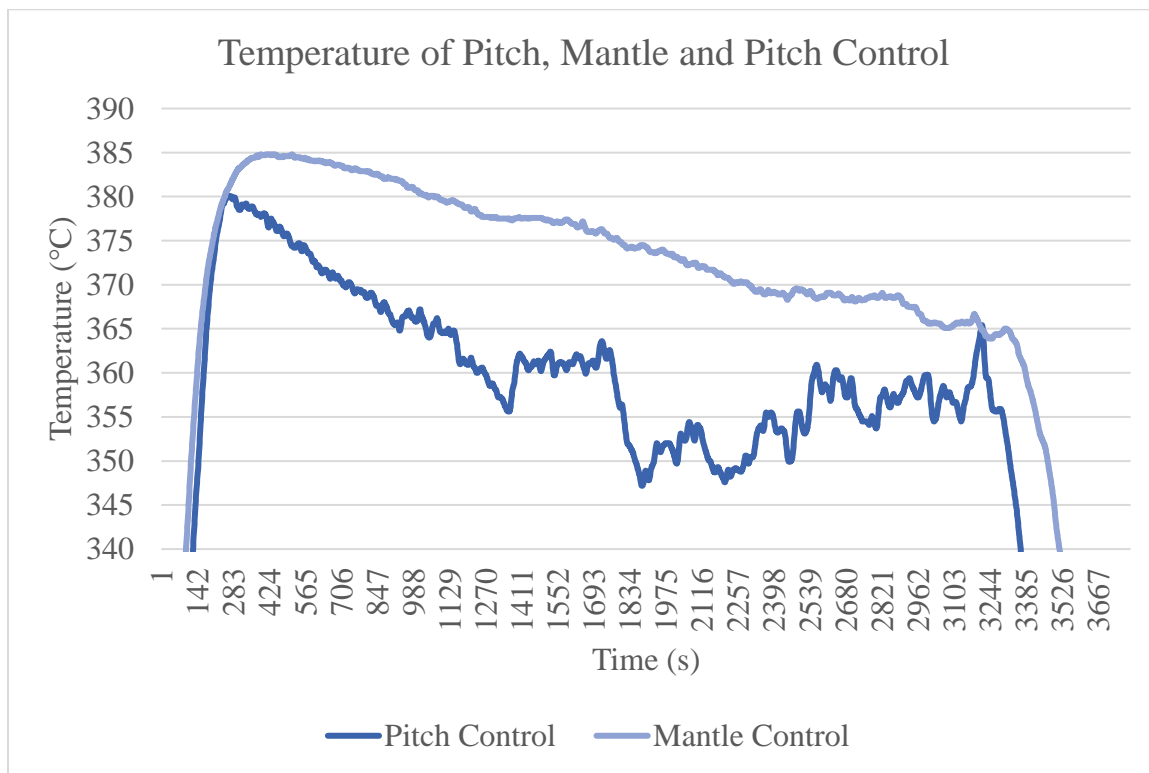


Figure 2.3 A comparison of the pitch temperature during heat treatments with the temperature being controlled by the pitch thermocouple or the mantle thermocouple.

### 2.2.3 Heat Treatment

As previously stated, the goal was to create a thermodynamically favorable environment for the aromatic structures of the pitch and rGO to align and build larger polyaromatic structures. To accomplish this, nitrogen sparging was conducted in a 500 ml flask placed in a mantle heater set to a temperature of 425 °C. This mantle temperature was controlled by a PID controller and led to a pitch temperature of approximately 370 °C. The difference between the mantle temperature and pitch temperature was due to the heat losses

caused by the volatiles being removed from the pitch. These reactions led to difficulty in having a precise temperature for some heat treatments.

The thermal treatment lasted for 0.5, 1, 2, 3, and 4-hours, while the mantle was held isothermally at 425 °C, with a nitrogen flow rate of 30 l/hr (STP). The volatiles were condensed in a connected flask that was cleaned after each run by heating the flask to 500 °C for multiple hours in air. Additionally, insulation was wrapped around the treatment flask to prevent the loss of heat during treatments. Once the heat treatment was complete, the flask air cooled to room temperature with the flow of nitrogen continuing throughout the entire heating and cooling process. Then the pitch was removed from the treatment flask and weighed for mass loss.

#### 2.2.4 Insoluble Testing

The primary insoluble metric of interest was quinoline since it was the most widely reported insoluble in the literature and can be compared to the parent isotropic pitch QIs. To determine the quinoline insoluble portion of the heat-treated pitch, the following method was used and repeated in triplicate for each sample. Approximately 0.5 g of pitch was placed in a 50 ml beaker and quinoline was added with a pitch:solvent ratio of 1 g:20 ml. If the sample proved too difficult to filter because of a high concentration of insolubles, the test was repeated with a 0.25 g of pitch. The pitch-quinoline mixture was placed on a hot plate set to temperature of 120 °C for at least 1-hour with a watch glass to prevent evaporation of the solvent. The mixture was stirred every 15 minutes to help prevent pitch from adhering to the flask. The carefully pre-dried filter to be used for filtration was weighed in order to calculate insolubles. Using vacuum filtration system with a 0.7  $\mu\text{m}$  pore size borosilicate glass filter, the hot pitch-quinoline mixture was poured over the filter. Additional quinoline was used to rinse the 50 ml beaker and rinse the walls of the vacuum filter apparatus. Once the bulk of quinoline had been filtered, THF was used to further displace the quinoline from the pitch. This THF rinse was essential because of the high boiling point of quinoline, it is difficult to remove from the pitch by using only heat. After the THF rinse, the vacuum was left to filter for an additional 5-minutes. Then the filter with the quinoline insoluble pitch was placed in a small aluminum pan and placed on a hot plate

set to 100 °C to evaporate any remaining THF. After at least 2-hours the filter and pitch were weighed to calculate insolubles using equation 2.1.

$$QI (\%) = \frac{(Filter\ final\ mass) - (Filter\ initial\ mass)}{Pitch\ initial\ mass} \times 100 \quad [2.1]$$

### 2.2.5 Dynamic Mechanical Analysis (DMA)

Softening points were determined by using a TA Q800™ DMA with a compression clamp. A controlled force program was used to provide a constant force of 0.1 N applied to a small pellet of pitch while the temperature ramped from 25 °C to 450 °C at a rate of 5 °C/min. Once the pitch sample yielded (softened to liquid-like viscosity), the run was automatically stopped. To determine the softening temperature, the derivative of displacement with respect to temperature was plotted. Figure 2.4 shows a graphical representation of the DMA softening point test with the softening temperature marked.

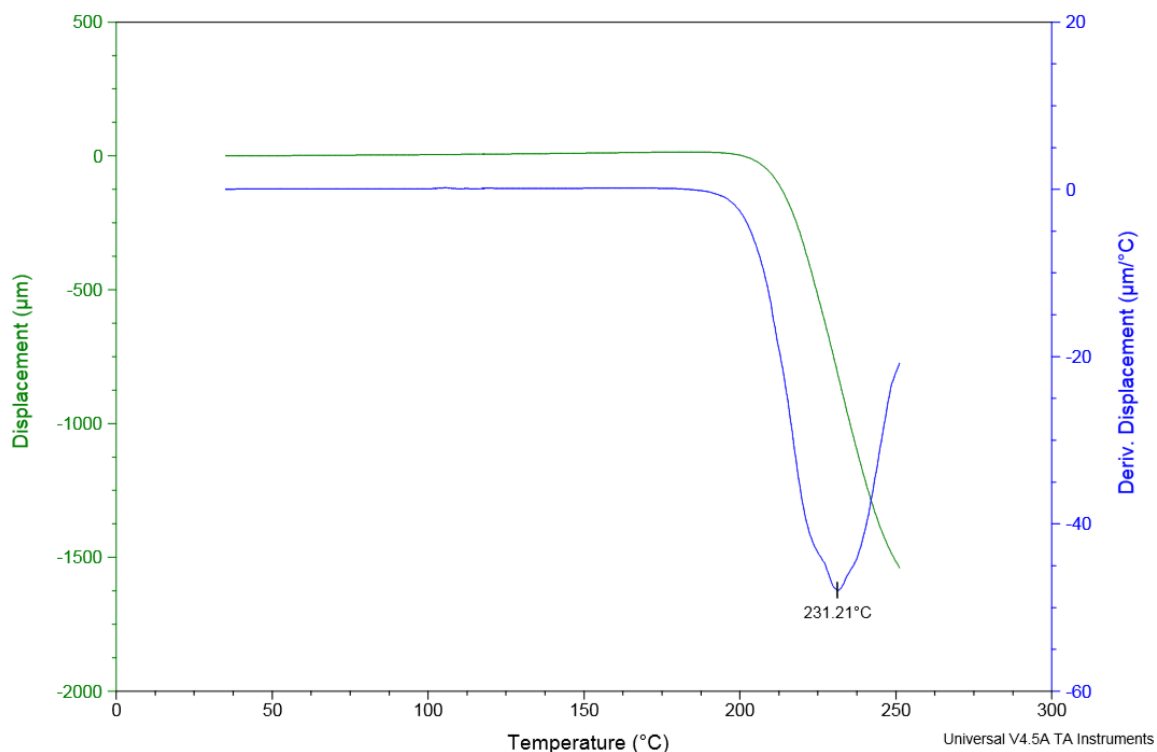


Figure 2.4 Example of a DMA analysis to determine the softening temperature of a pitch. The derivative of displacement with respect to temperature is plotted and the peak of this curve is representative of the softening temperature.

### 2.2.6 Polarized Light Microscopy

To determine the mesophase percentage of a sample ASTM 4616-95, Standard Test Method for Microscopical Analysis by Reflected Light and Determination of Mesophase in Pitch, was used. Approximately 1 g of the treated pitch was coarsely ground, mixed with a small amount of epoxy from Pace Technologies™ (ULTRA-3000R-128-resin and ULTRA-3000H-32 hardener), and then placed in a Leco® 25 mm mold. Additional epoxy was poured on top of the pitch: epoxy mixture for the “puck” to be polished in a Buehler EcoMet 3000™ with an AutoMet 200™ attachment. This epoxy-pitch “puck” cured in a convection air oven set to 50 °C for at least two hours. The “puck” surface was polished with five subsequent steps with tap water using 240 grit, 400 grit, and 600 grit sandpaper. The final two polishing steps were with a Buehler Ultrapol™ pad using 3-micron alumina slurry and a Buehler TexMet™ pad with a 0.05-micron alumina slurry. The samples were rinsed with tap water and patted dry with a cloth. An example of the final product is shown in Figure 2.5.



Figure 2.5 Example of a polished “puck” of pitch inside an epoxy. This “puck” was used for polarized light microscopy to determine the mesophase percentage of the heat-treated pitch. Puck was 1 inch in diameter.

The results of the polarized light optical microscopy analyses allowed for the designation of a volume % mesophase content within the pitches. This volume percentage was calculated by completing a 1000-point count of pitch on each puck and tallying a yes or no if mesophase was present, excluding the presence of epoxy. The 21-point reticule on the Leitz microscope was used as a marker for the yes/no tally. The mesophase was calculated by using equation 2.2.

$$\text{Percent Mesophase} = \frac{\text{Mesophase Counts (yes)}}{1000 \text{ (total counts)(yes and no)}} \times 100 \quad [2.2]$$

## 2.3 Results

### 2.3.1 Petroleum Pitch

The mesophase percentages per sample were averaged for each treatment time and the results comparing the three rGO wt% for the petroleum pitch are shown in Figure 2.7. As previously mentioned in section 2.2.2, the goal was to determine if the added rGO nucleated the mesophase at a very small concentration (0.01 wt.%) and a relatively higher concentration (0.10 wt.%).

The temperature controlling method stated in section 2.2.3, was to minimize the variation in the average temperature of the pitch once it reached treatment temperature. While this did lead to a decreased variation in treatment temperatures, there was still some variation in the temperature most likely due to the manual placement of the thermocouples and the endothermic volatilization. Since the formation of the mesophase was sensitive to the treatment temperature, when analyzing the results and averaging the mesophase percentages across all samples with replication, some error occurred.

The logged temperature of the pitch was used to determine the average temperature of the pitch once it reached the mantle set-point temperature of 425 °C until the controller cut power to the heating mantle and cooling began. The plot of the average pitch temperature of each petroleum heat treatment can be seen in Figure 2.6. The average temperature and mesophase percentage relationship do not appear to favor a specific sample. Table 2.1 shows the average temperature for all samples at each treatment time. The pitch temperature generally reached a maximum temperature towards the beginning of the run, then slowly decreased as the run progressed. Therefore, the longer the treatment time, the lower the average temperature tended to be. Even though the pitch temperature goal was 370 °C, after 0.5-hours, it was difficult to attain.

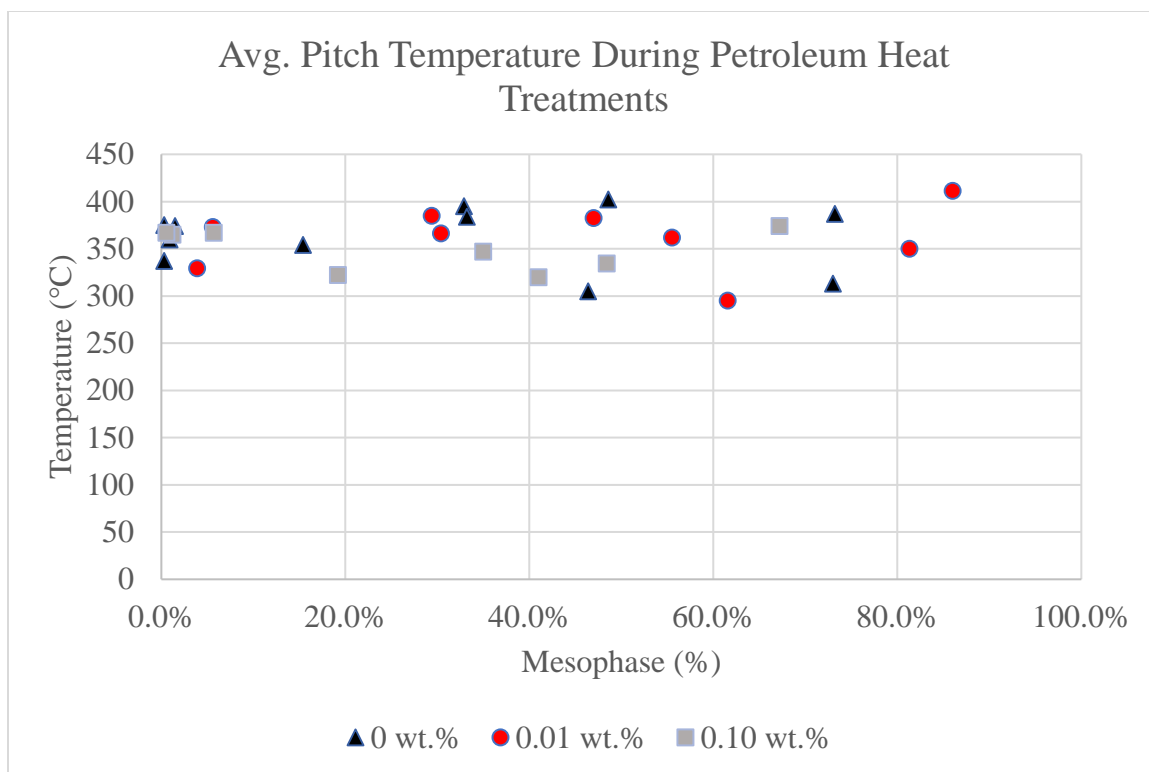


Figure 2.6 The average temperature of the pitch during the heat treatment for every petroleum pitch sample tested.

Table 2.1 Average temperatures at each treatment time with deviation.

<u>Treatment Time (hr)</u>	<u>Avg. Temp (°C)</u>	<u>Std. dev. (°C)</u>
0.5	373	16
1	351	28
2	357	33
3	355	27
4	338	27

This deviation in temperature was reflected in the deviation of mesophase percentage for the samples as seen in Figure 2.7. The largest mesophase deviation was with the 1-hour sample. When analyzing the results with the deviation in temperatures, the sample weight percentages of rGO that were tested suggest that rGO was beneficial for accelerating mesophase nucleation at 0.01 wt.%, especially at 2-hours. However, the rGO does not appear to assist in the nucleation of mesophase at 0.10 wt.% rGO. The largest differences in mesophase growth after nucleation appear at treatment times of 0.5,

1, and 2-hours. Then it appears that all the samples begin to slow in the rate of mesophase growth from 3 to 4-hours.

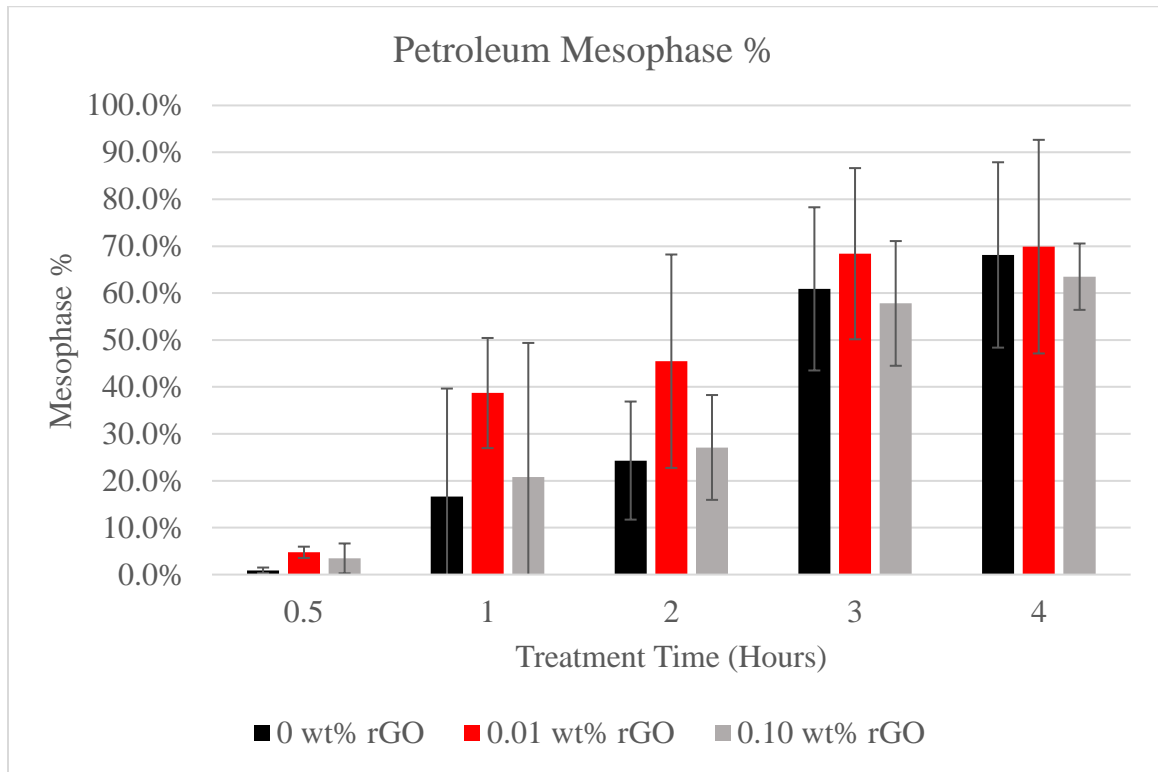


Figure 2.7 Petroleum mesophase percentage as determined by polarized light microscopy. Three samples were tested at three rGO weight percentages: 0 (baseline), 0.01, and 0.10.

To decrease the deviation in average temperatures to determine if the results were a function of temperature rather than rGO, samples with closer average temperatures were compared but this comparison removes the replication of each rGO wt.%. Table 2.2 list the average temperatures and the reduction of the deviation in temperatures. The mesophase percentages with closer related average temperatures, i.e. less deviation, is shown in Figure 2.8. With less deviation in the temperatures, it appears that the effects of rGO at 0.01 wt.% become more pronounced. The treatment time that had the smallest deviation in temperature is shown in Table 2.3. With a deviation of approximately 2 °C, the 0.01 wt.% sample had significantly more mesophase at 5.6% than the 0 wt.% and 0.10 wt.% at 0.9% and 1.2%, respectively.



Table 2.2 Comparing rGO wt.% with closer average temperatures. Target temperature was 370 °C.

<u>Treatment Time (hr)</u>	<u>Avg. Temp (°C)</u>	<u>Std. dev. (°C)</u>
0.5	362	2
1	336	12
2	339	31
3	377	23
4	323	13

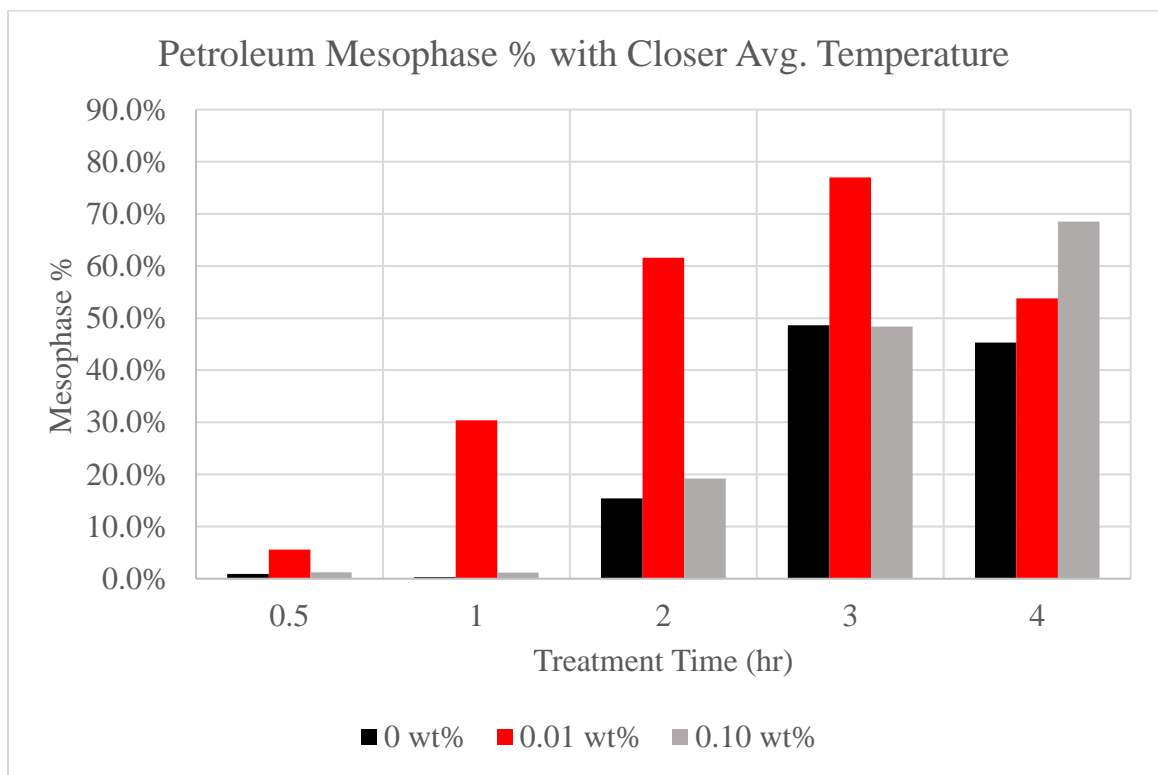


Figure 2.8 The mesophase percentage compared with less deviation in the average temperatures.

Table 2.3 Comparison of mesophase percentages for the 0.5-hour treatment samples that had the smallest deviation of average pitch temperature.

<u>rGO %</u>	<u>Treatment Time (hr)</u>	<u>Avg. Pitch Temperature (°C)</u>	<u>Mesophase %</u>
0	0.5	360	0.9
0.01	0.5	362	5.6
0.10	0.5	365	1.2

The highest difference in mesophase percentages occurred within the first 2-hours of heat treatment. With the dispersed rGO in the pitch, there were more opportunities for the mesophase to form because of the available PAHs nucleation sites. This suggests that the rGO at 0.01 wt% accelerated the overall mesophase growth by being a nucleation site. For all samples, it appeared that the growth of mesophase begets more mesophase. Therefore, with more mesophase initially, the 0.01 wt% sample can generate mesophase at a faster rate. Once the nucleation sites matured in the growth of mesophase, the rate of growth for the 0.01 wt% rGO sample more resembled a non-rGO sample as seen in the 3-hour and 4-hour treatment times.

As mentioned in section 2.2.6, polarized light microscopy was conducted on a Leitz microscope following the procedure outlined in ASTM 4615-95. Using a 20x air objective, 1000-points were counted for each puck to determine the mesophase percentage using a zig-zag pattern. Figure 2.9 shows the polarized light analysis of the base pitch petroleum product. No anisotropy (mesophase) was visible with the rotation of the analyzer or the rotation of the stage.

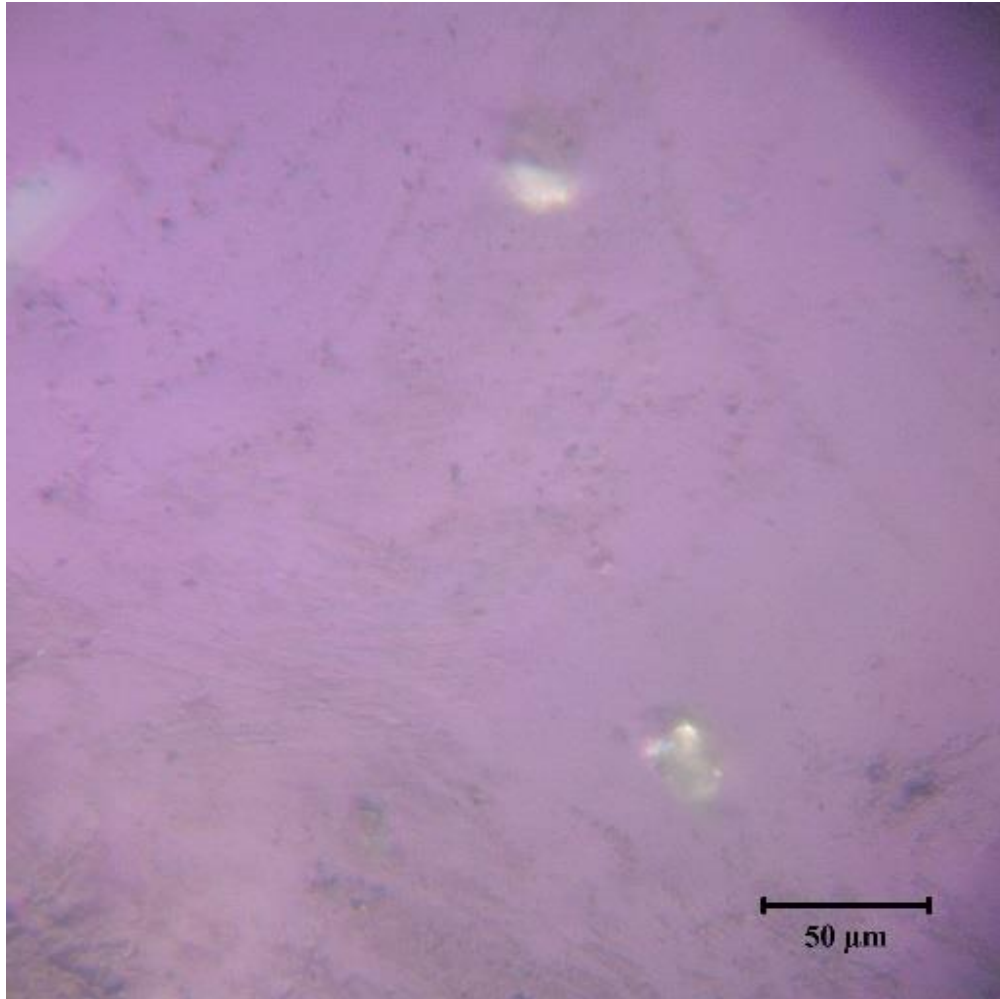


Figure 2.9 Isotropic petroleum-based pitch under polarized light. No mesophase content is present. The two white dots are epoxy.

When the heat-treated samples were analyzed under the polarized light, the mesophase content appears in tones of bright cyan, yellow and magenta, while the isotropic pitch matrix (and isotropic epoxy matrix) remained a static tone of purple. The isotropic matrix was the same color throughout because it reflected light at the same wavelength throughout the material. However, with the anisotropic material, the crystalline structure caused the polarized light to reflect at various wavelengths across the sample, yielding the variation of colors. This effect was seen by rotating the stage the sample was placed on by 90 degrees, which caused the colors to change from cyan to magenta and magenta to cyan.

An example of the nucleation of mesophase in the 0.01 wt.% sample can be seen with the polarized light images for the 0.5-hour samples as shown in Figure 2.10. The 0 wt.% sample did have small mesospheres form (Figure 2.10 (i)), but they were below the minimum 4  $\mu\text{m}$  diameter used to count mesophase as outlined in the ASTM. The 0.01 wt.% sample had similar sporadic areas of small mesophase nucleation with spheres that were slightly larger than the 0 wt.% sample. However, there were sites of large mesophase growth and coalescence within the 0.01 wt.% sample, as seen in Figure 2.10 (ii). These areas of mesophase could be the sites where the rGO allowed for the nucleation of mesophase, which then led to the earlier growth of mesophase. The 0.10 wt.% sample appeared to have larger spheres than the 0 wt.% sample sporadically dispersed in the isotropic pitch Figure 2.10 (iii), but there were not areas of mesophase growth as seen in the 0.01 wt.% sample.

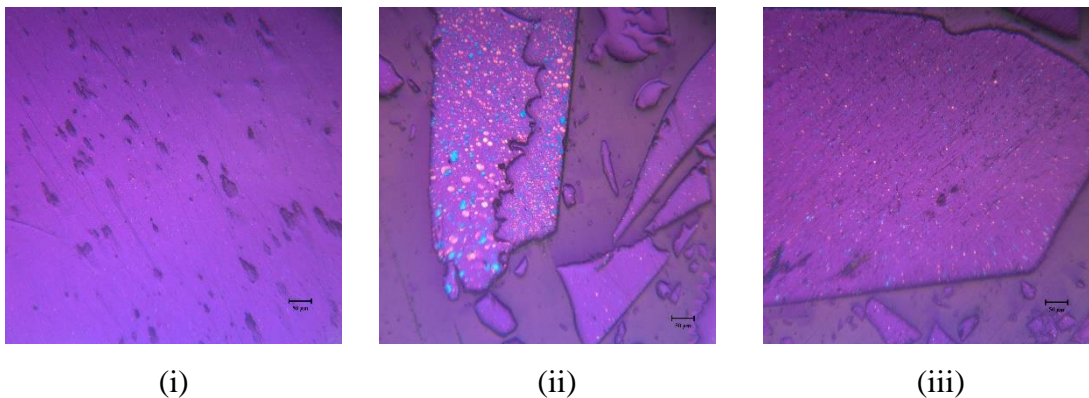
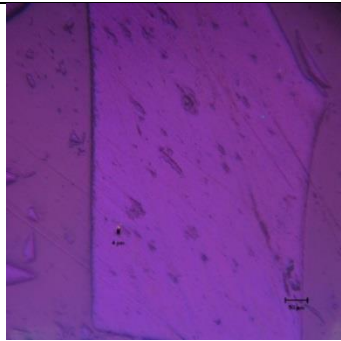
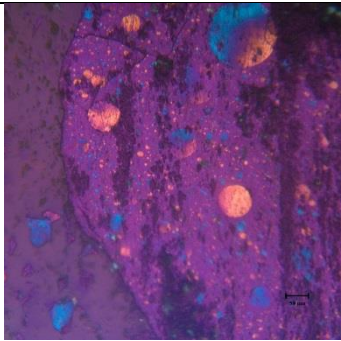
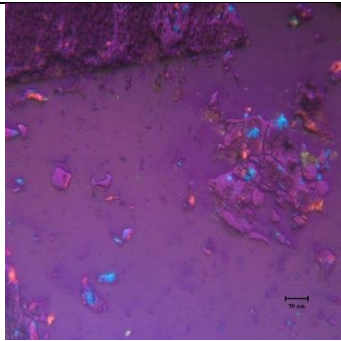
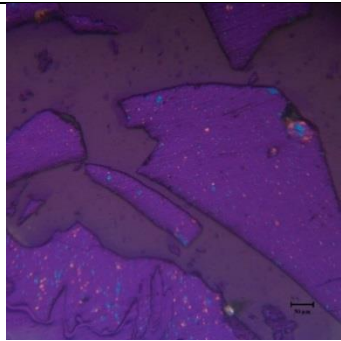
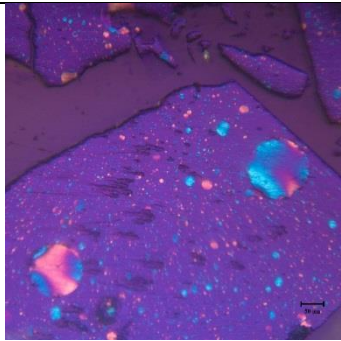
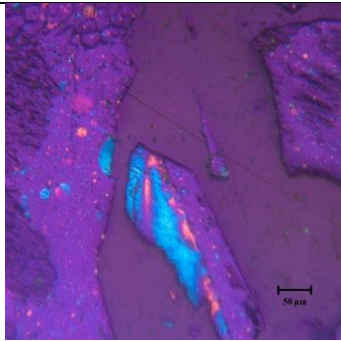
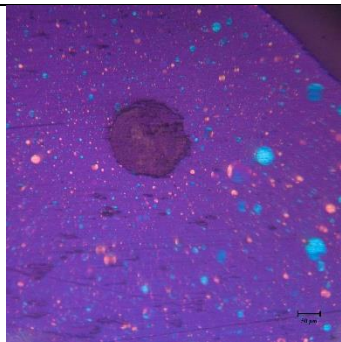
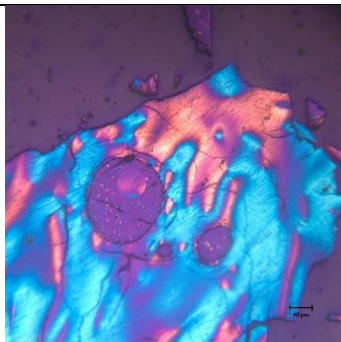
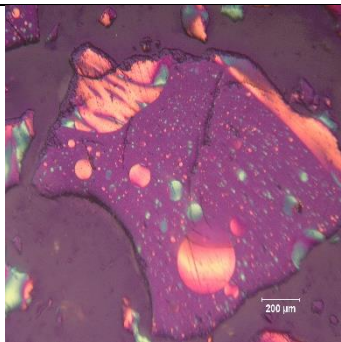


Figure 2.10 Mesophase growth comparison by polarized for 0.5-hours of thermal treatment for the 0 wt.% (i) 0.01 wt.% (ii) and 0.10 wt.% (iii) samples. Scale bar is 50  $\mu\text{m}$ .

The evolution of mesophase nucleation then growth for the petroleum sample is shown in Figure 2.11. All samples appeared to go through similar mesophase cycles of initial formation (nucleation), growth, and coalescence, but at different rates. Towards the end of the treatment times, even though the mesophase percentages begin to converge, the type of mesophase formed appeared to vary between the three samples. The 0 wt%

sample had larger dispersed spheres, the 0.01 wt% had more flow fields of mesophase and the 0.10 wt% had smaller dispersed spheres. The smaller dispersed spheres in the 0.10 wt% sample could be representative of the higher number of nucleation sites present that may be competing for coalescence with the other spheres present. The balance of promoting nucleation but not oversaturating the pitch could explain the higher mesophase percentages in the 0.01 wt% sample.

Petroleum Pitch		
0 wt % rGO	0.01 wt% rGO	0.10 wt% rGO
		
	(i)	
		
	(ii)	
		
	(iii)	

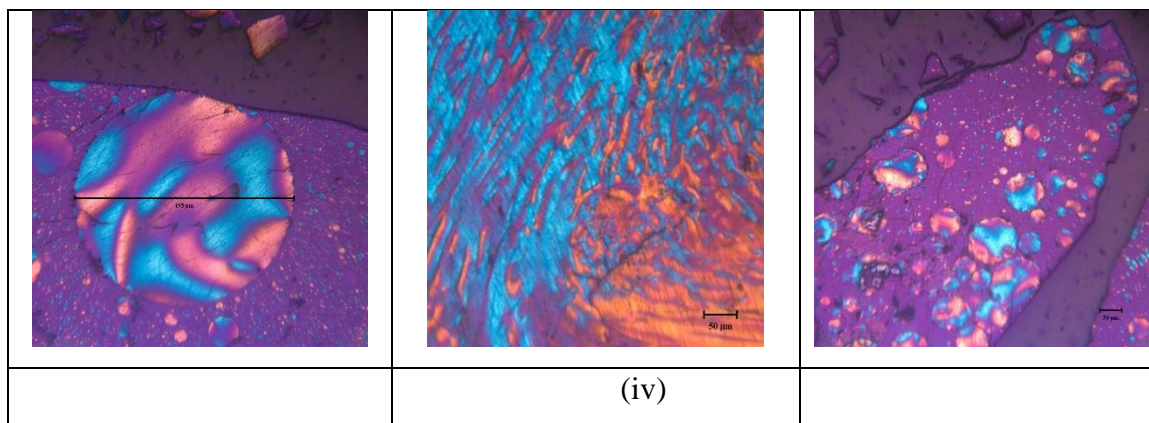


Figure 2.11. Mesophase content for the petroleum sample at treatment times of 1 hour (i), 2-hour (ii), 3-hour (iii), and 4-hour (iv).

After treatment, each sample was analyzed for softening point temperature. The important characteristic of softening temperature was determined by DMA. This test was to determine if the pitches once spun into fibers, could be oxidized without interfilament fusion and to estimate the melt spinning temperature. As the mesophase content increased (extended thermal treatment) the softening temperature increased as well, which is highlighted in Figure 2.12. The increase in softening temperature was because the mesophase molecular weight is generally larger than the isotropic molecular weight and therefore will have a higher softening temperature. The softening temperature of the pitch drastically increased from the parent pitch softening temperature of 110 °C after 0.5-hours of treatment to above 200 °C for all samples. After the initial 0.5-hours of treatment, the rate of softening temperature increase appeared to slow. This decreased rate suggests that the majority of the lighter molecular weight compounds present in the pitch are volatilized within the first 0.5-hours of heat treatment leading to the drastic increase in softening temperature. For all weight percentage samples and all treatment times, there was a similar softening temperature and the minimum temperature required for oxidation of 220 °C was reached within the first 0.5-hours. The slight softening temperature decrease from 3 to 4-hours was due to sampling pitches that had a lower treatment temperature at the 4-hour mark. It does not imply that if a portion of the same sample was tested at 3-hours then 4-hours, the softening temperature would be lower.



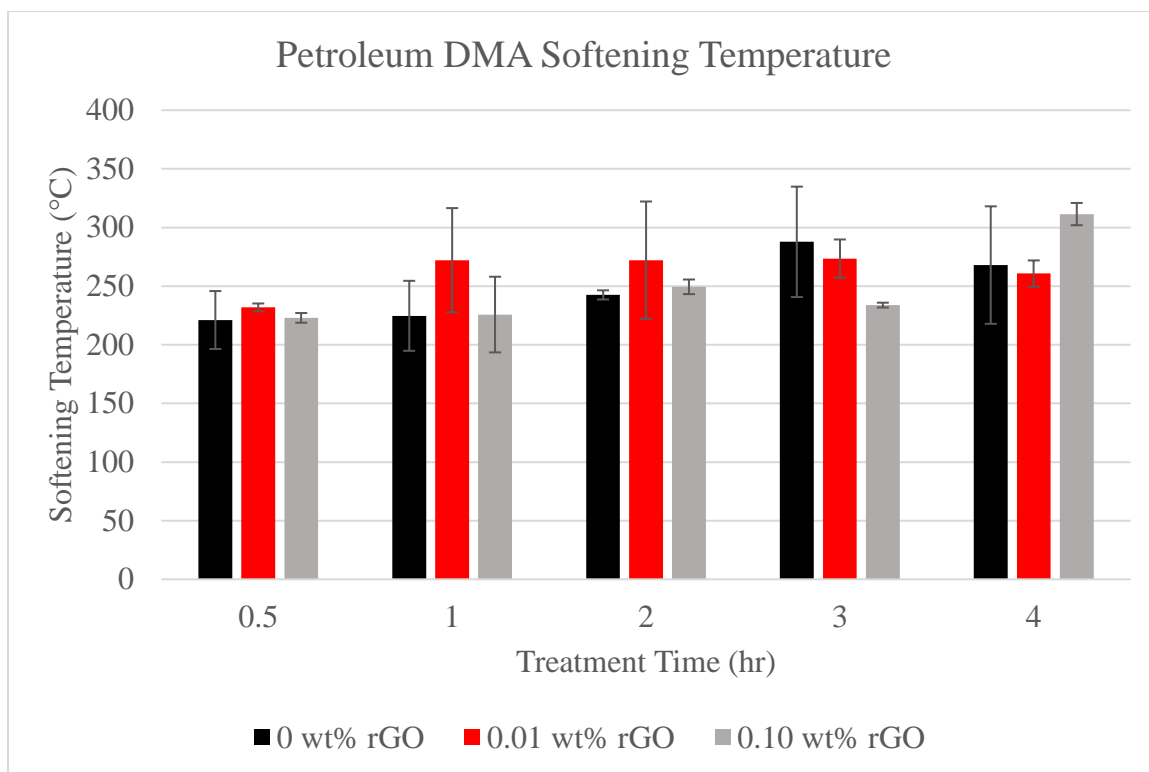


Figure 2.12 Softening temperatures of the pitches by DMA compression test for all petroleum pitches tested. The softening temperature was determined by a controlled force test. Then the derivative of displacement with respect to temperature was plotted.

Another important characterization of the heat-treated pitch was the amount of pitch insoluble in quinoline. After each heat treatment, approximately 0.5 g of the pitch was used for insoluble testing and completed in triplicate. The results are plotted in Figure 2.13. The QIs appeared to follow the trend of mesophase formation shown by point-counting, that is, as the mesophase content increased, as did the QIs. The 0.01 wt% sample had more initial QIs, but all the samples trend towards a similar QI percentage near four-hours.

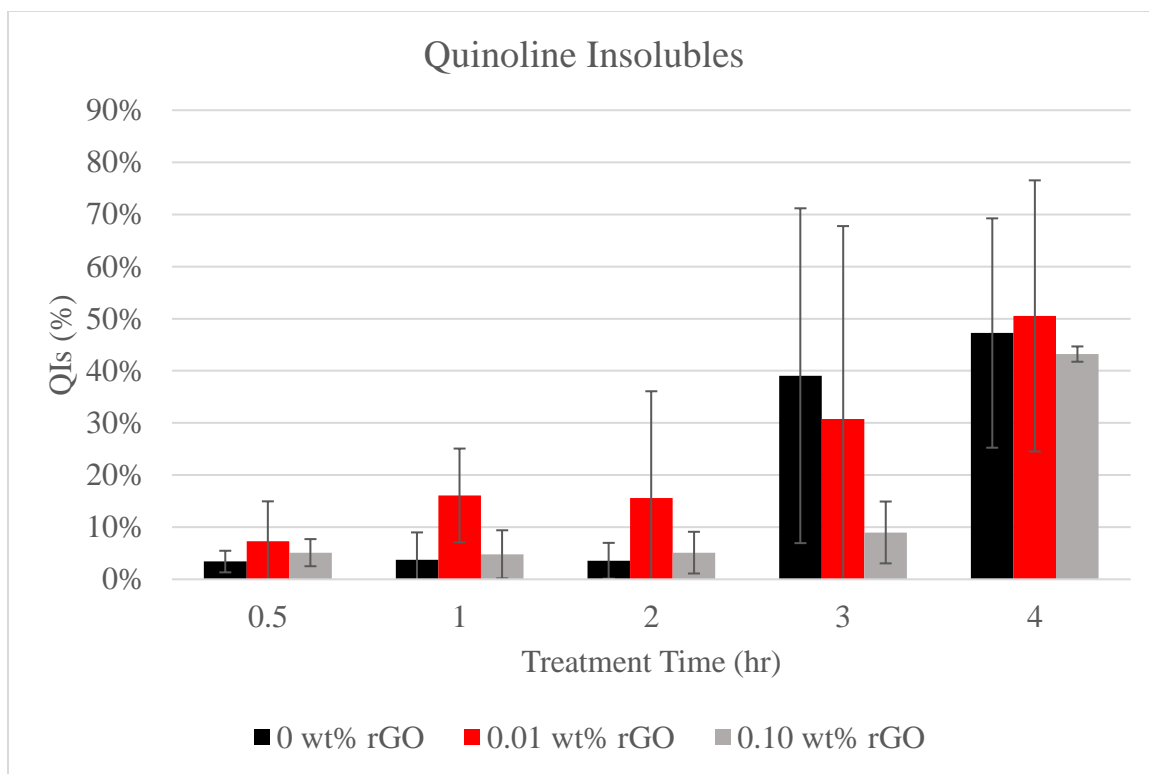


Figure 2.13 Quinoline insolubles (QIs) for all the petroleum pitches tested. As expected, the QIs increased with increased mesophase percentage.

### 2.3.2 Coal-tar Pitch

Following the same procedure used for the petroleum-based pitch, the mesophase percentages per sample were averaged for each treatment time and the results comparing the three rGO wt.% for the coal-tar pitch are shown in Figure 2.15. The goal was to determine if the added rGO nucleated the mesophase at a very small concentration (0.01 wt.%) and a relatively higher concentration (0.10 wt.%).

Since the same heat treatment arrangement was used for the coal-tar heat treatments as with the petroleum pitch heat treatments, there was variation in average temperatures across all samples. This variation is shown in Figure 2.14, where the average temperature during the heat treatments was plotted versus mesophase percentage. The deviations in the temperatures for each treatment time can be seen in Table 2.4. Except for the 0.5-hour treatment time, there were large variations across the average temperature. Additionally, with the same mantle set temperature of 425 °C used with the



petroleum samples, the coal-tar pitch samples on average had a lower average pitch temperature. The precise temperature control of the pitch proved difficult because of the endothermic volatilization. Even though the target pitch temperature was 370 °C, it was difficult to achieve for the longer treatment times.

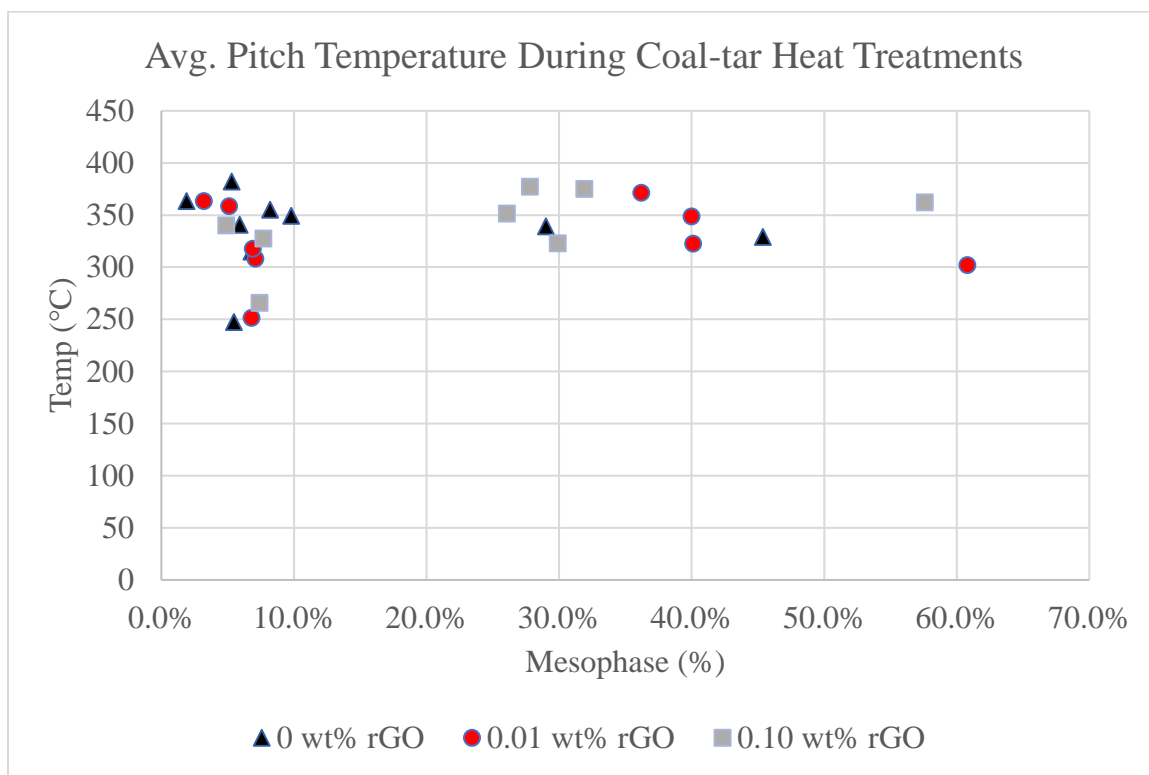


Figure 2.14 The average temperature of the pitch during the heat treatment for every coal-tar sample tested.

Table 2.4 Average temperature during the heat treatment for all coal-tar samples and the deviation of temperatures.

<u>Treatment Time (hr)</u>	<u>Avg. Temp (°C)</u>	<u>Std. dev. (°C)</u>
0.5	364	0
1	331	20
2	308	54
3	353	27
4	330	9

The deviation in temperatures led to more deviation of mesophase in the coal-tar samples than with the petroleum samples. This led to no apparent trend once all samples were averaged for mesophase percentages as shown in Figure 2.15. To separate the effect of temperature with the effect of rGO on mesophase growth, samples with less deviation of average pitch temperatures were analyzed. Table 2.5 shows the improved deviation of average temperature once outlier average temperature samples were removed. Figure 2.16 shows the mesophase percentages but again, this removes replication.

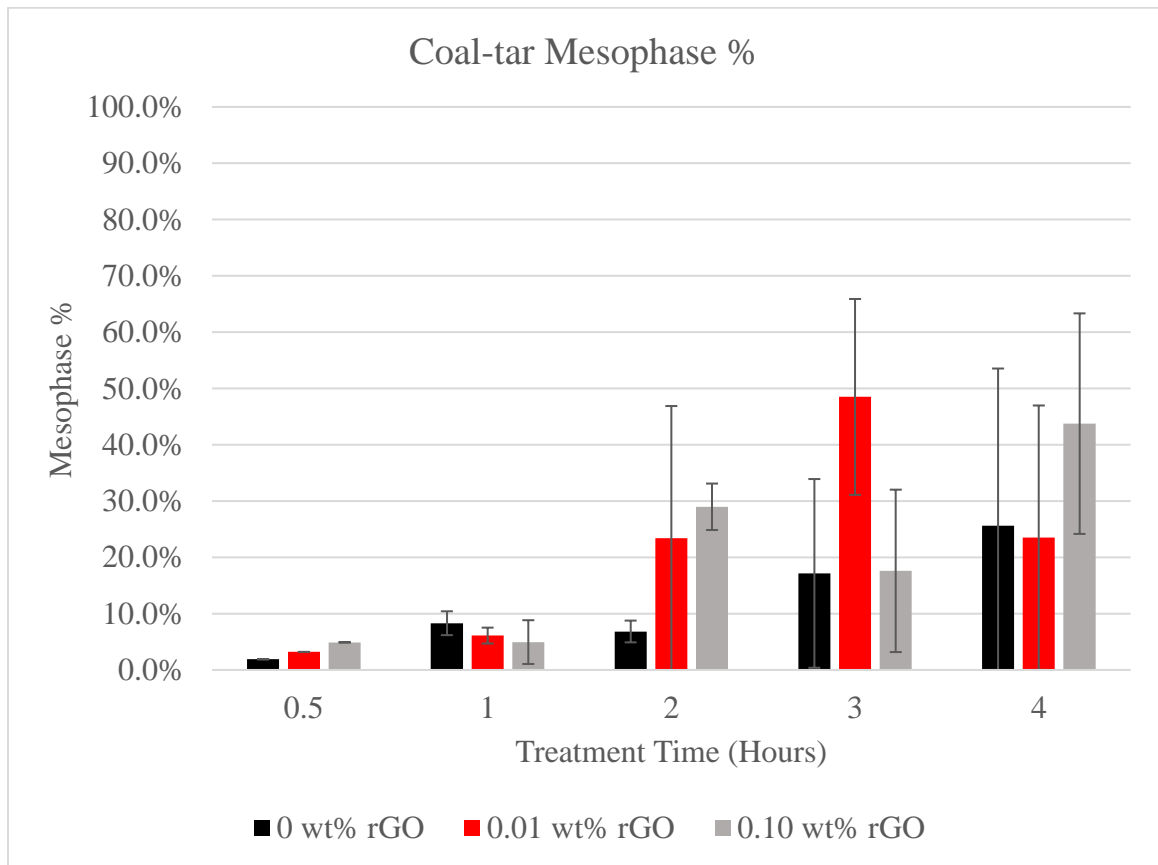


Figure 2.15 Coal-tar pitch mesophase percentage as determined by polarized light microscopy. Three samples were tested at three rGO weight percentages: 0 (baseline), 0.01, and 0.10.

Table 2.5 Comparing rGO wt.% with closer average temperatures. Target temperature was 370 °C.

<u>Treatment Time (hr)</u>	<u>Avg. Temp (°C)</u>	<u>Std. dev. (°C)</u>
0.5	364	0
1	327	17
2	360	12
3	376	4
4	326	3

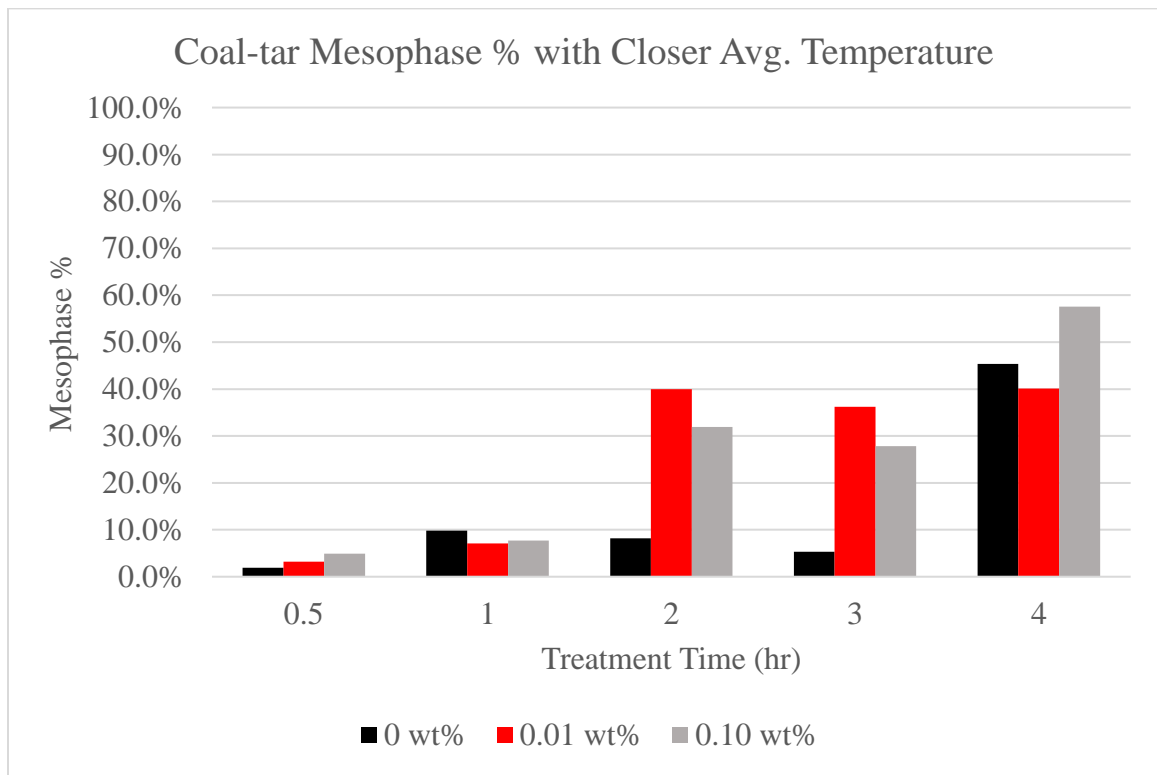


Figure 2.16 The mesophase percentage compared with less deviation in the average temperatures.

Once the deviation in average temperature was decreased, the addition of rGO appears to assist in the growth of mesophase. This effect of an increased nucleation of mesophase was similar to the petroleum sample where the largest difference in mesophase growth was around the 2-hour treatment time. Similarly, as the heat treatment

times progress, the amount of mesophase for each sample converges to a similar amount at 4-hours.

At 0.5-hours of treatment time, shown in Table 2.6, all samples had the same average temperature. With the rGO samples, the mesophase percentages were higher than the sample with 0 wt.% rGO, suggesting the rGO assisted in the rate of mesophase development. For the rGO samples of 0.01 wt.% and 0.10 wt.%, the mesophase percentages were 3.2 % and 4.9 %, where the 0 wt% rGO sample had 1.9 % mesophase. The amount of mesophase for all three samples were similar to the mesophase percentages at 0.5-hours with the petroleum pitch.

Table 2.6 Mesophase percentage for coal-tar pitch samples with same average temperature heat treated for 0.5-hours.

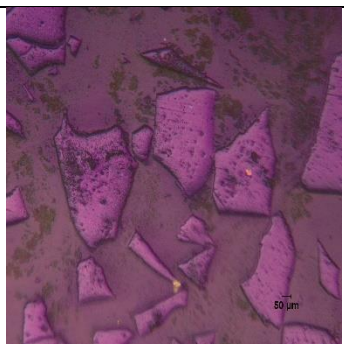
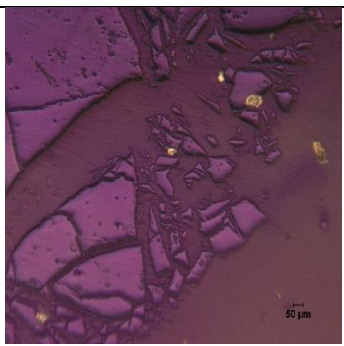
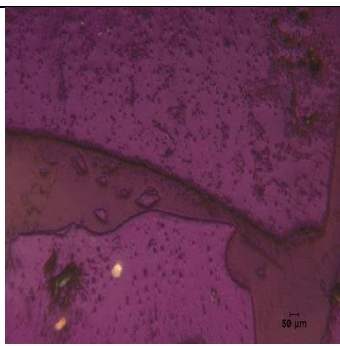
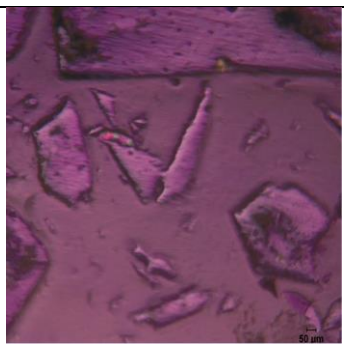
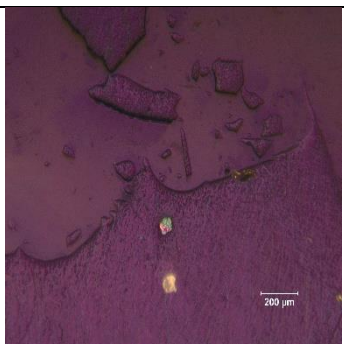
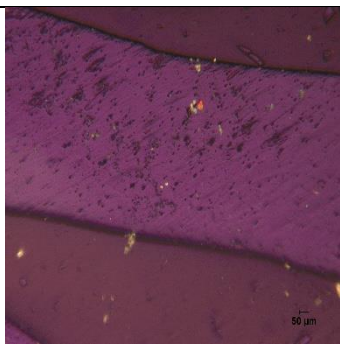
<u>rGO %</u>	<u>Treatment Time (Hour)</u>	<u>Avg. Pitch Temperature (°C)</u>	<u>Mesophase %</u>
0	0.5	364	1.9
0.01	0.5	364	3.2
0.10	0.5	364	4.9

For the coal-tar sample, both rGO wt.% were similar in mesophase growth. Additionally, the amount of mesophase growth in the coal-tar sample was lower than the petroleum sample. This lower growth may be due to the lack of mobility in the coal-tar molecular structure. Since the coal-tar had less aliphatic areas, the energy and time required to generate mesophase was higher than that of the petroleum sample.

Polarized light microscopy was conducted on a Leitz microscope following the procedure outlined in 2.2.6. Using a 20x air objective, 1000-points were counted for each puck to determine the mesophase percentage using a zig-zag pattern. Figure 2.17 shows the polarized light analysis of the base pitch coal-tar product. No anisotropy (mesophase) was visible with the rotation of the analyzer or the rotation of the stage. The nucleation and growth of mesophase is shown with the polarized light images in Figure 2.18.



Figure 2.17 Isotropic coal-based pitch under polarized light. No mesophase content is present. The white dot is epoxy.

Coal-tar Pitch		
0 wt % rGO	0.01 wt% rGO	0.10 wt% rGO
		
(i)		
		

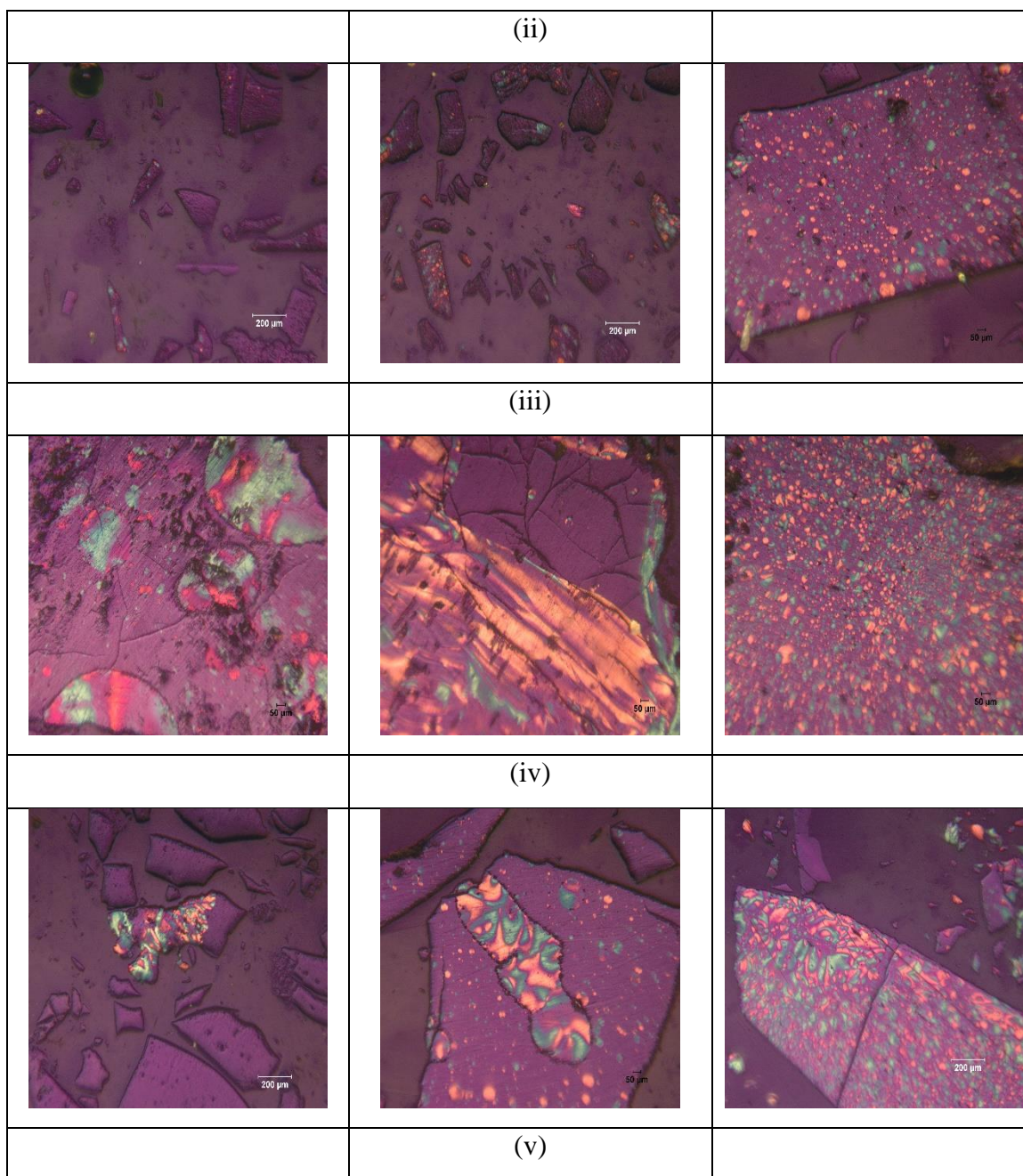


Figure 2.18. Mesophase content for the petroleum sample at treatment times of 0.5-hours (i), 1-hour (ii), 2-hour (iii), 3-hour (iv), and 4-hour (v).

Softening temperature of the coal-tar pitches followed a similar trend as the petroleum pitches and are shown in Figure 2.19. The softening temperature drastically increased from the baseline of 100 °C to near 200 °C within the first 0.5-hours of treatment. However, the rate of increase for the softening temperature decreased as the



length of the heat treatment increased. Again, this suggests the majority of the lighter molecular weight compounds were volatilized during the first 0.5-hours of the heat treatment. From 2-hours to 4-hours, both petroleum and coal-tar samples have a similar softening temperature.

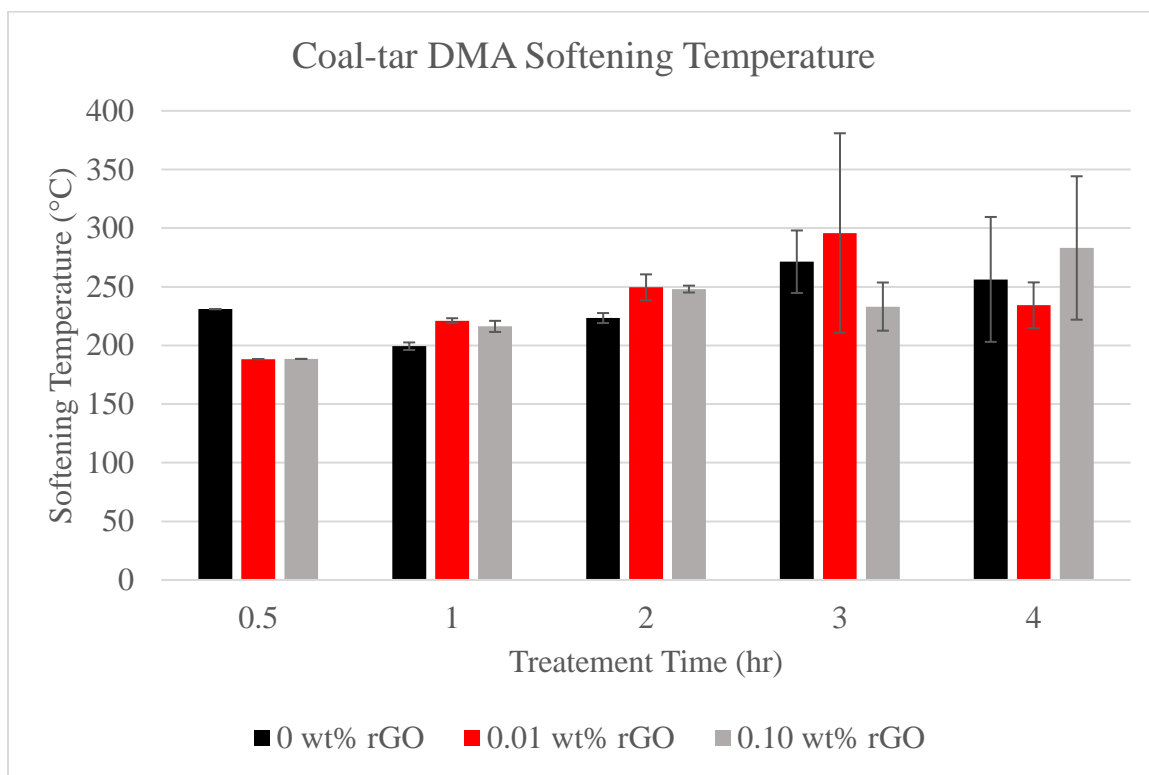


Figure 2.19 Softening temperatures of the pitches by DMA compression test for all coal-tar pitches tested. The softening temperature was determined by the derivative of displacement with respect to temperature.

The QIs were measured following the heat treatments with the same procedure outlined in 2.2.4 and the results are shown in Figure 2.20. The QIs for the coal-tar pitch samples do not have the same drastic difference as shown between the petroleum pitch samples. Overall, the QIs for all samples increase at a similar rate as the treatment times increase. The disparity of the polarized light results and the QIs could be from the size of mesophase formed for each sample or polymerization of the isotropic matrix[35].

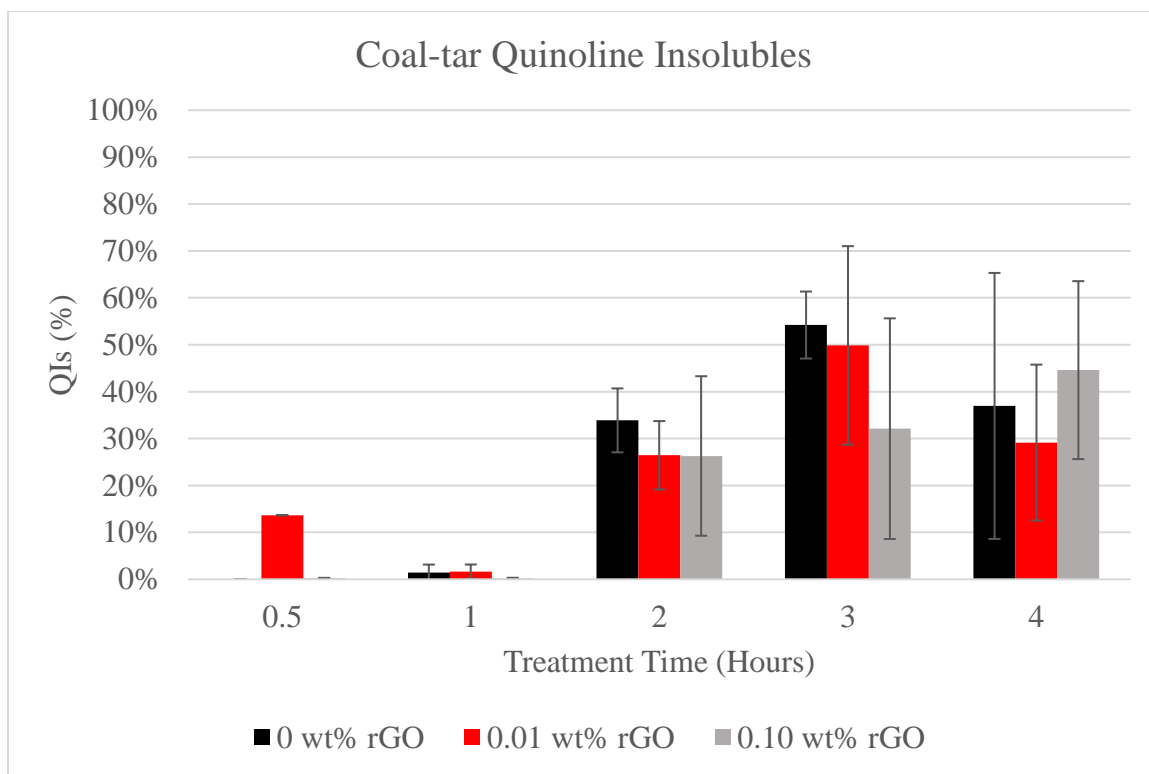


Figure 2.20 Quinoline insolubles (QIs) for all the coal-tar pitches tested. As expected, the QIs increased with increased mesophase percentage.

Polymerization of the isotropic matrix could have caused the PAHs to form longer poly aromatic chains instead of stacking. Since the coal-tar pitch molecular structure is not as mobile as the petroleum pitch, it is a possibility this occurred. It has been shown that the molecular weight of the isotropic matrix is not constant throughout the heat treatment process, and continuously transforms[36]. Therefore, if a sample has lower mesophase content because of the isotropic matrix polymerization, it could still yield a higher insoluble content because of the long-chained, insoluble isotropic molecules.

### 2.3.3 Observations During Heat Treatments

During the heat treatments, the type of volatiles produced for the petroleum and coal-tar pitch varied significantly by visual inspection. While the weight percentage losses were similar between the samples (40-60 wt.%), the coal-tar pitch had more



volatiles condense in the condensing flask, where the petroleum volatiles mainly condensed in the fume hood. The “dirtier” heat treatment of the coal-tar pitch may be due to the complexity of the mixture of organic compounds present in the pitch[37]. While the nitrogen was used for mixing the molten pitch by sparging, the flow rate of the nitrogen had a significant effect on the mesophase development which is supported by empirical evidence from previous experiments. The higher the nitrogen purge flow rate, the more aggressive the removal of volatiles from the heat treatment vessel. This aggressive flow rate of nitrogen mitigated the condensation of the lighter and more volatile species evolved during the heat treatment and facilitated the development PAH condensation into mesophase pitch.

Once the sample had cooled to room temperature, the isotropic pitch fraction tended to have a shiny, glassy appearance, while the mesophase pitch appeared more matte grey. The difference in appearance suggests phase separation of the mesophase and isotropic phases during cooling. Separation occurred because the mesophase was of a higher density than the isotropic pitch, therefore tended to settle on the bottom of the flask[38].

#### 2.2.5 Milled Mitsubishi and THF Insolubles

A synthetic mesophase pitch, Mitsubishi AR, was used as a seed crystal to test if it affected mesophase growth similar to rGO when dispersed in the petroleum-based pitch. This experiment was important because it helped probe the novel nature of rGO as a nucleation site compared to other similarly structured catalysts upon which the mesophase could nucleate. The AR pitch was ground in a ball mill and then tested at concentrations of 0.01 wt.% and 0.10 wt.% for 0.5 hours of heat treatment following the same procedure for the rGO doped samples. The growth of mesophase was lower than the pitch with rGO as a seed crystal yielding 2.1% and 0.8% mesophase versus 5.6% and 1.2%, respectively. Therefore, the results showed that rGO is better at mesophase generation than a mesophase seed crystal, Mitsubishi AR. The surface area only of the rGO and the relatively short length scale of rGO compared to milled AR pitch appear to be the most important factors that allowed it to be a novel solution as a nucleation site of mesophase.

Also, an experiment was conducted to determine the influence the insolubles of the pitch had on the mesophase growth since insolubles were not removed from the pitch-THF mixture during the heat treatment process. This experiment was important because the THF insolubles in pitch could have affected the homogenous dispersion of rGO. An experiment was conducted with each concentration of rGO to remove the insolubles to determine the effect this had on mesophase growth. After sonication, the samples were placed in a centrifuge at ambient air temperatures with a rotation speed of 500 rpm for one hour. The solution was decanted, and then heat treated the same as previous samples at 1 and 2-hours. There was an average of 12 wt.% THF insolubles for all samples. No discernable difference was observed in the growth of mesophase in these centrifuged samples compared to the non-centrifuged samples.

## 2.4 Conclusion

In these experiments rGO was used as a nucleation site, “catalyst”, in petroleum and coal-tar pitch to assist in the formation of mesophase. The petroleum pitch results suggest that an exceptionally low concentration of rGO (0.01 wt.%) dispersed into an isotropic pitch acts as nucleation sites to aid in the development of mesophase domains. The results of the 0.01 wt.% were promising because of the high cost of rGO, the less material that can be used would make the addition of rGO a more economically viable process. The type of mesophase growth varied as well. With 0 wt.% rGO the mesophase was less dispersed throughout the isotropic matrix and consisted of larger mesophase spheres. For the 0.01 wt%, the mesophase had a similar dispersion to the 0 wt%, but the nucleation of mesophase was more rapid. This nucleation of mesophase is because the 0.01 wt% concentration of rGO possibly lowered the energy required for the PAHs to stack and form mesophase structures. The 0.10 wt% mesophase was more dispersed with smaller mesospheres than the other weight percentages and did not appear to coalesce as quickly. For all petroleum samples the softening temperature increased drastically in the first 0.5-hours of treatment from 100 °C to approximately 220 °C suggesting the volatilization of lighter compounds occurred in the beginning of the heat treatment process. After the first 0.5-hours, the softening temperature gradually rose to over 250 °C at the 4-hour treatment time.

The coal-tar pitch results suggested when looking at similar average treatment temperatures, the addition of rGO assisted in the growth of mesophase for both the 0.01 wt% and the 0.10 wt% samples. However, overall the results of the coal-tar sample were more enigmatic than the petroleum sample. These results could be from the lack of mobility of the coal-tar sample compared to the petroleum sample that would make it more sensitive to variations in temperature. Also, for the coal-tar pitch, the aggressive volatilization of the lighter compounds may have contributed to the higher QIs and smaller sized formation of mesophase because the isotropic solvent was removed too aggressively or polymerized early in the process. Since the coal-tar pitch compounds were less mobile than the petroleum pitch, it may require a less aggressive nitrogen flow rate during the growth phase of mesophase. This could allow the lighter compounds to act as a solvent in which the mesophase could form.

The following chapters will discuss the efforts to melt spin the treated pitch into fiber, and to characterize graphitized fibers by tensile testing for tensile properties. Moreover, the morphology of the graphitized fibers was analyzed by SEM imaging of fracture surfaces.

## Chapter 3. MELT SPINNING

### 3.1 Introduction

As mentioned, the goal with melt spinning was to transition the solid pitch into a softened state then quickly vitrify in air while applying tension in order to draw a green fiber. There were two methods used at UKY to melt spin; a single filament extruder and a single filament pressure capsule. Generally, pressure spinning with the capsule was used for smaller batches of experimental pitches (<40 g) or to test the spinnability of certain pitches. This was useful because certain pitches, especially mesophase pitches, can require multiple runs to optimize the spinning conditions. When pressure spinning, multiple spinning runs can be completed on the same day because fewer parts are required to clean. The extruder, while useful for bulk continuous filament spinning, requires significantly more time to get started and clean, and therefore only a few runs per day are possible. Prior to the work in this thesis, approximately 100 spinning runs were completed between the extruder and pressure spinning apparatus. The goal of these runs was to understand the operational parameters (pressure, temperature, take-up speed) effect on generating a green fiber. With experimental pitches, it was difficult to predict the best-operating conditions prior to spinning. Therefore, it was appropriate to start with general estimated conditions, then slowly adjust the available parameters to generate green fiber. However, unlike isotropic pitches, mesophase pitches require precise temperature control due to their highly non-Newtonian behavior[24].

The temperature dependence of mesophase pitch can be characterized using rheological analysis. The mesophase shows a shear thinning (non-Newtonian) behavior as the shear rate increases. Therefore, at a constant temperature the viscosity of the mesophase pitch decreases as the shear rate increases (Figure 3.1), where the viscosity for an isotropic pitch would remain constant. At low shear rates, the domains of the mesophase liquid crystalline structure are stretched and the size of the mesophase structure decreases, which decreases the viscosity of the pitch. If the shear rate increases still, the mesophase domains shift into a monodomain field[39] (oriented in the same direction) which leads to the viscosity slightly increasing, or remaining constant.

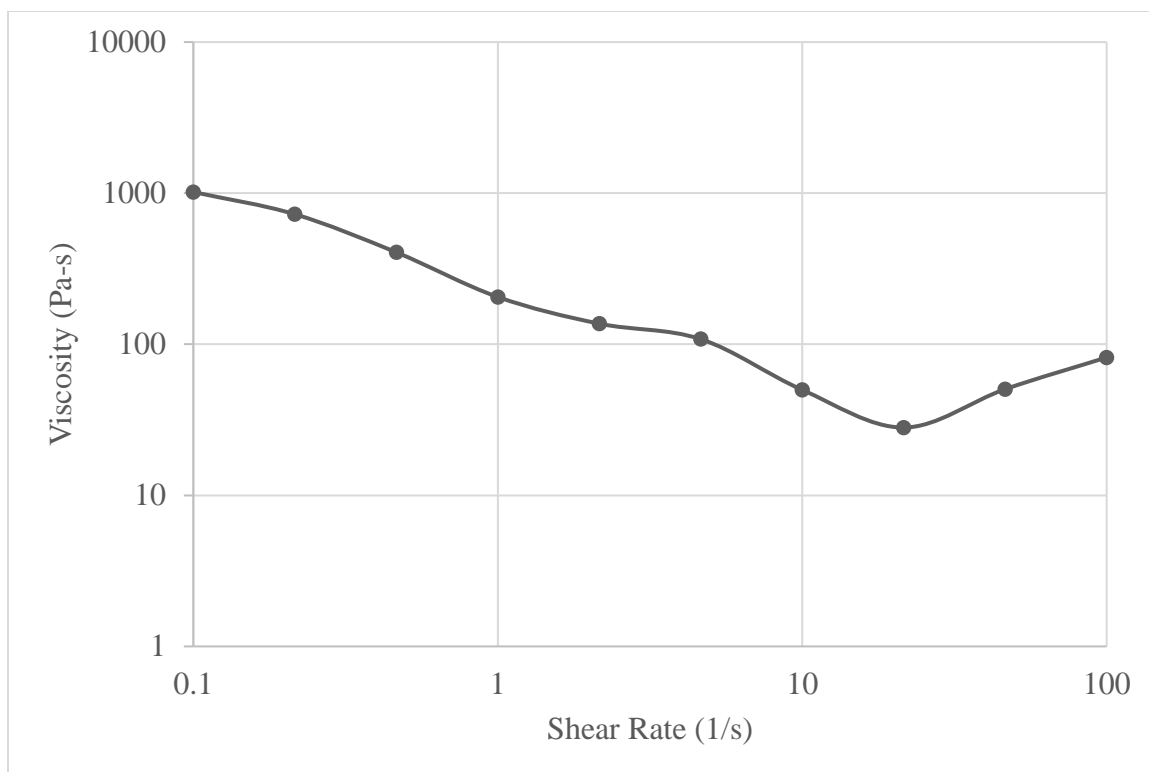


Figure 3.1 Representative shear rate sweep for a 100% mesophase pitch.

The following sections discuss the extruder and pressure melt spinning process as well as the spin runs conducted with the pitches specific to this thesis. For the rGO pitches, since the dispersed rGO is significantly smaller than the diameter of the spinneret and the filter, it was not expected to affect the fibers generated. Additionally, the phenomena of melt pool spinning is discussed and the difficulties it caused in generating a small, consistent diameter green fiber without voids. The variation of operating parameters with an isotropic and mesophase pitch will be discussed by examining the previous Wayne Extruder (WEXT) and pressure spinning runs. While various pitches have been spun with the WEXT and pressure capsule, a comparison of the operating conditions for the isotropic petroleum pitch and the 100-percent mesophase Mitsubishi AR pitch will be discussed.

### 3.1.1 Wayne Extruder (WEXT) Spinning

Extruder melt spinning was an involved process where multiple parameters require adjusting to ensure the molten pitch was at the right temperature, pressure, and flow rate to generate green fiber.

An extruder functions by using a screw to meter finely ground pitch (0.15-0.70 mm) through heated zones to gradually soften the pitch and force it through a capillary into a spinneret. A screw was used to generate pressure by adjusting the RPM and tapering threaded flutes in the direction of flow. The friction between the solid pitch and the wall of the capillary provides the necessary force required to push the pitch through the various temperature zones and generate the necessary pressure at the end of the screw, which vary for isotropic and mesophase pitches. An example of an extruder screw is shown in Figure 3.2. The hexagonal right side of the screw was coupled with the motor to turn the screw. As the flutes move from right to left, the height decreases from approximately 1.0 mm to 0.5 mm. Generally, the melt spinning run began with a screw speed of 20 RPM and was adjusted throughout the run to reach the optimal flow rate. This leads to a range of pressures depending on the flow characteristics of the pitch. For an isotropic pitch, the pressures were usually around 100 psi while the mesophase pitches ranged from a few hundred psi to near 1000 psi. Additionally, an important factor with melt spinning by extrusion was feeding the ground pitch to the screw at a constant rate. Without a consistent feed rate and properly sized pitch (function of flute size), successful extruder melt spinning was not possible. A hopper cannot be used to feed the pitch because it becomes bound in the throat of the hopper due to the pitch adhering to the walls of the feed hole.



Figure 3.2 Extruder screw for the WEXT.



- |                          |                         |                            |
|--------------------------|-------------------------|----------------------------|
| 1. Zone 1 heater (C)     | 5. Melt temperature (M) | 9. Emergency stop          |
| 2. Zone 2 heat (C)       | 6. Start                | 10. Amperage (M)           |
| 3. Die Zone 1 heater (C) | 7. Stop                 | 11. Screw RPM display      |
| 4. Die Zone 2 heater (C) | 8. Barrel screw RPM (C) | 12. Pressure display       |
|                          |                         | 13. Input for pitch powder |

Figure 3.3 Side view of the WEXT with the listed monitored (M) and controlled (C) parameters.

Figure 3.3 shows a side view of the WEXT with the controls listed. A basic schematic of the extruder was shown in section 1.7.1. In order to control these parameters, the WEXT had four temperature zones, the screw RPM which varies flow rate and therefore pressure, and spinnerets which range from 0.30 - 1.00 mm in diameter. The temperature zones and pressure transducer location are shown in Figure 3.4. As

mentioned, the goal with the extruder was to provide sieved pitch (0.15-0.70 mm) to the screw which metered the pitch by friction with the wall through the temperatures zones to soften the pitch to a liquid-like viscosity. The maximum size of the ground pitch needed to be smaller than the maximum height of the screw flutes, else the screw could not force the pitch through the capillary. The melt temperature thermocouple was located near where this softening transition occurs. The spinneret was located below Die Zone 2, and this was where the single filament fiber forms.



Figure 3.4 Controlled temperatures zones for the WEXT where the pitch transitions from right to left. Melt temperature and pressure transducer location are shown.

To manage the shear thinning behavior on the WEXT, the four temperature zones must be properly set (by experimentation) to have a successful run. While the DMA softening temperature assisted in setting the initial spinning parameters, ultimately, they were adjusted throughout the run as the behavior of the pitch was observed. This was not necessarily the case with isotropic pitches or low mesophase pitches (< 20%) where the softening temperature was used to set parameters near the optimal operating conditions.



After multiple spinning experiments, the following ratios were generated (equation 3.1) in order to quickly estimate a baseline target of temperatures for the start of each run. This table was generated from the most successful spin runs on the extruder and calculates the four zone temperatures as a ratio of the DMA softening temperature ( $T_{sp}$ ). The four zones are shown in Figure 3.4, Zone 1 ( $Z_1$ ), Zone 2 ( $Z_2$ ), Die Zone 1 ( $DZ_1$ ), and Die Zone 2 ( $DZ_2$ ).

$$Z_1 = \frac{T_{sp}}{1.17} \quad Z_2 = \frac{T_{sp}}{0.86} \quad DZ_1 = \frac{T_{sp}}{0.86} \quad DZ_2 = \frac{T_{sp}}{0.86} \quad [3.1]$$

For an isotropic pitch with a 110 °C softening temperature, green fibers were spun with starting zone temperatures of 94 ( $Z_1$ ), 127 ( $Z_2$ ), 127 ( $DZ_1$ ), and 127 °C ( $DZ_2$ ). These temperatures were systematically adjusted to 90, 145, 150, and 150°C to generate the most consistent and smallest diameter fiber throughout multiple runs by monitoring the flow characteristics of the pitch as it exited the spinneret. The range of adjustment to temperatures was standard for any isotropic pitch spun. However, these ratios of temperatures did not apply for mesophase pitches since they generally required different set temperatures depending on the source of the pitch, the softening temperature, and mesophase content. For example, the Mitsubishi AR pitch required zone settings of 225 ( $Z_1$ ), 320 ( $Z_2$ ), 330 ( $DZ_1$ ), 330 °C ( $DZ_2$ ) with a 286 °C softening temperature to generate a green fiber. The ratios of these temperatures applicable to this specific mesophase pitch were not applicable to other mesophase products. Multiple spin runs were required to determine ideal temperatures for other high-percentage mesophase pitches. Once the temperature ratios were properly set (as determined by experimentation) and with a consistent feed rate of ground pitch, small diameter fibers were spun. Figure 3.5 shows the carbonized fibers of 100-percent mesophase pitch melt spun from an extruder.

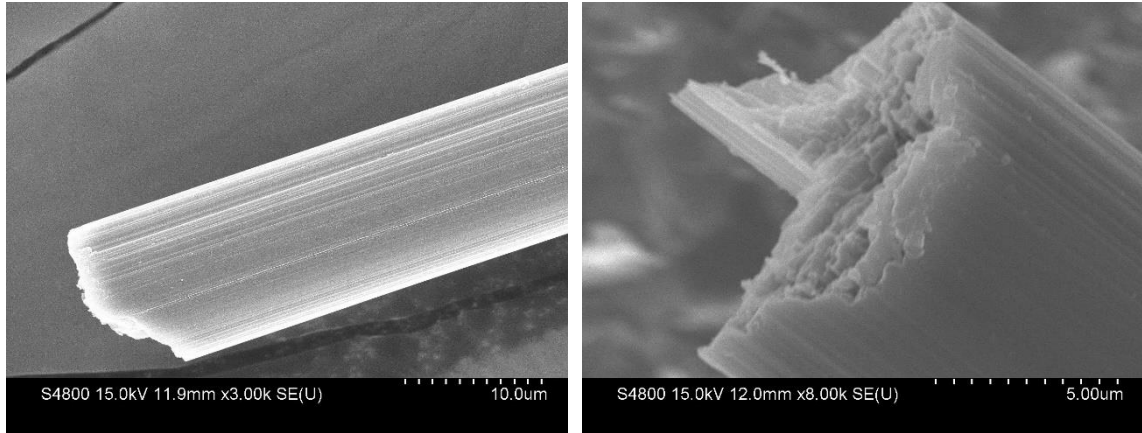


Figure 3.5 Extruder melt spun mesophase carbon fibers.

### 3.1.2 Pressure Spinning Capsule

As mentioned, pressure spinning was advantageous for small amounts of experimental pitches generated on a research scale. While the goal of generating a small diameter ( $< 20 \mu\text{m}$ ) fiber was the same as extruder melt spinning, there was only one temperature zone to set and pressure was applied by nitrogen instead of a screw. The methodology of choosing a starting temperature and pressure, then iteratively adjusting both to obtain continuous fiber filament spinning was the same as the extruder. Figure 3.6 shows the pressure spinning capsule used at UKY CAER.

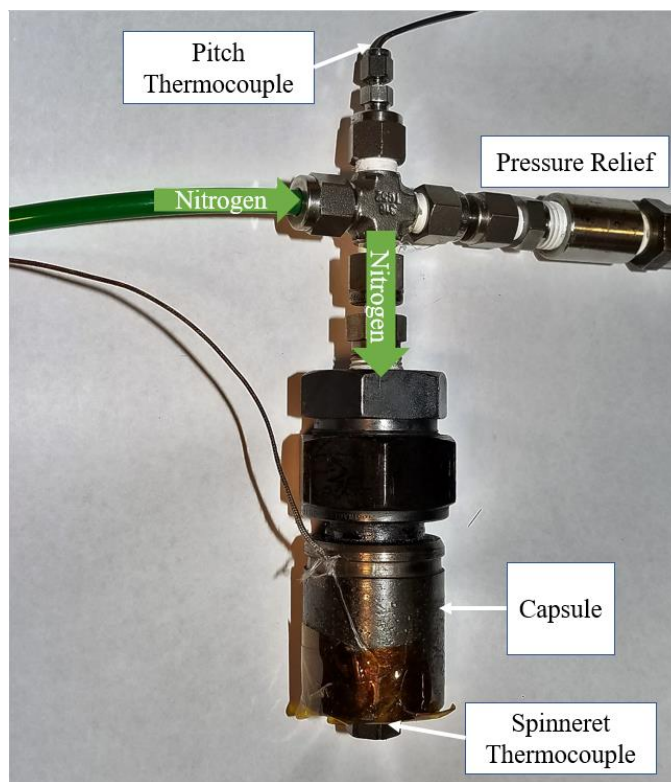


Figure 3.6 UKY CAER pressure spinning capsule with monitored pitch temperature, controlled spinneret temperature, and controlled nitrogen flow.

For pressure spinning, the pitch did need to be ground to a specific size. Course grinding was sufficient to fill the pressure capsule. After the capsule was filled with pitch it was important to flush the capsule with nitrogen prior to heating to prevent polymerization of the pitch in the air. A low pressure of 5 psi was used to provide an inert atmosphere while the capsule was heating. The general starting temperature for pressure spinning was 30-40 °C above the softening temperature, however, an initial heat soak was used near the softening temperature of the pitch to ensure homogeneous softening. The location of the spinneret thermocouple with respect to the band heater led to the difference in temperatures for the same pitch. Two thermocouples (TCs) were used, one for controlling and one for monitoring temperatures. One TC was placed at the edge of the spinneret for controlling the band heater (Spinneret TC) and a second was placed through the top of the capsule to monitor pitch temperature (Figure 3.7). The temperature was controlled by the TC near the spinneret because it leads to more consistent

temperatures as compared to controlling the heater by the pitch temperature. The same problem of controlling temperature by the pitch appears that occurred during heat treatments. There was significant lag between the heater turning on, and the pitch thermocouple reaching the desired temperature. When the heater was controlled by the pitch temperature, there was more variation in the temperature over time. However, the manual placement of the spinneret TC still caused a variation in the spin temperature used for each run of a few degrees Celsius, even with the same pitch sample used. For example, the petroleum isotropic pitch that was spun on the WEXT was initially set to 100 °C for ten minutes before ramping to the spinning temperature of 135 °C. This temperature was 15 °C lower than the DZ2 temperature used for the WEXT.

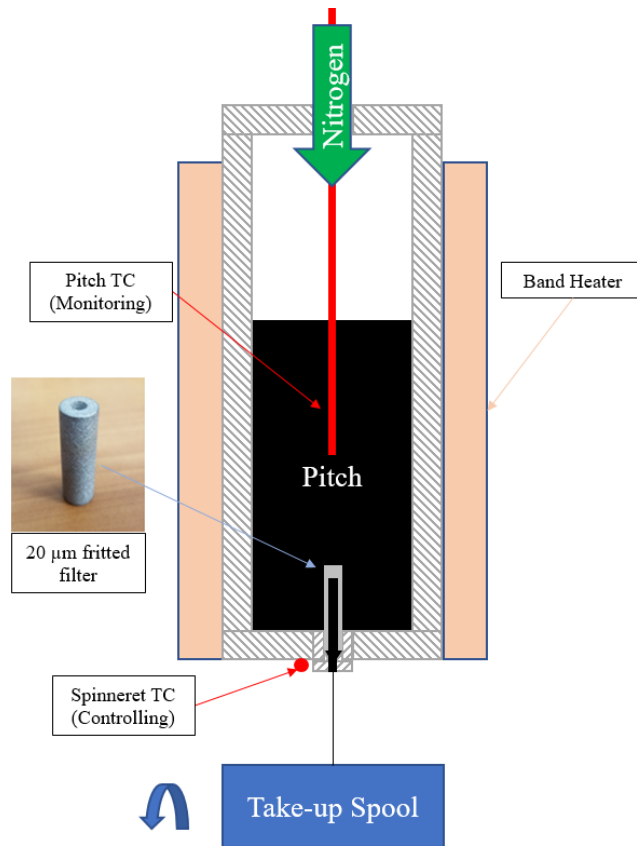


Figure 3.7 Melt spinning apparatus used for spinning green fibers. A 20  $\mu\text{m}$  fritted metal filter was used during spinning to filter out particulates. The parameters controlled for pressure spinning are shown: nitrogen pressure, spinneret temperature, and take-up spool RPM.

A fritted stainless-steel candlestick filter (with a nominal pore size of 20  $\mu\text{m}$ ) was used to filter the molten pitch prior to entry into the spinneret to ensure no solid, insoluble particles became embedded in the fiber. Previous experiments with melt spinning have shown that a 20- $\mu\text{m}$  pore size was sufficient to properly filter the molten pitch without requiring excessively high pressures to force pitch through the filter. However, spinning time was reduced as the in-line filter became blinded. The time for the filter to become blinded depended on the pitch used, but generally limited the spin run to less than 20 minutes for high-mesophase content pitches.

As with the WEXT, multiple mesophase and isotropic pitches have been pressure spun to ascertain the spinnability of pitches and to generate small-scale fibers. The isotropic pitches were resilient to changes in nitrogen pressure and spin temperature. The isotropic petroleum pitch was able to be spun successfully at temperatures ranging from 120-140  $^{\circ}\text{C}$  with pressures ranging from 5-65 psi. However, the mesophase pitch was much more difficult to spin in the pressure capsule because the temperature was not as precisely controlled compared the WEXT. Pressure spinning the AR mesophase sample used for the WEXT required a set temperature of 365  $^{\circ}\text{C}$  in order to begin to generate a fiber, compared to 330  $^{\circ}\text{C}$  when spun using the WEXT. Figure 3.8 shows fibers that were generated by pressure spinning and the graphitic structure after graphitizing. It is important to note that voids were present in the fiber, which was common during the pressure spinning process if the fibers were too large in diameter. These voids may be removed by conducting a vacuum distillation slightly above the spinning temperature of the pitch.

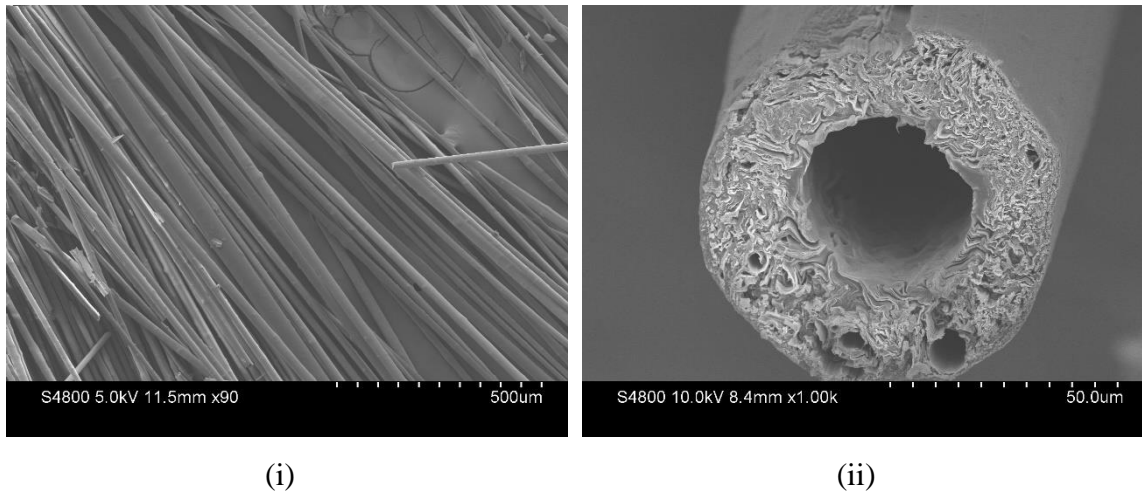


Figure 3.8 Green fibers after being pressure spun for a mesophase pitch (i). Graphitized mesophase fiber with desired graphitic sheets and undesired voids in the fiber (ii).

### 3.1.3 Melt Pool Spinning

The difficulty of melt spinning was further compounded by the phenomena of melt pool spinning which was a common occurrence with the extruder and pressure capsule. A pool was formed on the face of the spinneret from where the nascent fiber was drawn. With the fibers spinning from a pool it was tremendously difficult to calculate a draw down ratio (DDR) or accurately control the flow of the pitch. The draw down ratio is the ratio of the fiber diameter exiting the spinneret to the diameter of the fiber collected on the spool. Figure 3.9 provides an example of melt pool spinning on the extruder as a function of time and shows that the pitch wets and pools on the surface of the spinneret prior to being pulled into a fiber. This isotropic pitch was spun from a 330  $\mu\text{m}$  spinneret and the melt pool grew to 3.7 mm (Figure 3.9 (E)) before being pulled into a fiber (Figure 3.9 (F)). The viscoelastic behavior of the pitch, surface energy of the spinneret, spinneret temperature, and pitch flow rate were possible variables that caused the melt pool to form.

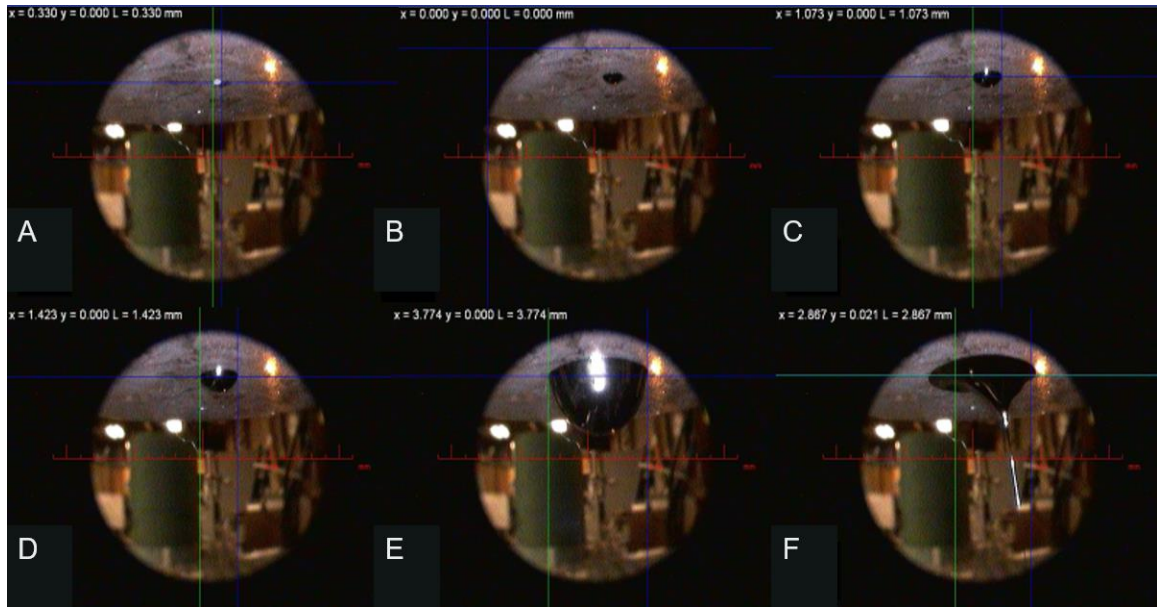


Figure 3.9 Melt pool spinning where only the exit of the spinneret is shown at  $330\ \mu\text{m}$  (A), the pitch exits and begins to swell to a pool size of  $3.774\ \text{mm}$  (E) and decreases to  $2.867\ \text{mm}$  once pulled into a fiber (F).

### 3.1.4 Lessons Learned

Melt spinning fiber regardless of the method used was a delicate process that required significant experience to intuitively know how to change the parameters to produce quality fiber. While initial conditions were estimated, pitches usually needed multiple runs with varying parameters to determine the optimal operating parameters. For isotropic pitches, these operating parameters were generally linear in nature and could translate from one isotropic to another. However, high-percentage mesophase pitch generally needed multiple test runs with precise temperature control to generate a small diameter fiber without voids. Additionally, the properties of the fibers were highly dependent on the processability of the pitch during spinning. The mechanical properties were a function of the mesophase percentage, but also a function of voids present in the fiber and diameter of the fiber. The voids and diameter were highly dependent on the spinning process (spin temperature, pressure, capillary shape, spinneret diameter, etc.). The melt spinning process still requires optimization in order to prevent melt pool

spinning, accurately predict optimal spinning conditions, and consistently generate a small diameter fiber without voids.

### 3.2 Method

For the rGO experiments, because the quantities of pitch produced were generally tens of grams, the pressure capsule method was used for spinning fibers. The spinning procedure followed the progression outlined in section 3.1.2 where specific starting conditions were chosen for the pitches (Table 3.1) and systematically adjusted to the optimal levels. These samples were chosen because the results suggested 0.01 wt.% rGO assisted in mesophase development for the petroleum pitch and possibly the coal-tar pitch. Therefore, to judge the efficacy of using rGO to assist in mesophase development, the rGO doped pitch was melt spun to determine if adding rGO was a viable method for the entire fiber production process. For each base pitch, two variations of the pitch were spun, one baseline 0 wt.% and one containing 0.01 wt.% dispersed rGO, all heat-treated at 4-hours. The 4-hour treatment time was chosen in order to spin with higher mesophase percentages. The nitrogen pressure, capsule temperature, and spool RPM were the three variables adjusted to ensure continuous fiber spinning. The Spin Temp listed was the starting temperature used for the heat soak of the pitches.

Table 3.1 Initial spinning parameters for experimental pitches. Filter pore size, nitrogen pressure (P), spinneret diameter ( $\emptyset$ ), spinneret temperature (Spin Temp), take-up spool setting (RPM), and meters per minute (m/min) of fiber collected.

<u>Filter (<math>\mu\text{m}</math>)</u>	<u>P (psi)</u>	<u>Spinneret <math>\emptyset</math> (<math>\mu\text{m}</math>)</u>	<u>Spin Temp (<math>^{\circ}\text{C}</math>)</u>	<u>RPM</u>	<u>m/min</u>
20	20	660	225	150	78

After the initial heat soak, the initial settings for each pitch were systematically adjusted to optimize the spinning process. Once the fiber started to form with the optimized settings, it was allowed to reach the spool before any external force was applied. This allowed time to observe the flow of the molten pitch, the vitrification point of the fiber, and the uniformity of the vitrified fiber. To attach the fiber to the spool,



double-sided tape was placed on the spool. Immediately after the fiber was attached, the motor was started to turn the spool.

The non-heat-treated base pitch samples were not included in the experiments because of their low softening points. While petroleum and coal-tar base pitches have spun remarkably well into green fiber in previous experiments, their softening temperatures of 110 °C and 100 °C respectively, were too low to avoid fusion of fibers during oxidation.

### 3.3 Results

While the spinning conditions were similar for all pitches (Table 3.2), the difficulty of spinning each varied. It is important to note that even with similar mesophase percentages and the same base material, the size of the mesophase spheres and polymerization of the isotropic phase could vary between samples and therefore affect the spinnability of the pitch. An additional factor, melt pool spinning, mentioned in section 3.1.3 affected all spin runs leading to variation in the flow path of the molten pitch and vitrification point of the fibers. As mentioned, melt pool spinning was when the pitch wetted the surface of the spinneret upon exiting the capillary. This surface wetting could be caused by the high surface energy of the spinneret used (steel) and the flow rate of the pitch (function of temperature and pressure) and was a laborious problem to solve. When wetting occurred, it was extremely difficult to determine the draw down ratio (DDR) of the fibers as well as the flow characteristics of the pitch. Certain steps may be taken to overcome melt pool spinning including a silicon spinneret spray and adjusting starting temperature and pressure. Each step was attempted to resolve melt pool spinning but it still occurred during all spin runs. Generally, once wetting began during a spin run, it was not possible to stop without restarting the spin run with a clean spinneret surface. All pitch samples showed a tendency to wet during spin runs and therefore all fiber samples were collected under melt pool spinning conditions. Additionally, voids were present in all fibers but were more prominent in the coal-tar samples, possibly due to more volatiles evolving in the fibers that condensed in the pitch during heat treatment.

Table 3.2 Optimization of spinning conditions for each heat-treated pitch; petroleum (Pet.) and coal-tar (Coal) with listed mesophase percentage (M), softening temperature ( $T_{sp}$ ), controlled spin temperature (Spin T), monitored pitch temperature (Pitch T), nitrogen pressure (P), and spool take-up speed (RPM)

<u>Sample</u>	<u>rGO %</u>	<u>M %</u>	<u><math>T_{sp}</math> (°C)</u>	<u>Spin T (°C)</u>	<u>Pitch T (°C)</u>	<u>P (psi)</u>	<u>RPM</u>
Pet.	0	45	205	270	280	40	284
Pet.	0.01	54	248	275	288	40	300
Coal	0	29	220	280	303	60	224
Coal	0.01	29	215	275	287	40	178

Figure 3.10 shows a typical band of green fiber as taken up by the rotating spool. This green fiber was exceptionally fragile and required oxidation before it could be more readily handled. The fiber was attached to the spool by using double-sided tape near the edge of the spool and single filaments may be seen in the image. After multiple revolutions of the spool, the fibers formed a “band” of fibers as shown. In this case, unwinding of the filament was nearly impossible. Linear traversers may be used to extend the collection of fibers to the ends of the spool in a helical pattern, which is more amenable to unwinding. However, for these small research samples, no traversing of the spool was required since the fibers were cut from the spool and placed in ceramic boats for oxidation.

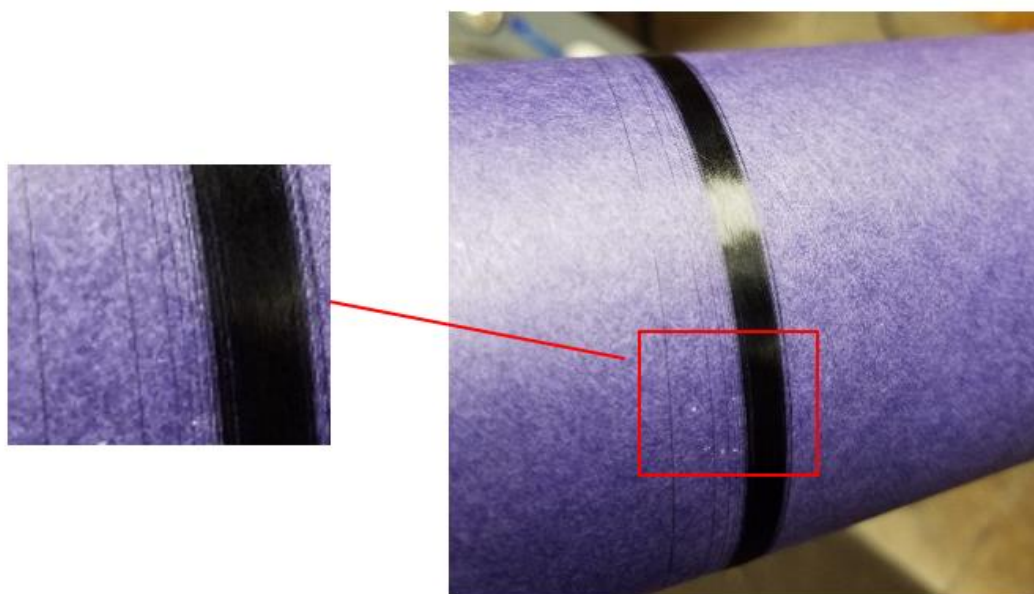


Figure 3.10 Green fiber melt spun pitch sample. The collection of fiber forms a band around the spool. Individual filaments are highlights in the callout image.

### 3.4 Conclusion

The initial spin conditions (pressure, temperature, spool RPM) chosen for the pitches were adjusted to optimize the single filament fiber production for each sample. With these optimized conditions, green fiber was collected from each sample. The most robust pitches during the pressure spinning tests were the petroleum pitch with 0.01 wt.% rGO and coal-tar pitch with 0 wt.% rGO. Melt pool spinning conditions made it difficult to predict the DDR and affected the further optimization of the melt spinning process. Therefore, because of melt pool spinning conditions, no precise conclusions can be made about the effect of rGO on fiber production other than fibers were able to be produced from the pitches that contained rGO. The green fibers of the selected pitches were successfully spun, although their quality appeared to be less conclusively related to the rGO content and more determined by spinning conditions.

## Chapter 4. THERMAL CONVERSION AND CARBON FIBER PROPERTIES

### 4.1 Introduction

After green fiber is melt spun from a pitch source, it must be thermally treated to convert it to a carbon fiber. Green fiber is only vitrified pitch molecules, largely polyaromatic hydrocarbons, assembled in a fiber form. These hydrocarbons must be thermally converted to a fully carbon, graphitic state. The processes to do so begins with oxidative stabilization, where oxygen is introduced to the green fibers by an addition reaction where the oxygen diffuses through the fibers and reacts to crosslink the polyaromatic hydrocarbons. The softening temperature of the fibers increases at a faster rate than the oxidation heating rate which dramatically increases the softening temperature such that the filaments were infusible upon further heating and carbonization. Carbonization occurs in an inert atmosphere where most of the non-carbon atoms of the stabilized fiber were driven off as volatiles. Lastly, and particularly for mesophase derived fiber, the fibers are treated to graphitization temperatures (nominally greater than 2000 °C). The thermal energy allows for atomic rearrangement of the constituent carbon atoms into a well-defined graphite crystal, oriented with the basal planes (graphene planes) parallel to the fiber axis. After graphitization, the fibers are nearly a complete carbon structure with over 99 wt.% carbon content.

Through the described thermal conversion and subsequent tensile testing of the fibers, the goal was to determine if rGO, dispersed in the parent pitch to generate more mesophase and then spun into green fiber, affected the carbon fiber morphology, mechanical properties or the overall mass conversion to carbon fiber relative to the green fiber (or carbon yield). Characterization of the graphitized fibers was completed through scanning electron microscope (SEM) imaging to peer into the fiber morphology, and tensile testing to probe their mechanical properties.

Tensile testing entailed careful mounting of individual filaments into a FAVIMAT+ tensile testing machine where a stress-strain test was conducted. The tension in the filament was recorded as a function of applied strain. At small elastic strains, the apparent modulus defined the slope of the stress-strain curve. All fibers were quite linearly elastic to failure. The tensile strength was recorded as the highest stress on the

curve. Each sample had fibers tested at four-gauge lengths (20 mm, 30 mm, 40 mm, and 50 mm) to determine the average break tenacity and initial modulus. The multiple gauge lengths were used to calculate a system compliance, which accounts for the error introduced by the FAVIMAT+ due to the spring constant of the instrument clamp and the load cell being of similar magnitude of the high modulus (more resistant to strain) pitch carbon fibers. However, because the compliance requires an accurate cross-sectional area of the carbon fibers which was generally non-uniform for the experimental samples, accuracy of compliance calculations and therefore the accuracy of the break strength (MPa) and Young's modulus (GPa) could not be determined with reasonable accuracy. For these reasons, the compliance results are only included in Appendix A as a reference and the tensile testing results are reported in textile units which is discussed in section 4.2.3.

## 4.2 Mechanical Properties

### 4.2.1 Thermal Conversion

After the green fibers had been collected on the spool, the fibers were cut from the cardboard spool in a single location and released as a length or bundle of collimated fiber. The bundle was laid straight, with no tension, in a ceramic boat for oxidation. Mass and length of the fibers were measured before and after oxidation. Oxidation took place in a Herathem™ General Protocol Convection oven for up to 24 hours, reaching temperatures up to 350 °C. The fibers were allowed to air cool and visually inspected for fusion and no oxidized fiber sample appeared to be fused. Once the change in mass and length of the fibers were noted, the fibers were placed in a graphite crucible in a Thermal Technology™ (1000-3060-FP20) graphitization furnace where they underwent carbonization and graphitization within the same run. The temperature was ramped to 800-1000 °C for carbonization with a dwell for many minutes. Then the temperature was quickly ramped to a graphitization temperature over 2000 °C with a dwell for many minutes. The changes in mass and length of the fibers were noted after graphitization and are shown in Table 4.1.

Table 4.1 Change in lengths and masses for the petroleum (P) and coal-tar (C) pitches with 0 wt% and 0.01 wt % rGO. Initial green fiber carbon yield (CY) after graphitization.

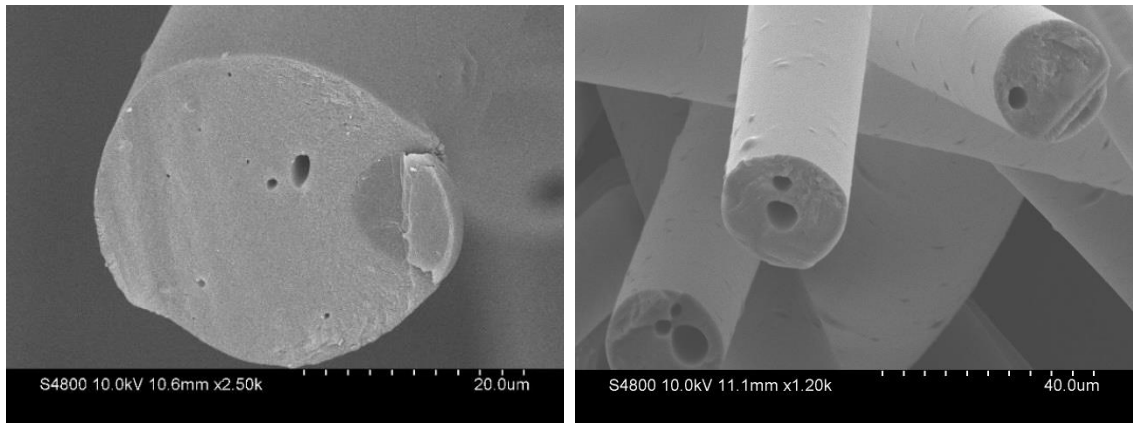
<u>Sample</u>	<u><math>\Delta</math>Mass (%)</u>	<u><math>\Delta</math>Length (%)</u>	<u>CY (%)</u>
P - 0 wt%	-26%	-7%	74%
P - 0.01 wt%	-28%	-7%	72%
C - 0 wt%	-19%	-7%	81%
C - 0.01wt%	-18%	-7%	82%

After graphitization, the petroleum pitches had more mass loss than the coal-tar pitch samples, most likely due to the petroleum pitch initially having more aliphatic structures. Concerning the thermal conversion process and the final carbon yield, rGO did not appear to affect the processability of the fibers towards graphitization (other than mesophase nucleation), most likely because it was inert to the thermal conversion process. Additionally, the higher carbon yields of the coal-tar pitch fibers could be attributed to the initial C/H ratio of the coal-tar base pitch being higher than the petroleum base pitch (Table 1.1). Overall, the carbon yield (CY) of the petroleum and coal-tar samples were similar to the CY common among pitch-based fibers[8].

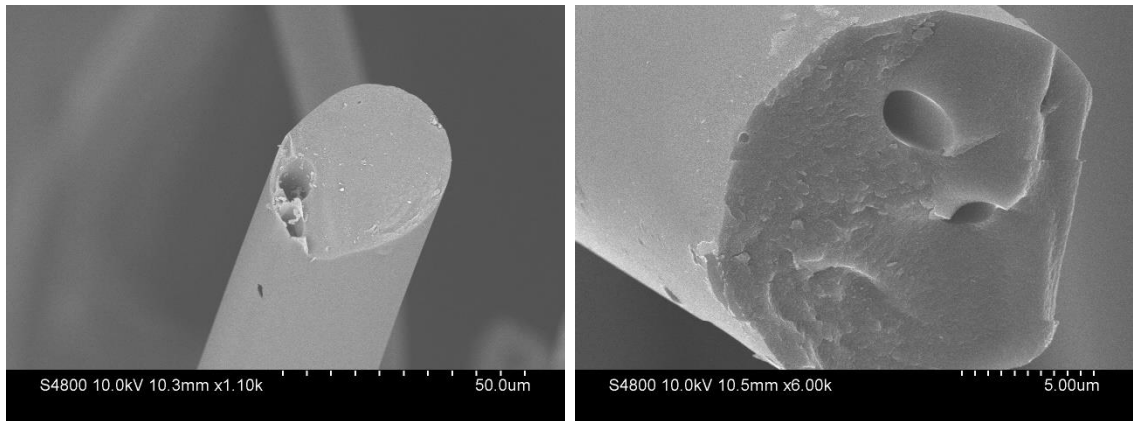
#### 4.2.2 Microscopy

After graphitization, the fibers were Au sputter coated and imaged using a Hitachi S4800 field-emission SEM. The fiber fracture surfaces were imaged for the presence of internal voids. The fiber surfaces were also imaged to investigate roughness and diameter uniformity. Voids in the fiber can drastically reduce the tensile strength of the fiber and in addition to reducing the filament cross sectional area (relative to a nominal diameter-defined area), voids function as stress risers. Moreover, the fiber modulus, which also depends on the actual cross-sectional area of the fiber, can be measured to be lower than expected with the presence of large internal voids. Variations in diameters and the presence of voids were from of the spinning process. This variation could be due to fluctuations in temperature near the exit of the spinneret or caused by the pitch evolving a small amount of volatile gas, at spinning temperature, when the pitch quickly goes from high pressure to low pressure upon exit of the spinneret.

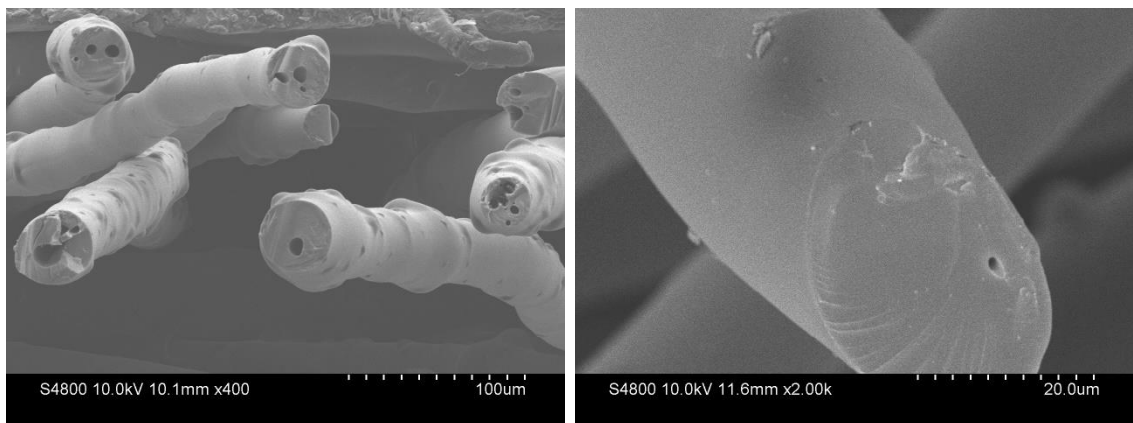
Since diameters were primarily dependent on consistent and stable spinning conditions, the pitch with the most stable spinning generally had the smallest fiber diameter. All fiber samples collected had voids present and variations in diameter. Figure 4.1 shows images of all the graphitized fibers starting with petroleum 0 wt.% (i) (45% mesophase), petroleum 0.01 wt.% (ii) (54% mesophase), coal-tar 0 wt.% (iii) (29% mesophase), and coal-tar 0.01 wt.% (iv) (29% mesophase).



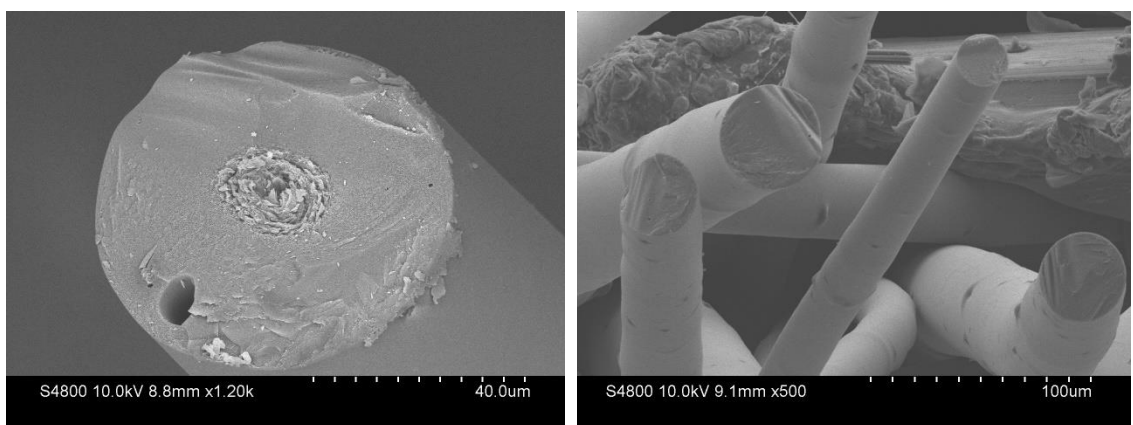
(i)



(ii)



(iii)



(iv)

Figure 4.1 SEM images of melt-spun graphitized (i) petroleum pitch 0 wt.% rGO (ii) petroleum pitch 0.01 wt.% rGO (iii) coal-tar pitch 0 wt.% rGO (iv) coal-tar pitch 0.01 wt.% rGO.

The petroleum pitch fibers had the smallest and most uniform diameter (i-ii) as measured by the SEM (Table 4.2). The smoothness of the petroleum pitch fibers may be due to the aliphatic areas of the pitch allowing the mesophase to flow more easily in a molten state or less volatiles present in the petroleum pitch. Thus, the petroleum pitch would experience less tensile stress at the vitrification point and a higher faster take-up RPM could be used. This may be the case since the petroleum pitches were collected from 284-300 RPM and the coal-tar pitches were collected from 178-224 RPM. Again,



these take-up speeds were optimized for each pitch and represent the maximum allowable value where fiber collection was still possible.

Average diameters measured using SEM are listed in Table 4.1 with the petroleum fibers with 0.01 wt% rGO showing the smallest diameter, which generally correlates to the best spinnability. Therefore, it may be the case that since higher RPMs can be used with the petroleum fibers, smaller diameters were formed, and with smaller diameters there was less of a chance for voids to form.

Table 4.2 Diameter ( $\emptyset$ ) of the four graphitized fibers samples as measured by SEM. Petroleum (P) and coal-tar (C) pitch.

<u>Sample</u>	<u>Average <math>\emptyset</math> (<math>\mu\text{m}</math>)</u>	<u>Std Dev.</u>	<u>N</u>
P - 0 wt%	23.50	5.30	15
P - 0.01 wt%	15.90	1.80	15
C - 0 wt%	33.10	10.50	15
C - 0.01wt%	33.00	11.90	15

For fibers spun from the neat coal tar derived pitch, there were more significant variations in fiber diameter possibly due to insolubles and non-uniform shrinkage in the axial or transverse direction during thermal conversion where varying diameters would cause different rates of reaction. The different rates of reaction during thermal conversion can lead to “crimped” fibers (Figure 4.2). The nodules (insolubles) primarily present in the coal-tar pitch fibers (iii-iv) can also cause variations in the diameters of the fibers as seen in Figure 4.1 (iii). The coal-tar pitch fibers with 0.01 wt% rGO were the only fibers with potentially some graphitic texture visible, shown in Figure 4.1 (iv).



Figure 4.2 Example of a fiber that had non-uniform shrinkage during thermal conversion. Here the fiber was approximately 120 mm in length and approximately 30  $\mu\text{m}$  in diameter.

### 4.2.3 Tensile Testing

The single filament tensile testing was completed using a Textechno FAVIMAT+ with (AI)ROBOT2 equipped with auto feed. This robotic system uses a sample storage case consisting of magazines capable of loading 25 fibers each and uses a robotic arm with a transfer clamp to move one fiber at a time to the testing clamp. When using the auto feed to grab the fibers, due to the brittle nature of graphitic pitch fibers, the robotic arm mechanical clamp of the auto feed would often break the pitch fibers. Therefore, all fibers were manually loaded. To load the fiber, the testing clamps were set to the proper gauge length and the fiber was manually mounted with rubber tipped tweezers and the clamps were manually closed. Each fiber sample was tested with ten fibers at four-gauge lengths ( $L$ ) ( $N = 40$ ), 20, 30, 40, and 50 mm. After the fiber was properly pretensioned, the FAVIMAT+ measured the linear density of the fiber and calculated the diameter ( $D$ ) of the fiber, with the assumption the fiber was circular and solid. The FAVIMAT+ uses ASTM D1577, Standard Test Methods for Linear Density of Textile Fibers, with the vibration method to determine the fiber's linear density ( $\mu$ ) by using the pretension ( $T$ ), gauge length ( $L$ ), and resonant frequency ( $f_n$ ) to calculate the linear density ( $\mu$ ) (equation 4.1). With a user inputted volumetric density ( $\rho$ ) the diameter can be calculated (equation 4.2).

$$\text{Linear Density } (\mu) = \frac{T}{4 \cdot f_n^2 \cdot L^2} \quad [4.1]$$

$$\text{Diameter } (D) = \sqrt{\frac{\mu}{\rho} \cdot \frac{4}{\pi}} \quad [4.2]$$

An in-line load cell (210 cN max) measured the axial tension in the fibers until breakage with a cross head speed of 1 mm/min and a pretension of 1.0 cN/tex. Since the non-circular shape of the fibers caused discrepancies in the diameter measurements as

compared to the SEM diameter measurements, linear density was used for mechanical property analysis. The units of force per linear density (cN/dtex, or grams-force/decitex) stem from the textile industry and are used in place of force per cross sectional area. Where “dtex” is an abbreviation for deci-tex, which is a unit of measurement equal to one gram of mass per 10-km of length. In fact, the linear density unit of measurement is largely a proxy for cross sectional area and is rooted in the difficulty of measuring the cross-sectional area of irregularly shaped textile filaments (e.g. sheep wool fiber). Therefore, the textile analog of strength is called tenacity, in units of force at break per linear density. With these textile units the stress-strain curve was produced and plotted by the FAVIMAT+ along with the force per linear density measurements. The break stress and modulus values were calculated and reported by the instrument testing parameters and can be found in Appendix A[40], [41].

#### 4.3 Results

The results of the single filament tensile testing on experimentally produced mesophase pitch carbon fibers are shown in Table 4.3. Results are reported in textile units of break tenacity (cN/dtex) and modulus (cN/dtex) which helps account for the presence of voids by normalizing to linear density (dtex) and using the break force (cN). Four fiber samples were not included for the coal-tar pitch 0.01 wt.% sample because the results indicated multiple fibers may have been mounted for one test, leading to tremendously high values.

Table 4.3 Break Tenacity (T)(cN/dtex) and Initial Modulus (E)(cN/dtex), and Coefficient of Variance (COV) of the graphitized pitch fibers. Shown are petroleum (P) and coal-tar (C) with 0 wt.% and 0.01 wt.% rGO.

<u>Sample</u>	<u>T</u>	<u>COV</u>	<u>E</u>	<u>COV</u>	<u>N</u>
P - 0 wt.%	2	73%	199	68%	40
P - 0.01 wt.%	13	51%	215	18%	40
C - 0 wt.%	2	61%	276	50%	40
C - 0.01 wt.%	4	70%	331	67%	36

Although diameter was not accounted for with textile units, as mentioned in Chapter 3, the smaller diameter can be indicative of a sample that spun better and therefore has less voids. Analysis of the mechanical property results of the fibers in textile units of cN/dtex shows the smallest, most uniform, diameter fiber sample had the highest Break Tenacity (T), which was the petroleum with 0.01 wt.% rGO (Figure 4.3). Voids are a gross defect in the fiber and will cause the force at breakage to be much lower than a comparable fiber with less voids. The other three samples have no difference in the Break Tenacity and significantly large coefficient of variances (COV). In addition to voids, the large variances could be explained by the occasional crimp in the fibers tested. This crimp could cause the fiber to not be completely pre-tensioned and therefore cause an error in the natural frequency calculation of the fiber where the length (L) was slightly longer than the FAVIMAT+ was measuring (equation 4.1).

Additionally, because of the varied spinning conditions, it was difficult to draw any conclusions of the influence rGO had on the mechanical properties of the fibers. While both 0.01 wt.% rGO pitch samples had slightly better tenacity and modulus than the comparative 0 wt.% sample (Figure 4.3, 4.4), with the current information and analysis, no definite conclusions can be made to the influence of rGO on mechanical properties.

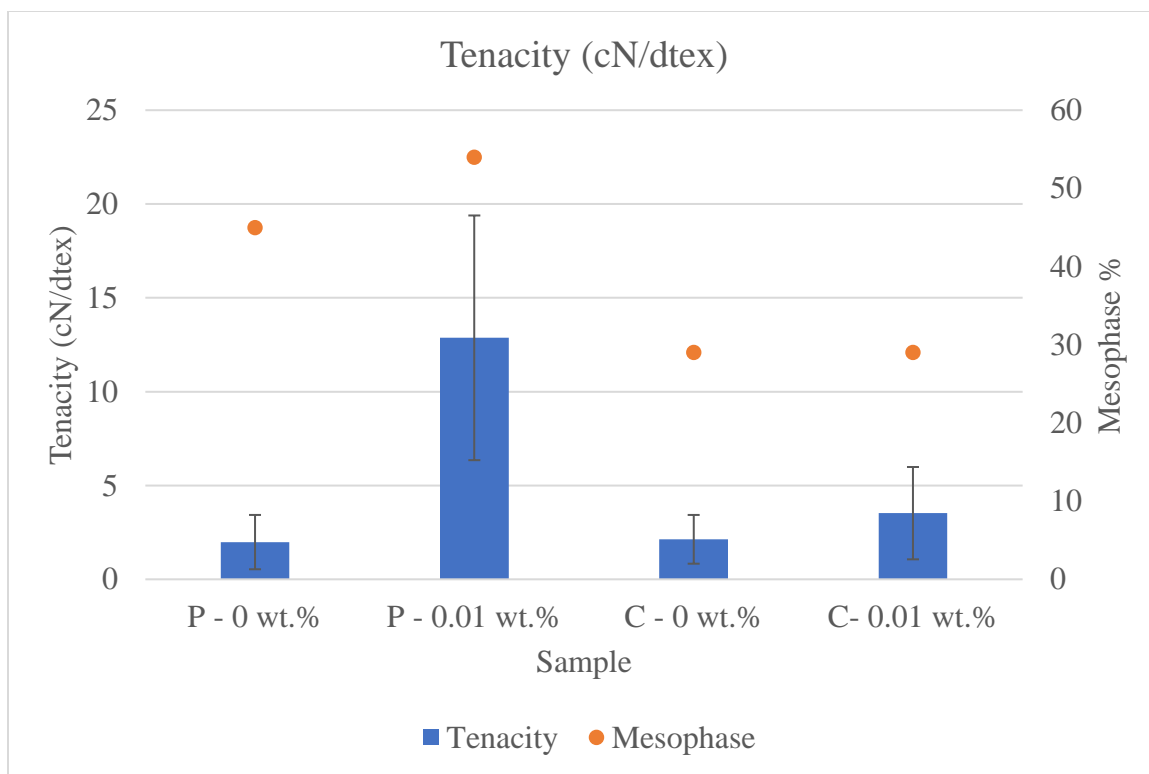


Figure 4.3 Break stress of the graphitized petroleum (P) and coal-tar (C) pitch fibers in textile units (cN/dtex) with mesophase percentage.

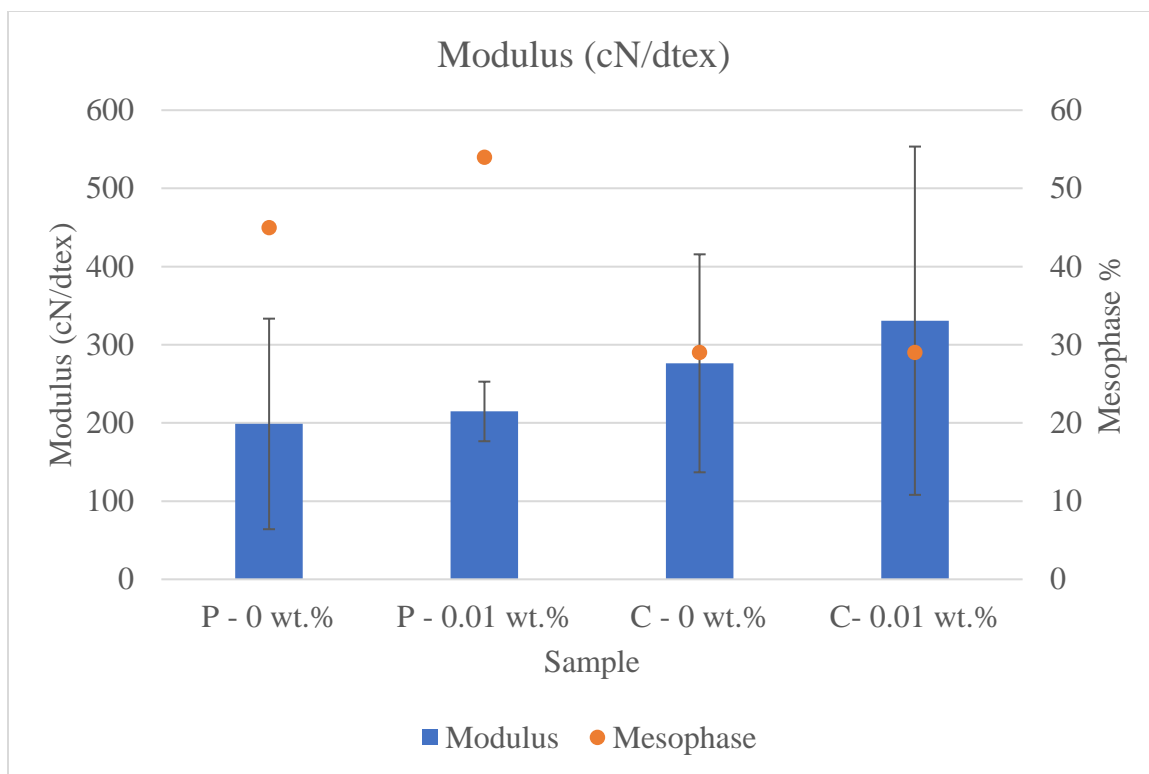


Figure 4.4 Modulus of the graphitized petroleum (P) and coal-tar (C) pitch fibers in textile units (cN/dtex) with mesophase percentage.

#### 4.4 Conclusion

SEM imaging and single filament tensile testing were used to determine if there were any effects from the dispersed rGO in the parent mesophase pitch on the structure and mechanical properties of the resultant graphitic fibers. Graphitic texture representative of high mesophase content was only observed slightly in the coal-tar 0.01 wt.% sample (Figure 4.1 (iv)) but was not prevalent throughout the sample as determined by SEM imaging. Additionally, the coal-tar samples appeared to have a higher degree of voids than the petroleum samples, which were influenced by the volatiles present in the coal-tar samples and thus reflected with difficulty spinning. This led to the diameters measured by the SEM showing the petroleum samples had smaller diameters and less variance of diameters.

While it was found that the 0.01 wt.% rGO samples had slightly better mechanical properties than the 0 wt.% samples, the variances were large enough to prevent a

definitive conclusion that the improvement was due to the rGO. Overall, fibers generated from all pitch samples showed similar mechanical properties except for the relatively high Break Tenacity of the petroleum 0.01 wt.% sample. For all samples, the influence of the melt spinning process appears to dominate the fiber structure as determined by SEM and subsequently the tensile testing results. Regardless of the pitch used or rGO concentrations, the properties and structure of the fiber were set by the spinning process. Therefore, it was difficult to conclude the influence, if any, rGO had on the mechanical properties of petroleum or coal-tar pitch carbon fibers considered for these experiments.

## Chapter 5. CONCLUSION

The specific questions addressed in this thesis were; determining if rGO influences the growth of mesophase in an isotropic petroleum and coal-tar pitch and if the addition of rGO influences the processability of the created mesophase pitch into carbon fibers (melt spinning, thermal conversion). The central findings and conclusions of this work are reviewed in the following.

Using low QI isotropic petroleum and isotropic coal-tar pitch from UKY CAER, rGO was dispersed into a pitch-THF mixture using sonication and systematically heat treated to promote the growth of mesophase. For the petroleum and coal-tar pitches two concentrations of rGO were tested, 0.01 wt.% and 0.10 wt.%, with respect to the base isotropic pitch. The length of heat treatments varied from 0.5-hours to 4-hours using a mantle temperature of 425 °C which led to an average pitch temperature of approximately 370 °C. Nitrogen sparging was used to create an inert atmosphere and generate shear in the molten pitch. The quantification of mesophase was conducted by using polarized light microscopy to determine an estimated volumetric mesophase percentage for each sample. Additionally, softening temperature and quinoline insolubles were measured and correlated to spinnability for each sample.

For the petroleum pitch, it was found that the 0.10 wt.% rGO sample did not assist in the growth of mesophase at any treatment time. However, the 0.01 wt.% rGO results suggested the rGO assisted in the accelerated growth of mesophase, particularly for 0.5-2-hours of heat treatment. This accelerated growth of the 0.01 wt.% sample led to an average increase of mesophase to 3.9% (0.5-hours), 38% (1-hour), and 45% (2-hours) compared to the 0 wt.% sample of 0.9% (0.5-hours), 16% (1-hour), and 24% (2-hours) respectively. However, after 2-hours, the rate of mesophase growth for the 0.01 wt% rGO sample slows significantly and at 4-hours of treatment time the average mesophase percentage of all samples nearly converge to 68% (0 wt.%), 70% (0.01 wt.%), and 64% (0.10 wt.%).

For the coal-tar pitch, the results showed a slight correlation to the rGO assisting mesophase growth in the first 2-hours of treatment time for the 0.01 wt.% sample.



However, the error for the coal-tar samples makes it difficult to say definitively whether the rGO was beneficial as with the petroleum pitch.

The petroleum and coal-tar samples all had a dramatic increase in softening temperature after the first 0.5-hours of heat treatment from approximately 100 °C to over 200 °C. This increase in softening temperature suggests the aggressive removal of lighter weight species present in both pitches. The softening temperature continued to increase but at a slower rate to a softening temperature > 260 °C for all samples treated for 4-hours. Additionally, the QIs appeared to correlate with the increase in mesophase percentage where more mesophase generally meant more QIs.

For melt spinning the pitch into green fibers four samples were tested. All samples were heat treated for four hours, petroleum 0 wt.% and 0.01 wt.% and coal-tar 0 wt.% and 0.01 wt.%. Each sample was successfully melt spun into green fiber and then stabilized, carbonized, and graphitized where carbon yields ranged from 72-82 wt.% (with respect to the initial green fiber mass). The graphitized fibers were imaged by SEM and variations in diameter and internal void occurrence were observed for each sample. All samples had varying degrees of voids, but both petroleum samples had the most uniform diameters. Graphitic texture was observed only for a few fibers with the coal-tar 0.01 wt.% rGO sample. The mechanical properties of the graphitized fibers were quantified by break tenacity (cN/dtex) and initial modulus (cN/dtex) which are units that stem from the textile industry where linear density is used in place of cross-sectional area. This proved useful for all pitch fiber samples tested because of the variation in diameters and voids present in the graphitized fibers.

Mechanical properties of the graphitized fibers were determined using single filament tensile testing to determine the effect of rGO on mechanical properties. The results showed that the 0.01 wt.% rGO sample of both base pitches had slightly better initial modulus than the 0 wt.% samples. For the petroleum 0.01 wt.% rGO sample, the break tenacity was significantly higher than the 0 wt.% rGO sample. However, due to the melt spinning process, it was difficult to determine the effects of rGO on mechanical properties because of the voids present in the fibers. Therefore, further research would be needed to determine if the variations were due to the rGO or melt spinning process.

## 5.1 Future Work

The fibers generated for this thesis appeared to be primarily influenced by the melt spinning process and therefore made it difficult to ascertain the influence, if any, rGO had on graphitic fiber production. Future work should focus on investigating additional rGO loadings and the precise control of the pitch heat treatment temperatures, as well as optimizing the melt spinning process. This optimization could include more precise temperature control, vacuum distillation to remove volatiles from pitch prior to spinning, and a heated air quench for higher spinning temperatures. While the results suggested a benefit to using rGO as a nucleation site for the growth of mesophase in an isotropic pitch, further studies would be needed to understand the mesophase nucleation with higher, precise temperatures. Increasing the heat treatment temperature of the pitch to above 370 °C could potentially allow for quicker mesophase nucleation and subsequent growth than shown here. Additionally, varying weight percentages of rGO between 0.01 wt.% and 0.10 wt.% of isotropic pitch could be studied to determine if there was a more efficient weight percentage to be used as a nucleation site.

## APPENDIX

### System Compliance

The calculated modulus of the fibers needs to be adjusted due to the spring constant of the tensile testing machine being of the same magnitude of the fibers. Due to the stiff nature of carbonized fibers, the system introduces an error into the calculated modulus values. To correct for this error, a corrected compliance ( $C$ ) is calculated using an average indicated compliance ( $C_a$ ) and an extrapolated y-intercept system compliance ( $C_s$ ) from the plot of  $C_a$  against each gauge length. Using the diameters calculated through frequency resonance measurements, the corrected modulus ( $E_c$ ) can be calculated.

$$C = C_a - C_s \quad [A.1]$$

$$C_a = \frac{l_0}{E_a \cdot A} \quad [A.2]$$

$$E_c = \frac{l_0}{C \cdot A} \quad [A.3]$$

$C$  = Corrected Compliance

$C_a$  = Indicated Compliance

$C_s$  = System Compliance

$l_0$  = Gauge length

$A$  = Cross-sectional area of fiber

$E_a$  = Average modulus

$E_c$  = Corrected modulus

## Weibull Analysis

The spinning and thermal conversion processes of carbon fibers causes defects to form in the fibers. These defects greatly affect the mechanical properties and can lead to large variations when calculating break stress. A Weibull modulus is used to help quantify the variation in calculated break stress, where a higher Weibull modulus indicated less variation in the data.

<u>Sample</u>	<u>Weibull Modulus</u>
Pet.	2.02
Pet.	2.03
Coal	1.74
Coal	1.45

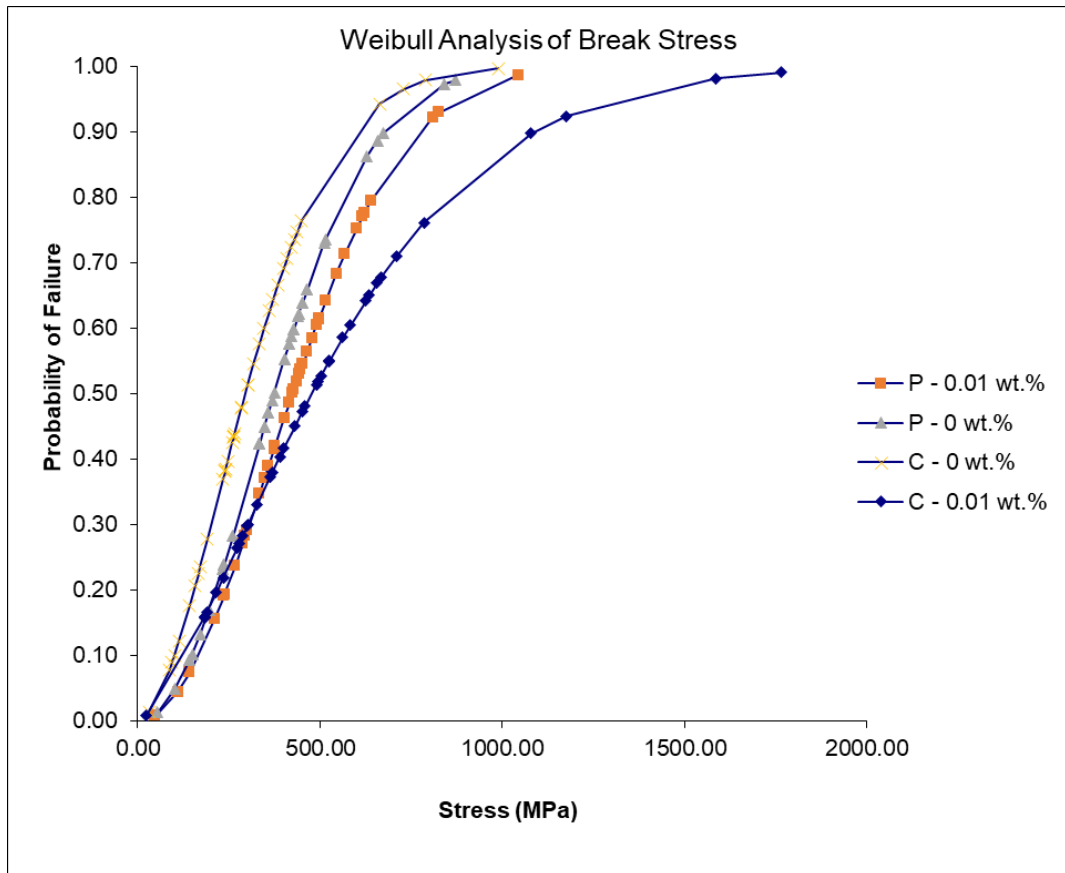


Figure 5.1 Distribution of the tensile stress against probability of failure using a Weibull analysis of graphitic fibers

## REFERENCES

- [1] Toray, "Toray Composite Materials America, Inc." [Online]. Available: <https://www.toraycma.com/page.php?id=661>. [Accessed: 01-Oct-2018].
- [2] Mitsubishi, "Pitch Fiber - Mitsubishi Chemical Carbon Fiber Composites." [Online]. Available: <http://mccfc.com/pitch-fiber/>. [Accessed: 01-Oct-2018].
- [3] T. Matsumoto, "Mesophase pitch and its carbon fibers," *Pure Appl. Chem.*, vol. 57, no. 11, pp. 1553–1562, 1985.
- [4] D. D. Edie and M. G. Dunham, "Melt spinning pitch-based carbon fibers," *Carbon N. Y.*, 1989.
- [5] A. Singh Gill, D. Visotsky, L. Mears, and J. D. Summers, "Cost Estimation Model for Polyacrylonitrile-Based Carbon Fiber Manufacturing Process," *J. Manuf. Sci. Eng.*, vol. 139, no. 4, p. 041011, 2016.
- [6] S. Ohtani, "Japan Patent," S41-15728, 1966.
- [7] S. Ohtani, K. Watanabe, and T. Araki, "Japan Patent," S49-8634, 1974.
- [8] J. The Society of Fiber Science and Technology, *High-Performance and Specialty Fibers*. Springer, Tokyo, 2016.
- [9] K. Azami, S. Yamamoto, T. Yokono, and Y. Sanada, "In-situ monitoring for mesophase formation processes of various pitches by means of high-temperature <sup>13</sup>C-NMR," *Carbon N. Y.*, vol. 29, no. 7, pp. 943–947, 1991.
- [10] J. Madias and M. De Cordova, "Foundry Coke Without Coal More Than Half-century of Production in Argentina," pp. 144–154.
- [11] R. J. Andrews, T. Rantell, D. Jacques, J. C. Hower, J. Steven Gardner, and M. Amick, "Mild coal extraction for the production of anode coke from Blue Gem coal," *Fuel*, vol. 89, no. 9, pp. 2640–2647, Sep. 2010.
- [12] J. D. Brooks and G. H. Taylor, "The formation of graphitizing carbons from the

- liquid phase,” *Carbon N. Y.*, vol. 3, no. 2, pp. 185–193, Oct. 1965.
- [13] T. Maeda, S. Ming Zeng, K. Tokumitsu, J. Mondori, and I. Mochida, “Preparation of isotropic pitch precursors for general purpose carbon fibers (GPCF) by air blowing-I. Preparation of spinnable isotropic pitch precursor from coal tar by air blowing,” *Carbon N. Y.*, 1993.
- [14] R. H. Hurt and Z. Chen, “Liquid Crystals and Carbon Materials,” *Phys. Today*, vol. 53, no. 3, pp. 39–44, Mar. 2000.
- [15] I. Mochida, Y. Korai, C.-H. H. Ku, F. Watanabe, and Y. Sakai, “Chemistry of synthesis, structure, preparation and application of aromatic-derived mesophase pitch,” *Carbon N. Y.*, vol. 38, no. 2, pp. 305–328, Jan. 2000.
- [16] I. Mochida, S.-H. Yoon, and Y. Korai, “Mesoscopic Structure and Properties of Liquid Crystalline Mesophase Pitch and Its Transformation into Carbon Fiber,” *Chem. Rec.*, vol. 2, no. 2, pp. 81–101, Mar. 2002.
- [17] I. Mochida, Y. Korai, C. H. Ku, F. Watanabe, and Y. Sakai, “Chemistry of synthesis, structure, preparation and application of aromatic-derived mesophase pitch,” *Carbon N. Y.*, vol. 38, no. 2, pp. 305–328, 2000.
- [18] I. Mochida, Y. Korai, C. H. Ku, F. Watanabe, and Y. Sakai, “Chemistry of synthesis, structure, preparation and application of aromatic-derived mesophase pitch,” *Carbon N. Y.*, vol. 38, no. 2, pp. 305–328, 2000.
- [19] Diefendorf et al., “Forming Optically Anisotropic Pitches,” 4208267, 1980.
- [20] L. S. Strehlow, R.A.; Singer, “High-temperature centrifugation - application to mesophase pitch,” 1970.
- [21] A. D. Cato and D. D. Edie, “Flow behavior of mesophase pitch,” *Carbon N. Y.*, vol. 41, pp. 1411–1417, 2003.
- [22] E. M. Dianov and D. S. Starodubov, “The viscoelastic behavior of pitches,” *Library (Lond.)*, vol. 2777, no. May 2010, pp. 60–70.
- [23] K. Lafdi, S. Bonnamy, and A. Oberlin, “Mechanism of anisotropy occurrence in a

- pitch precursor of carbon fibers: Part I- pitches a and b,” *Carbon N. Y.*, vol. 29, no. 7, pp. 857–864, 1991.
- [24] O. Fleurot and D. D. Edie, “Steady and transient rheological behavior of mesophase pitches,” *J. Rheol. (N. Y. N. Y.)*, vol. 42, no. 49, 1998.
- [25] A. D. Cato, D. D. Edie, and G. M. Harrison, “Steady state and transient rheological behavior of mesophase pitch, Part I: Experiment,” *J. Rheol. (N. Y. N. Y.)*, vol. 49, no. 101, 2005.
- [26] D. Grecov and A. D. Rey, “Steady state and transient rheological behavior of mesophase pitch, Part II: Theory,” *J. Rheol. J. Rheol.*, vol. 49, no. 85, 2005.
- [27] P. Morgan, *Carbon Fiber and Their Composites*, 1st ed. Boca Raton, FL: CRC Press, 2005AD.
- [28] D. D. Edie and M. G. G. Dunham, “Melt spinning pitch-based carbon fibers,” *Carbon N. Y.*, vol. 27, no. 5, pp. 647–655, Jan. 1989.
- [29] J. J. McHugh and D. D. Edie, “The orientation of mesophase pitch during fully developed channel flow,” *Carbon N. Y.*, vol. 34, no. 11, pp. 1315–1322, 1996.
- [30] D. D. Edie, N. K. Fox, B. C. Barnett, and C. C. Fain, “Melt-spun non-circular carbon fibers,” *Carbon Vol*, vol. 24, no. 4, pp. 477–482, Jan. 1986.
- [31] I. Mochida, S.-H. Yoon, N. Takano, F. Fortin, Y. Korai, and K. Yokogawa, “Microstructure of mesophase pitch-based carbon fiber and its control,” *Carbon N. Y.*, vol. 34, no. 8, pp. 941–956, Jan. 1996.
- [32] Y. Kofui *et al.*, “Preparation of carbon fiber from isotropic pitch containing mesophase spheres,” *Carbon N. Y.*, vol. 35, no. 12, pp. 1733–1737, 1997.
- [33] Y. Zhu, S. Murali, M. D. Stoller, A. Velamakanni, R. D. Piner, and R. S. Ruoff, “Microwave assisted exfoliation and reduction of graphite oxide for ultracapacitors,” *Carbon N. Y.*, vol. 48, no. 7, pp. 2118–2122, 2010.
- [34] S. Pei and H.-M. Cheng, “The reduction of graphene oxide,” *Carbon N. Y.*, vol. 50, no. 9, pp. 3210–3228, Aug. 2012.

- [35] R. Menndez *et al.*, “On the chemical composition of thermally treated coal-tar pitches,” *Energy and Fuels*, vol. 15, no. 1, pp. 214–223, 2001.
- [36] R. A. Greinke and L. S. Singer, “Constitution of coexisting phases in mesophase pitch during heat treatment: Mechanism of mesophase formation,” *Carbon N. Y.*, vol. 26, no. 5, pp. 665–670, Jan. 1988.
- [37] A. Mianowski, S. Blazewicz, and Z. Robak, “Analysis of the carbonization and formation of coal tar pitch mesophase under dynamic conditions,” *Carbon N. Y.*, 2003.
- [38] F. R. Vieira, C. H. M. de Castro Dutra, and L. D. de Castro, “Determining the anisotropic content in a petroleum pitch – Comparison of centrifugation and optical microscopy techniques,” *Fuel*, vol. 90, no. 2, pp. 908–911, Feb. 2011.
- [39] O. Fleurot, D. D. Edie, and J. J. Mchugh, “Elastic behavior of mesophase pitch,” in *The American Carbon Society 22nd Biennial Conference*, 1995, pp. 268–269.
- [40] “ASTM Standard 3822-07,” 2007.
- [41] “ASTM Standard 3379.” .



## VITA

Name:

Aaron Michael Owen

Place of Birth:

Henderson, KY, USA

Education:

University of Kentucky

Bachelor of Science in Mechanical Engineering May 2017

Positions Held:

Undergraduate Research Assistant

Center for Applied Energy Research, University of Kentucky

January 2015 – May 2017

Graduate Research Assistant

Center for Applied Energy Research, University of Kentucky

May 2017 – July 2018

Conferences and Presentations:

Owen, A.M., M.C. Weisenberger, D.L. Eaton, and R.J. Andrews. 2018. "Assisted Development of Mesophase in Pitch with the Use of Dispersed Graphene." *Carbon 2018*. Madrid, Spain.